8-11-2020

Functions of Extracellular Pyruvate Kinase M2 in Fibrosis-related Diseases

Hongwei Han

FUNCTIONS OF EXTRACELLULAR PYRUVATE KINASE M2 IN FIBROSIS-RELATED DISEASES

by

HONGWEI HAN

Under the Direction of Zhi-Ren Liu, PhD

ABSTRACT

Fibrosis represents a pathological condition characterized by excessive deposition of the extracellular matrix. Myofibroblasts are the primary source of extracellular matrix in fibrosis. Their resistance to turnover and elevated collagen synthetic capacity play critical roles during organ fibrosis progression, mechanisms of which are not fully understood. Here we report that high levels of extracellular PKM2 are detected in lung fibrosis patient tissues. The extracellular PKM2 promotes lung fibrosis by protecting myofibroblasts from apoptosis and increasing collagen production in myofibroblasts. Further, our results show that the extracellular PKM2 interacts with integrin αvβ3 and activates integrin αvβ3-FAK-PI3K signaling axis in myofibroblasts. Moreover, neutralization of PKM2 with the antibody is effective in attenuating lung fibrosis.

Fibrosis is a hallmark of cancer. Fibrosis in cancer results from the increased deposition of a cross-linked collagen matrix by myofibroblasts. Fibrosis in cancer has been shown to enhance cancer growth and metastasis. High levels of PKM2 are identified in the blood circulation of cancer patients of many types. However, the effects of extracellular PKM2 on fibrosis in cancer has not been well studied. Here we show that the extracellular PKM2 promotes lung metastasis in breast cancer and neutralization of PKM2 with antibody reduces tumor burden and lung metastasis. These effects are accompanied by marked changes in collagen content and myofibroblast population.

In summary, extracellular PKM2 facilitates the lung fibrosis by enhancing survival and collagen production of myofibroblasts via integrin αvβ3-FAK-PI3K signaling axis. In addition, extracellular PKM2 increases fibrosis level in breast cancer which favors cancer growth and metastasis. Our study suggests a new therapeutic target for the treatment of fibrosis-related diseases.

INDEX WORDS: Pyruvate kinase M2, Lung fibrosis, Myofibroblast, Apoptosis, Arginase-1, Breast cancer

FUNCTIONS OF EXTRACELLULAR PYRUVATE KINASE M2 IN FIBROSIS-RELATED DISEASES

by

HONGWEI HAN

A Dissertation Submitted in Partial Fulfillment of the Requirements for the Degree of

Doctor of Philosophy

in the College of Arts and Sciences

Georgia State University

2020

FUNCTIONS OF EXTRACELLULAR PYRUVATE KINASE M2 IN FIBROSIS-RELATED DISEASES

by

HONGWEI HAN

Committee Chair: Zhi-Ren Liu

Committee: Ritu Aneja

Charlie Garnett Benson

Electronic Version Approved:

Office of Graduate Services

College of Arts and Sciences

Georgia State University

August 2020

DEDICATION

I would like to dedicate my dissertation to my parents, Kai Han and Aiping Wei, my brother and my sister-in-law, Hongwu Han and Mali Chen. Thank you for your love and support. I will always love you all.

I would like to dedicate my dissertation to my grandparents for their love and care since my childhood. The memories with you are so fresh and I miss you both so much. Please rest in peace.

I would like to dedicate my dissertation to my little niece, Maiyatang. You are so little and so lovely. Bless you grow up healthily and happily.

ACKNOWLEDGEMENTS

I would like to thank my supervisor, Dr. Zhi-Ren Liu, for his supervision and guidance during my Ph.D. study. I would like to express my gratitude to my committee members Dr. Ritu Aneja and Dr. Charlie Benson. They encouraged me a lot and gave me valuable suggestions and comments on my dissertation. I would also like to thank Dr. Jenny Yang for her inspiration and her care about me in both research and life. Moreover, I want to give special thanks to Dr. Liangwei Li and Dr. Yinwei Zhang for their fundamental work, which sets a strong step stone for my project. In addition, I want to thank Dr. Siming Wang for her support in the Mass Spectrometry technique. I thank Dr. Jingjuan Qiao for her kind support and help. Besides, I would like to thank Maureen Meister for the linguistic assistance during the preparation of this manuscript. I would also like to give my appreciation to Guangda Peng for his countless support. Last but not least, I want to take this chance to thank all lab members of Dr. Zhi-Ren Liu's group for their help and valuable suggestions.

TABLE OF CONTENTS

LIST OF TABLES

LIST OF FIGURES

1 INTRODUCTION

1.1 Glycolysis

Glycolysis is the metabolic pathway that breaks down glucose into the three-carbon compound pyruvate and generates energy. Glycolysis is a sequence of ten enzyme-catalyzed reactions which take place in the cytoplasm of a cell. This process is an oxygen-independent metabolic pathway so that it can happen in the presence or absence of oxygen. The wide occurrence of glycolysis in many different species indicates that it is an ancient metabolic pathway.

Glycolysis has 10 steps, and each of the steps is catalyzed by its own enzyme. In general, the glycolysis pathway can be separated into two main phases, five of which are in the preparatory phase (or investment phase) and five are in the pay-off phase.

In preparatory phase, glucose, as the starting material, is phosphorylated by an enzyme called hexokinase to form glucose 6-phosphate (G6P). This step makes a more active form of sugar, G6P. And it also decreases glucose concentrations, which leads to continuous transport of glucose into the cell through the plasma membrane transporters. In addition, it also traps glucose inside the cell since the cell lacks transporters for G6P. G6P is not able to cross the cell membrane readily because it contains a phosphate group. G6P is then rearranged into its isomer fructose 6-phosphate (F6P) by glucose phosphate isomerase.

A phosphate group is transferred from ATP and added to F6P, producing fructose-1,6-bisphosphate (FBP). This step is catalyzed by the enzyme phosphofructokinase, which is the rate-limiting enzyme.

The FBP is quite unstable due to the phosphate groups, allowing it to split and form two three-carbon sugars: dihydroxyacetone phosphate and glyceraldehyde-3-phosphate. They are isomers of each other, and dihydroxyacetone phosphate can be converted to glyceraldehyde-3-

phosphate. Only glyceraldehyde-3-phosphate can enter the next steps of glycolysis. When glyceraldehyde-3-phosphate is used for the next step, dihydroxyacetone phosphate is eventually converted by triosephosphate isomerase to glyceraldehyde-3-phosphate.

Because the phosphates used in these steps come from ATP. Two ATPs have been used up, this is why this phase is called investment phase or energy-required phase.

In the pay-off phase, glyceraldehyde-3-phosphate is converted into another three-carbon molecule, pyruvate, through a series of reactions. In this process, four ATP molecules are produced, along with two molecules of NADH.

Followed up with the preparatory phase, glyceraldehyde-3-phosphate is oxidized and form 1,3-bisphosphoglycerate while NAD^+ is reduced to NADH and H^+ with the help of glyceraldehyde phosphate dehydrogenase (GAPDH). A phosphate group from 1,3-bisphosphoglycerate is transferred to ADP by phosphoglycerate kinase, forming ATP and 3-phosphoglycerate. 3-phosphoglycerate is isomerized into 2-phosphoglycerate. 2-phosphoglycerate loses a molecule of water, becoming phosphoenolpyruvate which is an unstable molecule and easy to form pyruvate by losing a phosphate group in the final step of glycolysis. The conversion of phosphoenolpyruvate into pyruvate makes a molecule of ATP. Since glucose leads to two three-carbon sugar in the preparatory phase, each reaction in the pay-off phase occurs twice per glucose molecule. In total, four ATP molecules are produced, along with two molecules of NADH. The net gain of the glycolytic pathway is 2 NADH molecules and 2 ATP molecules per glucose.

1.2 Pyruvate Kinase

1.2.1 Pyruvate kinase

Pyruvate kinase is the enzyme which catalyzes the last step of glycolysis, one of the three rate-limiting steps. It catalyzes the conversion of phosphoenolpyruvate (PEP) into pyruvate,

producing one molecule of ATP. ATP is the energy currency for the cell. Pyruvate is either broken down to carbon dioxide to yield more ATP molecules in aerobic respiration through a series reactions of pyruvate oxidation, the citric acid cycle and oxidative phosphorylation, or is converted to lactic acid or ethanol in the absence of oxygen.

Pyruvate kinase has four distinct, tissue-specific isozymes in animals, isoform L, R, M1 and M2. The L isoform is present in liver tissue while R isoform is expressed in erythrocytes. Both of two isoforms are encoded by the same gene *PKLR* and they both have two distinct conformation states: the R-state and L-state. The R-state is the compact and active form of pyruvate kinase with a high affinity for the substrate and is stabilized by PEP and FPB. While the T-state is the looser and less active form of pyruvate kinase with a low affinity for the substrate and is stabilized by ATP and alanine. Therefore, the R-state promotes glycolysis, but the T-state does not.

The PKM1 isoform is dominantly present in muscle and brain tissues while PKM2 isoform is found in early fetal tissue. They both are expressed from the gene *PKM*. The *PKM* gene contains 12 exons and 11 introns. M1 and M2 isoform are alternative splicing products of *PKM* gene. The M1 isoform has exon 9 while the M2 isoform has exon 10. Therefore, M1 and M2 share a majority of sequence similarity except for the only difference encoded by two different exons. The sequence difference of these two isoforms lies in 23 amino acids in the C-terminal. PKM2 is primarily expressed in embryonic cells during embryonic stages, and it is also present in other tissues like the lung fat tissue, retina and the pancreatic tissue. It is also found in highly proliferative cells like tumor cells in a dimeric form. It is believed PKM2 is intensively involved in tissue repair and regeneration.

1.2.2 PKM1 and PKM2

Both PKM1 and PKM2 are tetrameric proteins consisting of four identical subunits (or monomers). Each monomer contains four structural domains: A, B, C, and N-terminal domain. The monomer dimerizes to form a dimer. The dimer then dimerizes to form a tetramer. Two dimers interact with each other via dimer-dimer interface which is localized in the C domain on the monomer. The 23 amino acid difference between PKM1 and PKM2 localizes in the C domain, thus affects tetramer formation. Under physiological condition, PKM1 is always present as a tetramer while PKM2 can be in the form of a tetramer or a dimer.

Secondly, the difference in the 23 amino acids also affects two proteins' allosteric regulation. Domain C is the place where allosteric activator FBP binds. FBP directly binds PKM2 and increases enzymatic activity of PKM2. The interaction of PKM2 and the allosteric activator on domain C of pyruvate kinase leads to the conformational change of the enzyme, which enhances the enzymatic activity of PKM2. On the contrary, FBP does not bind to PKM1 so it does not have any effect on PKM1 activity. FBP is the main regulator of pyruvate kinases enzymatic activity. Since FBP is the intermediate product in glycolic pathway, it serves as a feedforward stimulator. In addition to FBP, other metabolites, amino acids, and small molecules can affect PKM2 activity. PKM2 can be activated by serine and succinyl aminoimidazole carboxamide ribose-50 phosphate SDH succinate dehydrogenase (SAICAR). The pyruvate kinase enzymatic activity of PKM2 can be inhibited by many inhibitors such as L-Cysteine, pyruvate, tyrosine, phenylalanine, alanine, adenosine triphosphate, and thyroid hormone T3. The inhibitors can bind to the allosteric regulatory domain, which leads to the conformational change of PKM2. The tetramer PKM2 will transform from a compact state to a loose state and finally dissemble to dimer form.

PKM2 activity is also regulated by post-translational modification, such as phosphorylation, acetylation and oxidation, which favors the less active dimeric PKM2.

The third difference is in energy production and intermediate utilization. Since PKM1 constitutively exists as the active tetramer, its dominant function is to generate ATP for the cell. However, PKM2, apart from producing ATP, can switch to the less active dimeric form and promote glycolytic intermediates accumulation. Glycolytic intermediates are building blocks used for the biosynthesis of different biomolecules such as amino acids, phospholipids and nucleotides.

1.2.3 PKM2 expression regulation

The alternative splicing is regulated by the splicing factor family heterogenous ribonucleotide proteins (hnRNPs) including hnRNP 1 (or PTB), hnRNPA1, hnRNPA2. The hnRNPs enter the nucleus and release exon 10 by binding to exon 9 and promote PKM2 expression. The 3 splicing factors are under the regulation of c-myc. During hypoxic conditions, the HIF1-α upregulates hnRNPs so that the M2 isoform is upregulated. Insulin can also upregulate the expression of M2 isoform. Studies show that EGFR activation can upregulate PTB, which results in the increase in PKM2 expression. The alternative splicing is highly dependent on PTB. In addition to the different splicing mechanisms, researchers have shown that PKM2 expression is also closely controlled by MicroRNAs (miRNA).

Genetic deficiency of the pyruvate kinase causes the disease known as pyruvate kinase deficiency. This deficiency is destructive for cells who depend on glycolysis for energy. The red blood cells, which do not contain mitochondria for aerobic respiration, can undergo hemolysis if they lack pyruvate kinase, resulting in chronic nonspherocytic hemolytic anemia. This condition occurs when the *PKLR* gene is mutated.

1.2.4 PKM2 dimer and tetramer

The PKM2 has two forms: tetramer and dimer. Both forms are composed of the same monomer, however, their biological effects are distinct. The tetramer PKM2 has enzymatic activity and mainly serves as a catalytic enzyme, regulating the glycolytic process. The dimer PKM2 has very low enzymatic activity and does not work in glycolysis. The dimer PKM2 and tetramer PKM2 can swift between one another by various activators and inhibitors. PKM2 only has pyruvate kinase activity when it is in tetramer form. The conversion of dimer into tetramer is also considered as the activation process of PKM2 while the conversion of tetramer into dimmer is considered as the inhibition of PKM2. For example, high physiological levels of FBP can stimulate the dimerization of the PKM2 dimers to form an active PKM2 tetramer and stabilize tetramer PKM2. The tetramer PKM2 can actively push the glycolysis machinery rolling. When the level of FBP is low, PKM2 tetramer can dissociate to dimer PKM2.

1.2.5 PKM2's function and cellular location

PKM2 has diverse cellular locations and performs many non-glycolytic roles. In general, PKM2 can be present in the cell cytosol, nucleus and extracellular space.

PKM2 can enter the nucleus and modify gene regulation. Additionally, it can attach to the outer membrane of mitochondrial to regulate mitochondrial function and it can exist in the endoplasmic reticulum to release endoplasmic reticulum stress. It can also be secreted into the extracellular space to act as a ligand and trigger intercellular signaling pathways. Moreover, PKM2 can also be modified with phosphorylation, acetylation and other proteins. The cellular localization and functions of modified PKM2 become more complicated.

（1）The non-glycolytic role of dimeric PKM2 in the cytoplasm

PKM2 in the cytoplasm usually acts as a metabolic enzyme in glycolysis, as in enzymatic tetramer form. While dimeric PKM2 is also present in the cytoplasm of certain cell types and it does not facilitate glycolysis. The cancer cells have elevated levels of dimeric PKM2 in the cytoplasm. The dimeric form of PKM2 is also called Tumor M2-PK. It is discovered when people were studying the Warburg effect. In the early twentieth century, German biologist Warburg discovered that tumor cells prefer glucose glycolysis than oxidative phosphorylation even when surround by oxygen in high levels. Such aerobic glycolysis is termed as Warburg effect. It is found that the tumor M2-PK plays vital roles in cancer progression. Cancer cells prefer the dimeric form of PKM2 because the low enzymatic activity of dimer PKM2 blocks the normal flow of glycolysis, thus accumulation of glycolytic intermediates provides building blocks for the biosynthesis of biomolecules which helps increase proliferation of cancer cells. These intermediates are precursors of nucleic acids, phospholipids and amino acids, which are principal constituents of cells.

Tumor cells can increase dimer PKM2 at the post-translational level. To be specific, dimerization of PKM2 is elevated in tumor cells by its interaction of PKM2 with various oncoproteins such as A-Raf. Tumors can also increase PKM2 at the transcriptional level. Tumor cells increase the transcription of PKM2 in various ways, such as through hypoxia-inducible factor, which is activated under hypoxic conditions in tumor microenvironments.

Besides functioning as a metabolic enzyme, cytoplasmic PKM2 also acts as a signaling modulator under certain circumstances. This role in signal modulation usually requires its interaction with other proteins. For instance, PKM2 was shown to interact with various tyrosine kinases including A-Raf and fibroblast growth factor receptor 1 (FGFR 1). These interacting partners modify PKM2 and promote the dimer/tetramer switch of PKM2, which has an impact on

metabolic alteration. On the other hand, PKM2 also changes the catalytic kinetics, substrate affinity and cytoplasmic location of its interacting partners, which affects signal transduction.

It is reported the PKM2 binds to phosphor-tyrosine residue to access protein complexes in signaling pathways. The anti-apoptotic protein Bcl2 is identified as a PKM2 interacting partner. PKM2 translocates to the mitochondria under oxidative stress and interacts with Bcl2 to stabilize it by preventing it from degradation.

（2）PKM2 as a protein kinase and transcriptional regulator in the nucleus

PKM2 contains nuclear localization sequence (NLS). When PKM2 is in tetramer form, the NLS site is buried due to a stable charge-charge interaction between monomers. When PKM2 is in dimeric form, the NSL site is exposed and PKM2 can enter the nucleus. PKM2 can be phosphorylated to gain nuclear access. For example, Mitogen-activated protein kinase 1 (ERK2) phosphorylates dimer PKM2 and results in the conformational change of PKM2 which makes PKM2 accessible to the nucleus and regulates gene expression. Once entering the nucleus, PKM2 can act as a transcriptional co-activator and participate in gene regulation to promote cell growth and proliferation.

It is first found that PKM2 binds to Y333-phsphrylated-β-catenin, and the complex is recruited to nucleosomes to phosphorylate histone H3, which subsequently increases histone H3 acetylation. This acetylation of histone H3 helps to increase the transcription of β-catenin target genes. Consequently, the expression of CycinD1 is increased, and the cell cycle is regulated. Another report demonstrated the PKM2 directly phosphorylates signal transducer and activator of transcription 3 (STAT3) and enhances transcription of mitogen-activated protein kinase 5 (MEK5) by STAT3. It is also reported that nuclear PKM2 can phosphorylate extracellular signal-regulated kinase 1 and 2 (ERK 1 and ERK 2) to promote tumor cell growth. PKM2 can regulate PD-L1

expression in immune cells like macrophages as well as tumor cells. Beside transcription factors, PKM2 has been shown to phosphorylate myosin light chain 2 (MLC2) and BUB3. Moreover, PKM2 also acts as a transcription regulator in a phosphorylation-independent manner. For example, PKM2 is reported to bind with the transcription factor Oct4 and inhibit Oct4-mediated transcription in cell stemness. Other studies suggest PKM2 can interact with NF-κB and HIF-1α in the nucleus and activate the expression of HIF-1α target gene *VEGF-A*, which leads to an increase in levels of VEGF-A in blood circulation and sequentially an enhancement of tumor angiogenesis.

However, the role of PKM2 as a transcription regulator has been questioned by studies in PKM2 knockout cells. Hosios et al. showed that PKM2-mediated phosphorylation was not a common event in cells (Hosios, Fiske, Gui, & Vander Heiden, 2015).

（3）PKM2 as an extracellular signaling communicator

PKM2 is reported be present in exosomes, potentially involved in cell-cell communication and extracellular signaling. Buschow et al. first reported that PKM2 was identified in B-cell exosomes (Buschow et al., 2010). PKM2 is found in exosomes released by various cells supported by subsequent studies. It has been accepted that PKM2 is present in exosomes secreted by different cell types. The information is accessible in public extracellular vesicle databases like ExoCarta and EVpedia. This new area indicates that PKM2 could play a role in cell-cell communication, carrying messages from host cells to recipient cells.

Various cancer cells secrete PKM2 and PKM2 is found to exist in high levels in the blood circulation of cancer patients. It has been used as a biomarker for different cancer types. It is reported that PKM2 in blood circulation enhances endothelial cell migration and proliferation, promotes angiogenesis and thus increase tumor growth (Li, Zhang, Qiao, Yang, & Liu, 2014).

People also demonstrated that PKM2 enhanced colon cancer cell migration via PI3K/AKT and Wnt/β-catenin signal pathways (Yang et al., 2015). Another study showed that PKM2 increased breast cancer cell proliferation via epidermal growth factor receptor (EGFR) activation (Hsu et al., 2016). Kim et al. suggested that extracellular PKM2 mediated tumorigenesis of colon cancer cells by upregulating claudin, a main constituent of the tight junction complexes, through EGFR-PKC-claudin-1 pathway (Kim et al., 2019). A recent investigation showed that secreted PKM2 promoted lung cancer metastasis via the Integrin β1/FAK/PI3K signaling pathway (Wang et al., 2020). In addition to cancer cells, other cell types are also reported to secret PKM2. A research group claimed that neutrophils secreted PKM2 at wound sites to promote angiogenesis and accelerate the wound healing process (Zhang, Li, Liu, & Liu, 2016).

Another mystery is whether the extracellular PKM2 functions as free PKM2 or vesicle wrapped PKM2. Free circulating PKM2 is a large protein and cannot enter the cell readily. Its effect is likely through cell surface receptor like EGFR or β1. On the contrary, vesicle wrapped PKM2 could be endocytosed by cell and play the role similar like intracellular PKM2. It is not known which form of extracellular PKM2 is playing a role outside the cells or if it is both forms.

There remains a major knowledge deficit in terms of our understanding of PKM2, and the current knowledge remains up for debate. The PKM2 knockout mice, contrary to researchers' expectations of a suppression in tumor development, do not attenuate tumor growth. This study challenges our impression of the tumor promoting role of PKM2, indicating that PKM2 might not be required for tumor development (Israelsen et al., 2013). Moreover, PKM2 knockout mice are susceptible to develop hepatocellular carcinoma spontaneously due to the metabolism imbalance.

1.3 Fibrosis

1.3.1 Fibrosis and wound healing

Fibrosis is a term used to refer to scarring. It involves an irregulated wound healing process usually caused by continuant insults preventing the wound from completely healing. The extracellular matrices accumulation results in the formation of permanent scar in tissue. Fibrosis is characterized by excessive deposition of extracellular matrix (ECM), which is the key factor that makes the tissue harden and causes scaring. In the end stage, the scaring leads to organ function disruption and finally organ failure. Fibrosis and resulting organ failure accounts for at least one third of deaths worldwide (Rockey, Bell, & Hill, 2015).

According to Rockey et al., fibrogenic responses can be divided into four main phases (Rockey et al., 2015). The first phase is the initiation of the response, which is triggered by organ injury. Organ injury comes from various stimuli, including pathogenic infections, toxic substances, radiation and mechanical injury. All these insults are usually persistent and result in chronic inflammation and a fibrogenic response. Inflammation leads to injury of epithelial cells and endothelial cells, resulting in release of inflammatory mediators, including cytokines and chemokines, which will recruit a wide range of immune cells, including macrophages, leukocytes, eosinophils, basophils and mast cells. The second phase is the activation of effector cells, which is triggered by cytokine and growth factors released by immune cells. The primary effector cells are fibroblasts and myofibroblasts (also known as activated fibroblasts). Myofibroblasts are a dominant source of ECM components during fibrogenesis. The third phase is the expansion of extracellular matrix. The fourth phase is fibrosis formation and ultimately the end-stage organ failure.

Cellular level fibrogenesis involves complex activities executed by many different cells, include inflammatory cells (e.g., macrophages and T cells), epithelial cells, effector cells, endothelial cells, and others.

It is suggested that fibrosis in different organs share common pathogenic pathways. The important signal pathways include transforming growth factor beta (TGF-β), platelet-derived growth factor (PDGF), connective-tissue growth factor (CTGF), interleukin 10 (IL-10) and vasoactive factors (angiotensin II and endothelin-1). Furthermore, it is clear that integrins, which link extracellular matrix to cells, are critical in the pathogenesis of fibrosis. Among all factors, TGF-β is the critical factor and the core molecular pathway involved in all types of fibrosis. TGF-β is the most well-studied regulator of fibrogenesis. There are three isotypes of TGF-β in mammals, TGFβ-1, -2 and -3, all with similar biological activity. Tissue fibrosis is primarily attributed to the TGFβ-1 isoform, which is released mainly by macrophages and circulating monocytes.

Wound healing process includes the following phases:

Hemostasis (as known as blood clotting): When epithelial and/or endothelial cells are injured, in the first few minutes of injury, circulating platelets in the blood start to accumulate at the injured site and become activated. The activated platelets release chemical signals to promote blood-clot formation. Soon, fibrin is activated and forms a mesh and attracts platelets. This causes clot formation to stop the leaking of the blood vessel, preventing further bleeding (Guo & Dipietro, 2010).

Inflammation: in this phase, platelet degranulation promotes vasodilation which increases blood vessel permeability. Epithelial and/or endothelial cells excrete MMPs, the enzymes that break down the basement membrane, pave roads for inflammatory cells to the site of injury. On the other hand, injured epithelial cells and endothelial cells also secret growth factors, cytokines

and chemokines to recruit inflammatory cells. The fastest responders are macrophages and neutrophils, and they come to clear out the damaged and dead cells along with bacteria and any other invading pathogens through the process of phagocytosis,

Proliferation: In this phase, angiogenesis, collagen deposition, granulation tissue formation, epithelialization, and wound contraction occur. The cytokines and chemokines released by inflammatory cells act as mitogenic and chemotactic stimuli for endothelial cells and the migrated endothelial cells from new blood vessels, referred to as angiogenesis. During this period, lymphocytes and other cells also become activated and secrete cytokines and growth factors, such as TGFβ, FGF, EGF and PDGF, which further induce the activation of myofibroblasts. Myofibroblasts migrate into the wound and secrete extracellular matrix including collagen and fibronectin. The newly formed structure containing proliferative fibroblasts, new angiogenic vessels, together with infiltrated inflammatory cells in a loose extracellular matrix is called granulation tissue. Meanwhile, epithelial cells also proliferate and migrate over the basal layers and form a new layer of epithelium to cover the wound bed. In wound contraction, myofibroblasts contract the wound and decrease the wound to this normal tissue site. When these cells finish their job and are no longer functional, they undergo programmed death (Gonzalez, Costa, Andrade, & Medrado, 2016).

Maturation (remodeling): In this phase, collagens undergo cross-linking, and proper alignment to provide strength to the healing tissue.

However, persistent stimuli result in chronic inflammation, which gives rise to an excessive deposition of ECM components and ultimately leads to permanent fibrosis. Comparing the fibrotic process versus normal wound healing, the key seems to lie in the balance between collagen

synthesis and collagen degradation. When the rate of new synthesis exceeds the rate of resolution, the healing process turns in the wrong direction as fibrosis.

1.3.2 Fibrosis resolution

Although fibrosis has always been considered irreversible, evidence is emerging indicating fibrosis is reversible under some circumstances. Investigations are intensely performed in animal models, wherein the removal of injury sources leads to gradual resolution of fibrosis. As exemplified by the most commonly used animal model for lung fibrosis, bleomycin-induced mouse lung fibrosis by intratracheal administration. The bleomycin induces alveolar epithelial cell death followed by inflammatory cascades that ultimately progress to lung fibrosis. The cessation of bleomycin administration engenders spontaneous resolution of fibrosis, accompanied by restoration of tissue architecture. However, in humans, the injury sources are hard to remove in some cases, if not at all, and often people are unaware of the cause. Moreover, the translation of treatment strategies targeting fibrosis resolution from animal model to human patients is also challenging as animal models do not fully represent human cases. These are the obstacles we need to overcome or manipulate to target tissue resolution as a therapeutic strategy.

To resolve tissue fibrosis, three areas need to be taken into consideration: first of all, eradication the injury source; Then, degradation of the fibrotic ECM and the EMC-producing myofibroblasts, especially if cessation of stimuli is not possible or the stimuli is not identified (J.-I. Jun & Lau, 2018).

If the injury cause is clear, the most efficacious treatment to resolve the fibrosis is to eliminate the cause of injury, for example, the antiviral treatment in HBV-induced liver fibrosis.

The fibrotic ECM can be divided into two types: basement membrane at the base of the epithelial can endothelial cells as supporting structure which comprises Collagen IV, laminins

heparan sulfate proteoglycans; and interstitial ECM in the interstitial space coming predominantly from fibroblasts which is made up of Collagen I (most abundant), Collagen III, fibronectin, hyaluronan and proteoglycans. The interstitial collagens are eventually cross-linked to form more stiff and thick structure by lysyl oxidase (LOX) enzyme family and tissue transglutaminase (TG2).

The enzyme family Matrix Metalloproteinases (MMPs), a family of endopeptidases produced by a variety of cells play a central role in the degradation of intact collagens without cross-linking, including secreted collagenases such as MMP1, MMP8, MMP13, MMP18 and transmembrane collagenases such as MMP14 with MMP1, MMP13, with MMP14 being the most pivotal ones among a total of 24 MMPs.

The tissue inhibitors of metalloproteinase (TIMPs) are the enzymes that inhibit MMPs; and they have four subtypes (TIMP1-TIMP4). TIMPs bind to MMPs in a 1:1 ratio and the resultant MMP-TIMP complexes are recognized and cleared out by macrophages. The importance of the balance between MMPs and TIMPs in fibrosis resolution has been intensively studied but no applicable advances have been made due to the discrepancy in results. For example, overexpression of Timp 1 drives the severity of liver fibrosis, which is easily conceivable. However, the knockout of Timp1 and Timp3 in mice show enhanced liver fibrosis progression. A clearer answer of targeting TIMPs and MMPs as organ fibrosis resolution strategy needs to be addressed with a considerable amount of research in the future.

LOX and its homologs, LOX-like enzymes (LOXL1–LOXL4) are copper-dependent enzymes that cross-link collagen by catalyzing aldehyde formation from lysine residues in collagen and elastin. Inhibition of LOXL2 results in attenuated fibrosis and reverts the fibrosis in a range of organs like heart, liver and lung. However, a recent clinical trial of humanized ani-LOXL2 mAb (simtuzumab) does not exhibit a benefit for progression-free survival in IPF patients.

TG2 is another enzyme which catalyzes the cross-linking of collagen by forming inter- and intramolecular bonds between lysine and glutamine residues of proteins. However, the effect of TG2 on collagen turnover is tissue-specific as suggested by TG2-null mice who developed aggravated fibrosis in lung but showed no improvement for liver fibrosis.

In addition to depending on collagenase for collagen degradation, macrophages and myofibroblasts participate in collagen turnover by internalizing intact collagen for degradation. For example, myofibroblasts internalize intact collagen through integrins α2β1 and α3β1, as well as the fibroblast-derived transmembrane urokinase plasminogen activator receptor–associated protein (uPARAP), and collagen is internalized and packaged into lysosomes for degradation. uPARAP knockout mice develop exacerbated lung fibrosis. Macrophages uptake fragmented collagen via the extracellular glycoprotein milk fat globule–epidermal growth factor 8 (MFGE8), and Mfge8 knockout mice also exhibit stronger fibrosis development.

Elimination of myofibroblasts can be achieved by re-directing the fate of myofibroblast to apoptosis, senescence, de-differentiation and reprogramming.

Under normal wound healing processes, myofibroblasts are funneled for apoptosis after their job is complete. The loss of myofibroblasts is majorly mediated by extrinsic apoptosis pathways, triggered by TNF-α and Fas ligand which are released by immune cells. However, myofibroblasts under fibrotic conditions often display enhanced apoptosis resistance, acquired by survival signaling (e.g. NF-κB) and overexpression of anti-apoptotic proteins (e.g. BCL-2). The apoptosis resistance is induced by TGF-β1 and endothelin-1 (ET-1), both of which also serve as activators of myofibroblast differentiation, with FAK and PI3K/AKT being the downstream pathway. Moreover, the stiff ECM in fibrotic conditions also drives myofibroblast resistance to apoptosis through a mechanotransduction pathway involving Rho/ROCK signaling and leads to

activation of the mechanosensitive transcription factor megakaryoblastic leukemia 1 (MKL1), which will upregulate expression of anti-apoptosis related proteins. Inhibition of ROCK by Fasudil or loss of Mkl1 protects mice from lung fibrosis.

Therapeutic strategies focusing to abolish apoptosis resistance of myofibroblast have attracted researchers' enthusiasm. This includes the development of an IκB kinase (IKK) inhibitor (sulfasalazine) targeting NF-κB signal pathway, a histone deacetylase (HDAC) inhibitor (suberoylanilide hydroxamic acid) targeting downregulating antiapoptotic protein BCL-XL as well as upregulating proapoptotic protein BAK, an inhibitor targeting to block the caspase inhibitor XIAP and a fungal toxin gliotoxin which showed efficacy in liver or lung fibrosis experimental models. One matricellular protein CCN5 reverts pre-established cardiac fibrosis in part by inducing myofibroblast apoptosis.

Senescence is triggered by a broad range of stimuli such as DNA damage, oncogene activation, oxidative stress, followed by activation of the p52/p21 and/or p16INK4a/pRb tumor suppressor and the growth arrest and the senescence-associated secretory phenotype (SASP) in final step. Senescent myofibroblasts are recognized as αSMA-positive cells, positive for senescence markers, including p21, p16INK4a, and senescence-associated β-galactosidase (SA-β-gal). The senescent myofibroblasts also display particular SASP features including upregulation of ECM-degrading enzymes such as MMPs and downregulation of collagen and TGF-β1 and are ultimately eliminated by NK cells, CD4+ T cells, and macrophages for immunological clearance. The p53 and p16INK4a-deficent mice exhibit aggravated fibrosis. A matrix protein CCN1 is required for myofibroblast senescence as shown in the investigation of CCN1 mutated or deficient mice which displayed impaired myofibroblast senescence and exacerbated fibrosis (J. I. Jun & Lau, 2010). In addition to CCN1, the cytokine IL-22 also induce myofibroblast senescence via p53

activation through a STAT3-dependent pathway, supported by ectopic expression of IL-22 in mice ameliorate CCl4-induced liver fibrosis.

Although senescence in myofibroblasts has an antifibrotic effect, whereas senescence in epithelial and/or endothelial cells has pro-fibrotic effect by inducing further damage and exacerbated inflammation.

Myofibroblasts can be de-differentiated to inactive, quiescent fibroblasts. The de-differentiation of myofibroblasts has been observed in liver HSCs, wherein re-expression of PPARγ, which is lost during HSC transformation to myofibroblasts, reverts HSC-derived myofibroblasts to quiescent cells in vitro, accompanied by downregulation of fibrogenic genes, including *ACTA2* (encoding αSMA), *COLIA1*, *COLIA2*, *TIMP1*, and *TGFBR1*. This also occurs to lipofibroblast-derived myofibroblasts in lung as depletion of PPARγ in lung fibroblasts induces a profibrotic phenotype reversion to quiescent cells.

A considerable number of targets have been examined to target de-differentiation of myofibroblasts for fibrosis regression, including BMP7 which antagonizes TGF-β1; FGF-1 which reverses the myofibroblast by downregulating αSMA expression; prostaglandin E2 (PGE2) which blocks TGF-β1 and ET-1 signaling and inhibit FAK activation. Application of these discoveries to *in vivo* treatment has not achieved expected accomplishments. For instance, administration of PGE2 or erythroid 2–related factor 2 (NRF2) fails to protect mice from fibrosis.

The spontaneous lineage reprogramming rarely occurs, if at all, but it is documented as a potential approach for fibrosis resolution.

1.3.3 Lung fibrosis

Pulmonary fibrosis is the scarring in the lung. The lung parenchymal tissue is replaced by connective tissue consisting of dense extracellular matrix with the subsequent outcomes of alveolar architecture destruction, gas exchange blockage, and, ultimately, respiratory failure and death.

Pulmonary fibrosis occurs in association with other diseases as a secondary effect. Pulmonary fibrosis is caused by infection, air pollution, medication, scleroderma, and interstitial lung diseases (Rockey et al., 2015). In most patients, pulmonary fibrosis appears without any known cause. Such kind of pulmonary fibrosis is diagnosed as Idiopathic Pulmonary Fibrosis (IPF). IPF is progressive without substantial inflammation. Due to a lack of known inducers, the pathogenesis of IPF is poorly understood.

IPF shares some common fibrotic features with other types of pulmonary fibrosis. Alveolar epithelial cell injury is often observed which causes the release of different types of cytokines and drives fibroblasts to transform into matrix-producing myofibroblasts. Myofibroblasts induce apoptosis of alveolar epithelial cells, which leads to further myofibroblast activation and expansion of injury and effector-cell activation cycling.

Genetic and epigenetic factors make the epithelium susceptible to micro-injury from the outsources such as tobacco smoking, inhaled dust, infections (Barratt, Creamer, Hayton, & Chaudhuri, 2018; King, Pardo, & Selman, 2011). The injured epithelium undergoes repair process, interrupted by repetitive injury, which leads to the damage of the basement membrane and alveolar capillary barrier. The capillary proteins influx into interstitial and alveolar spaces, initiating the coagulation cascade, and aberrant vascular remodeling. Cells like fibroblasts are recruited to the site, proliferate, and differentiate to myofibroblasts. At the same time, cytokines and growth factor levels escalate, including transforming growth factor β1, platelet-derived growth factor, vascular

endothelial growth factor, and fibroblast growth factor. With the expansion of myofibroblast population and the pro-fibrotic signaling, the ECM is extensively deposited, and the fibrosis starts progressing (Barratt et al., 2018; Richeldi, Collard, & Jones, 2017).

Multiple drugs have been examined for pulmonary fibrosis, especially for IPF. Interferon γ-1b performs well in preclinical studies but fails in clinical trials with no effect in human patients. Endothelin-receptor antagonists do not benefit for human patients. Currently, only two drugs are approved by the FDA for the treatment of pulmonary fibrosis. One is pirfenidone, an anti-inflammatory medicine that slows fibrosis progression by suppressing the inflammatory response, however, its detailed mechanism is not fully known. The other is nintedanib, a pan-growth factor inhibitor, also has efficacy in treating pulmonary fibrosis, but substantial side effects are reported due to its blockage of multi growth factors. Diarrhea is a common side effect associated with nintedanib, while photosensitivity rashes are observed with pirfenidone. Additional gastrointestinal side effects are documented with both drugs. Although both medications slow down IPF progression, they cannot terminate the process. With the exception of these drugs, the treatment options for IPF patients are limited. Other therapies, including pulmonary rehabilitation and oxygen therapy help to slow the worsening and improve patients' quality of life. When it reaches a severe stage, lung transplantation is needed for patient survival if a qualified donor is available. Overall, more than 5 million people are suffering from pulmonary fibrosis globally. Due to the lack of suitable detection methods, most patients are already at a late stage when they are diagnosed and therefore life span is pretty low, generally less than five years.

The diagnosis of IPF involves a multi-disciplinary examination, requiring exclusion of known causes of interstitial lung disease (ILD) and the confirmation of usual interstitial pneumonia

(UIP) pattern using high resolution computer tomography (HRCT) or surgical lung biopsy if necessary (Barratt et al., 2018; Meyer, 2017).

1.3.4 Fibroblasts and Myofibroblasts

Fibroblasts are the most common cells in connective tissue. They are large-sized, spindle-shaped cells with a flat and oval nucleus. They have abundant rough endoplasmic reticulum and a large Golgi apparatus.

Fibroblasts are originated from mesenchyme characterized by the expression of vimentin, a typical marker of mesodermal origin. Fibroblasts are heterogeneous groups of cells with a variety of functions. They can come from adipocytes, pericytes, endothelial and epithelial cells. Fibroblasts are transformed from epithelial cells through a process termed as epithelial-mesenchymal transition (EMT). On the other hand, fibroblasts may also become epithelial cells by a counter process referred to as mesenchymal-epithelial transition (MET), which is observed in development, tissue regeneration and tumor malignancy. Fibroblasts and fibrocytes are the same cells with different states. Fibroblasts are in activated states. Fibrocytes are in less active states. Fibrocytes are bone marrow-derived mesenchymal cells that differentiate to fibroblasts when entering tissues.

Fibroblasts are present in interstitial spaces of the organ. In the lung, the fibroblasts are commonly found near the epithelium and endothelium. Fibroblasts play a central part in maintaining tissue integrity. Fibroblasts are the primary producer of extracellular matrix including collagen type I, III and IV, fibronectin, laminins and proteoglycans, responsible for supporting tissue structure by acting as a scaffold for cells.

Fibroblasts are key mediators in tissue injury and repair. Fibroblasts are among the early players in initiating inflammation. When tissue injury occurs, fibroblasts migrate to the damaged

site and participate in the wound healing process. They stimulate chemokine synthesis then the immune cells come to the injury sites to clear the pathogens and dead cells. Later, fibroblasts transform into myofibroblasts, which gain enhanced extracellular matrix synthesis ability to replace the wounded tissue. However, if the ECM production is beyond control, the excessive ECM replaces the normal connective tissue and leads to organ fibrosis (Kendall & Feghali-Bostwick, 2014).

As the principal source of ECM, the myofibroblast is considered a critical player in fibrosis progression (Stempien-Otero, Kim, & Davis, 2016). The prominent feature of myofibroblast, which can be utilized as minimum requirement for defining a myofibroblast, is that the myofibroblast acquires high contraction. The myofibroblast differentiation/activation is divided into two phases: fibroblasts to proto-myofibroblasts and proto-myofibroblast (Hinz, 2016). Proto-myofibroblasts are activated fibroblasts that have acquired enhanced proliferation and migration but have not yet developed stress fiber with increased contractile ability. The myofibroblasts are fully differentiated myofibroblasts with SMA expression and promoted cell contraction. The proto-myofibroblast can be induced by mechanical force coming from the stiff ECM in fibrotic conditions, undergo complete maturation into myofibroblasts only when stimulated by TGF-β.

Various origins of myofibroblast have been identified (Hinz et al., 2007; Wynn, 2008). The first source of myofibroblasts is local resident fibroblasts and mesenchymal cells. Additionally, the myofibroblasts can come from epithelial cells via epithelial–mesenchymal transition (EMT) and endothelial cells via a similar process called endothelial–mesenchymal transition (EndMT). Moreover, pericytes which are mesenchymal cells in bone marrow can be recruited into tissue and give rise to myofibroblasts.

In some type of tissues, myofibroblasts are also derived from tissue specific precursor cells. For example, in liver fibrosis, the pericyte-like stellate cells contribute to the majority of the myofibroblasts.

Although myofibroblasts are transformed from different cell origins, it is currently a mystery as to whether myofibroblasts from different sources have different roles in fibrogenesis.

Regulators that suppresses myofibroblasts have been explored with intensive studies (Hinz, 2016).

The basic fibroblast growth factor (bFGF, FGF-2) is reported to inhibit myofibroblast development and expression of α-SMA via the blockage of TGF-β1 signaling. In addition, the FGF-2 augments fibroblasts proliferation. Together, FGF-2 engenders the wound healing without generating fibrotic contraction. Interferon (IFN)-γ produced by T cells suppresses α-SMA expression in fibroblasts via activating repressor protein YB-1, which impairs Smad3-mediated transcription of TGF-β1-induced genes. This exhibits anti-fibrotic effects in mouse models of different organs by diminishing inflammation, collagen deposition and tissue contraction. However, IFN-γ is also a pro-inflammatory cytokine recruiting macrophages. TGF-β3 is stated to suppress myofibroblast in cell culture experiments and animal models. But the role of TGF-β3 is under debate. It is especially questionable because it shares nearly 70% sequence similarity of TGF-β1 and the same receptors, although explanation has been given to tissue specific distribution. Interleukin IL-1(IL-1) inhibits TGF-β1-induced α-SMA expression, shown in cultured dermal fibroblasts with the addition of IL-1 proteins. Other myofibroblast suppressors include PPAR-γ ligands, insulin-like growth factor (IGF)

The studies focused on myofibroblast activation and the relevant mechanisms never lose the interests of researchers. The connective tissue growth factor (CTGF or CCN2) is one of the

most well-studied factors to promote myofibroblast next to TGF-β1. CCN2 level in serum is found elevated in fibrosis patients, and mutations in the *CCN2* gene are observed in human fibrosis patients. CCN2 enhances the profibrotic action of TGF-β1 in a manner independent from TGF-β1. CCN2 deficient mice show declined fibrotic traits with abolished myofibroblast activation, via a probable pathway of Ras/MEK/ERK/STAT3. CCN2 in fibrotic conditions seems to come from fibroblasts, myofibroblasts and epithelial cells. Platelet-derived growth factor (PDGF) is believed to be another myofibroblast activator, suggested by a study in an animal model of lung fibrosis treated with specific antibodies blocking the PDGF receptors α and β wherein the myofibroblast formation was impaired. The possible mechanisms underlying the effect of PDGF can be TGF-β1dependent or independent. The Wnt/β-catenin signaling, which is upregulated in liver, skin, lung, kidney, and cardiac fibrosis deserves more attention as a potential therapeutic target. It is activated by TGF-β1, and suppression of Wnt ameliorates ECM accumulation in fibrosis. Moreover, Wnt is also involved in the EMT process, inhibition of which stops the transition of epithelial cells to fibroblasts thus dampens the myofibroblast precursor pool. However, extra care needs to be taken when it comes to applying the approach to target Wnt due to multiple critical roles of Wnt in normal cells.

Hyaluronic acid (HA) manipulates myofibroblast activation and persistence by facilitating the interaction between the HA receptor CD44 and the TGF-β1 receptor, thus affecting the TGFβ1 pathway. Other factors which promote myofibroblast activation are transient receptor potential vanilloid (TRPV) membrane channels which enhances pro-fibrotic effects of TGF-β1 and promotes activation of Smad2 and mitogen-activated kinases; vascular endothelial growth factor (VEGF) by co-acting with TGF-β1; hepatocyte growth factor (HGF) and IGF by cooperating with

TGF-β2; thrombospondin-1 (TSP-1) by converting latent TGF-β1 to the active form, and tumor necrosis factor-α (TNF-α).

Myofibroblasts are the ultimate cause responsible for excessive synthesis, deposition and accumulation of extracellular matrix proteins, most notably fibrillar collagens. The mechanisms that help myofibroblasts to persist in fibrotic tissues remain enigmatic. Our investigation improves current knowledge of the pathobiological mechanisms promoting the progression of organ fibrosis, the understanding of which is crucial to provide cellular and molecular targets for novel therapies that not only prevent progressive tissue scarring but also restore lost tissue function. Our discovery also can be applied as a novel therapeutic strategy that is not only poised to halt fibrosis but also has the potential to reverse established fibrosis and regenerate chronically injured tissues.

Myofibroblasts were initially regarded as a terminal state for fibroblastic cells, however recent evidence suggests that the myofibroblast phenotype is plastic and reversible. How their fates are determined or shifted and how the underlying cellular and molecular mechanisms are regulated remains unclear. The mechanisms that promote their survival and persistence in fibrotic disorders are poorly understood.

Fibrosis can also regress in organs with lower regenerative capacity than the liver, such as the lungs.

Patients with SSc-associated ILD show improved pulmonary functions in some randomized controlled trials, suggesting that tissue regeneration or regression of pre-existing fibrosis occurs in lungs.

Glutamine depletion in HSCs exhibits a profound reduction in basal respiration and adenosine triphosphate production, more so than glucose deprivation, indicating the role of glutamine as a preferred energy source (Harvey & Chan, 2018).

Myofibroblasts are also identified in the stroma surrounding the tumor; in other words, tumor microenvironment, the crosstalk of which with tumor cells supports tumor growth and metastasis. The myofibroblasts in the tumor microenvironment are also recognized as cancer-associated fibroblasts. Similar to myofibroblasts in wound healing and tissue repair, they are characterized by the high load of stress fiber in the cytoplasm with strong contractile ability and neo-expression of SMA. The cancer-associated fibroblasts play a pivotal role in promoting tumor proliferation, migration and survival, and supporting tumor cells to escape immune surveillance and form new niches in metastatic sites via enhanced cell contraction, cytokine and growth factor secretion, ECM synthesis and ECM degradation.

The incorporation of ED-A splicing product of fibronectin into the matrix is indispensable for latent TGFβ activation and the incorporation of αSMA into stress fibers (Bochaton-Piallat, Gabbiani, & Hinz, 2016).

1.3.5 Collagen production

(1) Collagen

The most common and repeated-occurred motifs in the amino acid sequence of collagen are Gly-X-Y, where every third amino acid in the collagen sequence is glycine, X frequently represents Pro and Y position is occupied by hydroxyproline (HYP). Together, proline and its derivative hydroxyproline compose around 23% of the total amino acids in collagen, as the second abundant amino acid found in collagen. Proline alone makes up around 11% of collagen. The hydroxyproline is specific to collagen, and approximately 99.8% of hydroxyproline amino acids in the body are stored in collagen structure, enabling it to be used as a marker for the measurement of the amount of collagen (Albaugh, Mukherjee, & Barbul, 2017). Hydroxyproline is originated from the hydroxylation of the proline post-translationally by the prolyl hydroxylase. Not only as

one of the dominant constituents, proline and hydroxyproline are also essential for maintaining the structure of collagen, as their cyclic structure restrains the spatial rotation of collagen helix so that the strength of collagen structure is reserved.

Collagen is regulated tightly transcriptionally by a range of factors, among which TGF-β is of great importance (Ricard-Blum, Baffet, & Théret, 2018; Stempien-Otero et al., 2016). TGF-β has two transmembrane serine/threonine kinase receptors, type I (TGFβRI) and type II (TGF-βRII). TGF-β binds to TGF-βRII and initiates the recruitment of TGF-βRI, which sequentially triggers the phosphorylation and activation of TGF-βRI, accomplished by signal transduction to R-Smad proteins (Smad2 and Smad3). R-Smad proteins are phosphorylated and bind to CoSmad Smad4 to form a complex. The heterodimeric complex enters the nucleus, binds to DNA (with the assistance of other factors in some cases), and initiates the transcription of TGF-β-target genes. One of the R-Smad proteins, Smad3, appears to be involved extensively in fibrotic pathways. The Smad-binding element (SBE), also known as CAGA box, exists in proximity of collagen promoters, and Smad3 is identified to bind to *COL1A2*, *COL3A1*, *COL5A1*, *COL6A1* and *COL6A3* promoters. Distinctively, the *COL1A1* promoter contains a CC(GG)-rich element, not a typical SBE, which is recognized by zinc finger family transcription factor SP1 and the complex Smad2-Smad4. However, surprisingly, in renal and liver fibrosis, the deletion of Smad2 does not reduce collagen expression, and its overexpression decreases collagen expression induced by TGF-β. A possible explanation is that Smads2 counteracts Smad3 on collagen production. Consistent with Smad3's role as a pro-fibrotic player, Smad2 knockout mice exhibit slow progression of fibrosis. The transcriptional factors which assist Smad-mediated TGF-β regulation include SP1, AP1 and the complex p300/CBP. NF-κB is also reported to promote fibrosis progression by facilitating TGF-β1-induced activation of fibroblasts. In addition to the classical Smad-mediated pathway,

TGF-β1 also activates non-Smad pathways, including mitogen-activated protein kinase (MAPK) such as p38 and Jun N-terminal kinase (JNK), Rho-like GTPase, and phosphatidylinositol-3-kinase PI3K/Akt pathways, some of which can also be activated by other cytokines or ECM. Other pro-fibrotic factors that regulate collagen expression include type 2 cytokines, such as interleukin-4 (IL-4) and interleukin-13 (IL-13). IL-4 and IL-13 are noted to regulate collagen I expression in human fibroblasts. Moreover, IL-13 enhances TGF-β expression in macrophage, which amplifies the signal cascades of fibrogenesis.

Furthermore, it is understood that some pro-inflammatory cytokines act as anti-fibrotic players, as exemplified by IL-1β which hampers TGF-β1-induced myofibroblast activation and collagen synthesis in dermal and lung fibroblasts; interferon gamma (IFN-γ) which abolishes COL1A2 and COL1A1 expression via interfering Y box-binding protein YB-1 with an IFN-γ response element; tumor necrosis alpha (TNF-α) which also impairs the expression of collagens by blocking the transcriptional coactivators of TGF-β target genes such as *COL1A2* via Jun/AP1 or NF-κB pathways. The IFN-γ induced JAK/STAT1 signal pathway antagonizes the TGF-β1 induced Smad pathway for COL1A2 expression via blockage of p300/Smad3 transcriptional coactivators, and the upregulation of Smad7, an inhibitor of R-Smads.

Collagen contains 30 members, all of which are characterized by triple helix structure made up of three α-chains, either identical (homotrimers) as in collagens type II, III, VII, VIII, X and others, or partially or completely (heterotrimers) as in collagen types I, IV, V, VI, IX, and XI (Gordon & Hahn, 2010). Collagen can be divided into two main categories, Fibrillar (Type I, II, III, V, XI) and Non-fibrillar which can be further distinguished and divided into several subfamilies, one of which is microfibrillar type VI collagen, the predominant component in the basement membrane. Fibrillar collagens are named so because their collagen monomers are

capable of assembling into highly orientated and arranged supramolecular structures, the so-called "fibril", featured by banding patterns of approximately 70nm periodically (Gelse, Pöschl, & Aigner, 2003).

Collagens synthesis starts with the transcription of the gene into alpha peptides. These alpha peptides go directly into the endoplasmic reticulum for post-translational processing where hydroxylation of lysines and prolines by the enzymes “prolyl hydroxylase” and “lysyl hydroxylase", respectively occurs, initiating the assembly of the three α-chains into trimeric procollagen. The procollagen enters the Golgi compartment and is packaged into secretory vesicles for its release into the extracellular space. Followed by secretion, the peptides on C and N terminals are removed by the membrane-embedded enzymes known as collagen peptidases, the procollagen N-proteinase and C-proteinase.

The fibrillar collagen types spontaneously aggregate into five-stranded fibrillar structures and further highly ordered larger fibrils (Gelse et al., 2003).

(2) proline-regulated collagen synthesis

Collagen is the most abundant protein in mammals, accounting for one-third of total protein. It is the major component of ECM in connective tissue in diverse organs such as skin, bone and blood and serves as the supporting structure. The vast majority (over 90%) of the collagen in the human body is type I collagen.

Proline comprises 10% of the total amino acid content in collagen. Proline is an indispensable constituent for the biosynthesis of collagen, and its availability is essential for collagen-associated physiologic activities like wound healing and tissue repair. Proline analogs which compete for proline, suppress collagen synthesis. The proline pool in body is replenished through de novo synthesis in cells and exogenous supply from the diet.

Proline is synthesized from arginine, glutamine and glutamate. The glutamate and glutamate-convertible glutamine are considered as the predominant sources for proline biosynthesis, with glutamine being the most abundant amino acid in the body, accounting for 20% of total free amino acids in blood circulation and 60% of the intracellular free amino acids. Glutamate is catalyzed by 1-pyrroline-5-carboxylate synthase (P5C synthase) to form 1-pyrroline-5-carboxylate (P5C), which is the essential amino acid connecting the citric acid cycle and urea cycle and, as such, is transformable to a variety of amino acids involved in citric acid and urea cycles. P5C is converted to proline by P5C reductase in the presence of NADPH.

Although glutamate is thought to be the common source of proline, investigations state that the increase in arginine (Arg) and arginine-derived ornithine (Orn) supplementation are the most effective in increasing collagen deposition. Arg is converted to Orn through the final step in the urea cycle by enzyme arginase, irreversibly. Orn is transformed to P5C by ornithine aminotransferase (OAT), which is a reversible reaction depending on the availability of substrate and products, with the reaction favoring the direction of the side with a low concentration. The biosynthesis of proline from arginine is more energetically efficient than from glutamate (Karna, Szoka, Huynh, & Palka, 2019). The synthesis of Pro from Arg consumes 2.5mol ATPs per mol product, while it requires 8 mol of ATPs to produce one mole of Pro. In terms of energy cost, arginase is widely spread in the animal kingdom for proline production. Cancer cells that exhaust Glu for energy purpose upregulate the arginine transporter, enhancing the intracellular arginine level, which acts as a critical precursor for proline synthesis to support cell growth and protein synthesis. Animals fed an Arg-deficient diet are subjected to the trauma of dorsal skin scratch, and supplementation of Arg does not influence the epithelialization of an artificial skin defect, underlining that Arg is involved in collagen deposition in wound healing (Barbul, 2008). In the

last phase of wound healing, the Arg is below detectable levels due to the active incorporation of Pro derived from Arg into collagen.

Arginine, glutamate, and glutamine are used as precursors for proline synthesis in a species- and cell-specific manner (Albaugh et al., 2017). All animals can produce proline from arginine with the aids of arginase (arginase I and arginase II), ornithine aminotransferase and P5C reductase, but the velocity varies among species. Various tissues including the small intestine, liver and kidney actively convert arginine to proline, albeit the synthesis is not high enough to satisfy the requirements of growth and tissue repair in the young or stressed adults. Proline conversion from glutamine and glutamate occurs in most mammals such as pigs, cattle and sheep via P5C synthase pathway. In contrast, the usage of glutamine or glutamate is not likely to happen in birds, cats, ferrets and many species of fish due to the lack of P5C synthase.

In the case of wound healing, the Pro level in wound fluid is more than 50% higher than in plasma, indicating a prerequisite of Pro in wound healing (Barbul, 2008). Additional supplementation of Pro in the diet does not result in increased collagen synthesis, albeit Pro availability is enhanced, suggesting that de novo synthesis of Pro is necessary due to possible metabolic disposal of Pro provided in supply. Additional supplementation of other citric cycle metabolites such as Gln, as Pro precursor, does not promote collagen synthesis in wound either, (Albaugh et al., 2017) whereas provision of Arg leads to a significant enhancement of collagen synthesis in the wound. This suggests that the Arg, rather than Glu is the primary source of Pro biosynthesis in wound repair.

(3) Arginine conversion to proline by Arginase

In the wound region, higher arginase activity is observed, associated with its role in converting arginine to proline for collagen synthesis.

Arginase comprises two isoenzymes, Arginase-1 and Arginase-2, which are encoded by distinct genes localized on different chromosomes (Caldwell, Rodriguez, Toque, Narayanan, & Caldwell, 2018). The two isoforms vary in many ways. Arginase-1 exists in the cytoplasm and is found predominantly in the liver. Arginase-2 is present in mitochondrial and mainly found in extrahepatic tissues such as the kidney. In airways, both Arginase-1 and Arginase-2 are identified in epithelial cells, endothelial cells, fibroblasts, myofibroblasts and alveolar macrophages. Nevertheless, both isoforms catalyze the same reaction converting arginine to ornithine, the last step in the urea cycle. The importance of Arginase-1 for collagen synthesis has been addressed in lung fibroblasts (Kitowska et al., 2008). Arginase-1 expression is strongly increased by TGF-β signaling during lung fibrosis process. Numerous investigations show that arginases play a vital role in fibrosis progression by converting arginine to proline, the building blocks of collagen (Maarsingh, Pera, & Meurs, 2008).

1.3.6 Integrin αvβ3

The integrins are a superfamily of transmembrane proteins. They are primary cell adhesion receptors that bind to the extracellular matrix and cell-surface ligands. They act as critical mediators in cell-matrix and cell-cell signal transduction and adhesion interactions. The integrin family transduces both inside-out signaling and outside-in signaling (Takada, Ye, & Simon, 2007).

Integrins are heterodimers. Each member of integrins is composed of two subunits: α subunit and β subunit. There are 18 α subunits and 8 β subunits in mammals. Around 25 integrin heterodimers are currently known, generated by the different combinations of α and β subunits. The amino acid sequence Arginine-Glycine-Aspartic acid is found in the interaction site of many extracellular matrix proteins, termed as a conserved integrin-binding motif (Horton, 1997). After integrins activation through ligand binding, the assembly of focal adhesion complex occurs,

followed by oligomerization and trans-autophosphorylation of tyrosine kinase FAK. The phosphorylated FAK binds Src family kinase such as Src and Fyn, through their SH2 domain. Subsequently, the Src family kinases phosphorylate FAK-associated proteins including paxillin. Phosphorylated FAK can bind with and activate PI3K, inducing intracellular proliferation and survival signaling. One of the common proliferation pathways stimulated by integrins such as αvβ3 is RAS-ERK signaling with Shc being an adaptor protein. Integrin, incorporation with growth factors, promotes RAS-MAK activation. Especially, integrin αvβ3 is known to be directly associated with the signaling of insulin and insulin-like growth factor receptors. While αvβ3 binding to its substrate, insulin receptor substrate (IRS)-1 can also interact with αvβ3. As a result, the insulin signaling is enhanced. The PDGF pathway can also be enhanced by αvβ3. Another essential role of integrins is the mediation of cell survival signaling. Cell adhesion is often required for the continued survival of cells. The interaction between the extracellular matrix and integrins provides a constitutive survival signal to cells via the PI3K-AKT pathway. The integrin family also regulates cell cycle, cell migration and cell transformation (Kumar, 1998).

Among all the members of integrin, the αvβ3, which is also known as vitronectin receptor, has been described to play a vital role in certain pathologies such as angiogenesis and cancer malignancy. It is expressed in platelets, osteoclasts, megakaryocytes, endothelium and vascular smooth muscles. Other pairs of αv integrin are more widely present in normal tissues. Besides vitronectin, αvβ3 interacts with many other extracellular proteins including fibronectin and fibrinogen. Integrin αvβ3 uses the classical RGD motif for recognition. However, some RGD proteins like collagen and laminin need to undergo conformational change before they can be bound by αvβ3. The interaction between integrin αvβ3 and extracellular matrix molecules is documented to be involved in the inflammatory response, tissue repair and remodeling, and bone

resorption. The evidence also indicates the role of αvβ3 in regulating cell proliferation, differentiation, migration and apoptosis. The integrin is intensively studied as a therapeutic target since upregulation of αvβ3 is found in disease conditions especially angiogenesis during tumor progression and bone diseases such as osteoporosis and bond metastasis. However, unexpectedly, β3 integrin knockout mice display marked increases in angiogenesis (Reynolds et al., 2002), tumor growth (Reynolds et al., 2002; Robinson, Reynolds, Wyder, Hicklin, & Hodivala-Dilke, 2004), elevated fibrosis (Friman et al., 2012), lung inflammation(Weng et al., 2003) and wound healing responses (Weis & Cheresh, 2011), probably due to compensatory effect of increased VEGFR2. Inhibition of αvβ3 through Cilengitide, a specific αvβ3(αvβ5) inhibitor, aggravates liver fibrosis (Patsenker et al., 2009).

1.4 Tumor microenvironment

1.4.1 Tumor microenvironment components

Cancer is still the leading cause of death globally irrespective of tremendous advances associated with treatment strategies and even the therapeutic paradigm due to myriad elucidations of the mechanisms in tumorigenesis, tumor progression and malignancy. The tumor microenvironment has drawn a growing body of attention in recent years as it is more and more recognized in fostering cancer, which brings a new insight into the therapeutic targets for cancer (Balkwill, Capasso, & Hagemann, 2012).

The tumor microenvironment is used to describe the stroma surrounding tumor cells, which are highly susceptible to be affected by tumor cells, and their communication with tumor cells and cells outside, in turn, manipulates tumor cells in a tumor-favoring manner which results in tumor growth and metastasis. Notably, the tumor microenvironment is critically involved in tumor progression. The tumor microenvironments consist of the vasculature (the newly formed, leaking,

angiogenic blood vessels wrapped by endothelial cells and pericytes), immune cells (including macrophage, lymphocytes, myeloid-derived suppressor cells), cancer-associated fibroblasts and extracellular matrix (Hirata & Sahai, 2017; Wu & Dai, 2017). All the components together compose the "soil" for the development of the tumor "seeds", notably the metastatic sites, which means the stromal cells form a favorable environment for tumor cells by the expansion of local resident cells or recruitment to prepare for the tumor metastasis.

Cancer-associated fibroblasts account for the largest population in the tumor microenvironment. Macrophages in the tumor microenvironment are termed as tumor-associated macrophages (TAMs), due to its tumor-supporting role in modulating the immune system in tumor stroma. TAMs are the most abundant immune cells in the tumor microenvironment. TAMs are activated by tumor cells, and they, in turn, promote epithelial-to-mesenchymal transition in tumor cell which is an indispensable process for tumor invasion. Cytotoxic T lymphocytes are the prominent warriors against tumor cells. However, their function is interfered by the tumor cells and other stromal cells. Tumor cells take advantage of the regulatory T cells and the myeloid-derived suppressor cells (MDSCs) to suppress immune attack. To satisfy the nutrition and oxygen demands along with the super expansion of tumor growth, the tumor cells use angiogenesis as a strategy, which promotes de novo formation of blood vessels. The tumor cells send out a message by secreting vascular endothelial growth factor A (VEGFA), then the endothelial cells in adjacent places migrate into the tumor microenvironments by beaching the surrounding ECM structure, and quickly proliferate and form angiogenic vessel sprouts. In addition, the endothelial cells secrete platelet-derived growth factor β (PDGFβ) to recruit pericytes from bone marrow to construct an outer layer for newly formed vessels and maintain endothelial cell survival and vessel stabilization. Moreover, the ECM structure, which comprises collagens, fibronectins and laminins, provides a

ground physically for tumor cell growth and avoids the anoikis caused by loss of contact with the basement membrane. Moreover, the ECM structure is concentrated with growth factors and cytokines within the microenvironment to support tumor growths and also acts as a barrier against attacks on tumor cells or therapeutic drug accessibility. Overall, the tumor microenvironment serves as fundamental support for tumor progression and, without doubt, is worth elucidation more extensively and delicately.

1.4.2 Cancer-associated fibroblasts

CAFs contribute to tumor cell growth by directly interacting with tumor cells and modulate the tumor microenvironment favoring tumor cell growth and survival by communicating with other stromal cells via signal cytokine, chemokines and growth factors secreted (Tao, Huang, Song, Chen, & Chen, 2017). CAFs are ascribed to ECM deposition by their considerable production of collagen and the remodeling of ECM by secretion of MMPs, which potentiates tumor cell migration and invasion.

CAFs are the most abundant stromal cell type among all the cell populations in the tumor microenvironment. CAFs are a heterogeneous population, originating from different cell types. As such, they manifest controversial roles for tumors as either tumor-promoting or tumor-suppressive reported in various investigations.

The fibroblasts in normal tissue are spindle-shaped mesenchymal cells that exist in interstitial space and are capable of collagen production. They can be activated in a given context under different situations such as wound healing and cancer. The activated fibroblasts in the tumor environment are so-called cancer-associated fibroblasts (CAFs). CAFs are usually larger in size than quiescent fibroblasts. They possess multi-branches of cytoplasm, more rough endoplasmic reticulum and free ribosomes. CAFs contain enhanced Golgi complex and stress fiber in the

cytoplasm and they have increased proliferation and migration capacity. They are characterized by the expression of α-SMA and enhanced ECM synthesis ability.

The CAFs are active producers of ECM components, including collagens of different subtypes, hyaluronan, fibronectins and laminins. The ECM deposition by CAFs forms a physical barrier to protect tumor cells against immune infiltration or drug access and also provides a structural platform enabling interaction between cells. Conversely, CAFs also control the ECM turnover by secreting EMC-degraded MMPs, which makes openings for tumor cell migration and allows the cytokine and chemokines accessible to adjacent normal tissue for educating them to serve for the pro-tumor purpose. CAFs are also a manipulator by producing a vast variety of cytokines, chemokines and growth factors, such as transforming growth factor-β (TGFβ), interleukin-6 (IL-6) and CC-chemokine ligand 2 (CCL2)

The origin of CAFs is complex, which encompasses six well-studied sources. The most common source of CAFs is the resident fibroblasts in tissue, which are activated by cytokines released by adjacent tumor cells. The resident fibroblast type varies in a given organ context, for instance, HSCs are the precursor cells for CAFs in liver tissue. Despite local sources, fibrocytes and mesenchymal stem cells in bone marrow can be attracted to tumor regions and turned into CAFs. Moreover, the epithelial cells and endothelial cells can contribute to the CAFs pool by undergoing EMT and EndMT, respectively. Other sources like adipocytes, pericytes and smooth muscle cells can also transdifferentiate into CAFs, albeit in rare cases. The heterogeneity of CAFs makes it hard to seek universal markers to identify CAFs. The recognized markers for CAFs are divergent, α-SMA, FAP, S100A4 and platelet-derived growth factor receptor-β (PDGFRβ), none of which is specifically expressed in CAFs. The preferred expression pattern of markers depends on the specific tumor environment.

Quiescent normal fibroblasts possess anti-tumor effects but can be reprogramed by factors released by tumor cells or stromal cells and tumor microenvironment stimuli such as hypoxia and oxidative stress. The most potent inducing factors include TGFβ, PDGF and IL-6. The exosomes secreted by tumor cells or stromal cells are capable of delivering growth factors and cytokines for CAFs activation. Epigenetic modulation is another approach to trigger fibroblast differentiation to CAFs.

CAFs are essential for tumor progression in many prospects. CAFs produce pro-angiogenic factors, such as VEGFA, PDGFC, FGF2, osteopontin and secreted frizzled-related protein 2 (SFRP2) to promote angiogenesis. CAFs drive the tumor cells to undergo EMT for enhancement of the invasive ability of tumor cells. To modulate the immune response, CAFs recruit monocytes from bone marrow and trigger macrophage polarization to M2 subtype, which is the type that suppresses inflammation and protects tumor cells from escaping immune surveillance, by secreting SDF1 and CXCL14. The TAMs with an M2 characteristic, in turn, enhance CAFs' capacity by inducing CAF activation. Additionally, CAFs release IL-6 and IL-8 to initiate the differentiation of MDSCs from tumor-infiltrated myeloid cells, featured by upregulated expression of S100A8 and S100A9. The MDSCs exhibit immunosuppressive power. CAFs can induce antigen-mediated activation-induced cell death (AICD) of the anti-tumor cytotoxic T lymphocytes (CTLs), contributing to tumor immune surveillance escape. Moreover, CAFs dampen the function of $CD8^+$ cytotoxic T cells by secreting plentiful FAS ligands which induce apoptosis of Fas-positive $CD8^+$ cytotoxic T cells, and by enhanced expression of programmed cell death ligand 2 (PD-L2) which silences the cytotoxic T cells via interaction between PD-L2 and the immune checkpoint protein PD-1 on T cells' surface. Besides, CAFs produce large quantities of TGFβ, which is a predominant immunosuppressive factor.

2 Extracellular PKM2 Facilitates Lung Fibrosis Progression

2.1 Abstract

Lung fibrosis is characterized by excessive deposition of the extracellular matrix, most notably fibrillar collagens. Myofibroblasts are the primary collagen-producing cells. Their resistance to turnover and elevated capacity for collagen synthesis play important roles in lung fibrosis development and progression, mechanisms of which are not fully understood. Here we report that the extracellular PKM2 facilitates progression of lung fibrosis by protecting myofibroblasts from apoptosis. Extracellular PKM2 upregulates Arginase-1 expression in myofibroblasts therefore facilitates proline production and subsequent collagen synthesis. Extracellular PKM2 interacts with integrin αvβ3 on myofibroblasts. Interaction of PKM2 with integrin αvβ3 activates FAK-PI3K-NF-κB survival pathway to prevent myofibroblasts from apoptosis. On the other hand, the interaction activates FAK-PI3K-PTEN to upregulate Arginase-1 in myofibroblasts. Our studies reveal a novel and crucial mechanism for lung fibrosis progression. More importantly, neutralization of PKM2 with the antibody attenuates lung fibrosis progression, suggesting a new therapeutic target for the treatment of lung fibrosis.

2.2 Introduction

Lung fibrosis is a progressive respiratory disorder that is characterized by excessive accumulation of extracellular matrix (ECM), especially collagens. Lung fibrosis affects more than 150,000 patients annually in the USA and over 5 million worldwide (Rangarajan et al., 2018). The fibrosis is triggered by continuous injury or chronic insults. The initial fibrogenic response attempts to repair injured tissue through replacing damaged tissue by newly synthesized ECM. However, it becomes dysregulated during fibrosis progression, which results in excessive amplification of profibrotic signals and massive accumulation of ECM. The ECM is predominantly

produced by activated fibroblasts, termed as myofibroblasts. Myofibroblasts are distinguished by the expression of α-Smooth Muscle Actin (α-SMA) and elevated contractile capacity. The persistence of myofibroblasts is one hallmark of lung fibrosis (Konigshoff et al., 2009). Notably, their persistence is associated with the acquisition of apoptosis resistance, an event that perpetuates fibrogenesis (Rangarajan et al., 2018). However, the mechanisms how myofibroblasts acquire apoptosis resistance have not been fully discovered.

Additionally, metabolism alteration in myofibroblasts has drawn increasing interest among researchers recently. Metabolic reprogramming is required for myofibroblast contractility and differentiation (Bernard et al., 2015). The augmented collagen synthesis of myofibroblasts is also associated with metabolism reprogramming (Ge et al., 2018; Hamanaka et al., 2019). Due to the unique amino acid composition of collagen, the rate of collagen synthesis greatly relies on the availability of two most abundant amino acids in collagen: glycine and proline. Proline-dependent regulation of collagen metabolism draws lots of attention recently (Karna, Szoka, Huynh, & Palka, 2019). Proline is mainly synthesized in cells by arginine – ornithine, catalyzing by arginase, and subsequent to proline or polyamine. Therefore, the arginase is the key enzyme during proline biosynthesis. The involvement of arginase in lung fibrosis has been described lately (Caldwell, Rodriguez, Toque, Narayanan, & Caldwell, 2018; Kitowska et al., 2008; Maarsingh, Pera, & Meurs, 2008).

Pyruvate kinase is an enzyme that catalyzes the last reaction in glycolysis. There are four isoforms of pyruvate kinases, L/R and M1/M2, which are expressed in different tissue types or under different physiological conditions. PKM2 can form a homodimer or a homotetramer. The tetramer is active as a pyruvate kinase (Elbers et al., 1991; Hacker et al., 1998), while the dimer is a protein kinase (Gao et al., 2013; Gao et al., 2012; Yang et al., 2012). Interestingly, a number of

recent studies show that PKM2 is functionally involved in multiple cellular processes, including metabolism control, transcription regulation, and chromatin packaging (Gao et al., 2012; Luo et al., 2011; Yang et al., 2011). High serum levels of PKM2 have long been observed in patients with various inflammation diseases (Hathurusinghe et al., 2007; Jeffery et al., 2009; Staib et al., 2006), indicating a potential association of extracellular PKM2 with inflammation responses. Notably, our previous studies demonstrated that the PKM2 released by cancer cells and neutrophils promoted tumor angiogenesis (Li et al., 2014) and wound repair (Zhang et al., 2016). The above evidence suggests a role of extracellular PKM2 in tissue injury repair and regeneration. In this report, we present evidence to show that the extracellular PKM2 is present in high levels in lungs of patients with lung fibrosis. Extracellular PKM2 facilitates fibrosis progression by protecting myofibroblast from apoptosis. Extracellular PKM2 also facilitates fibrosis progression by upregulating Arginase-1 (Arg-1) in myofibroblasts, which consequently promotes proline synthesis in myofibroblasts. PKM2 acts on myofibroblasts by interacting with integrin αvβ3 and subsequently activating the integrin αvβ3-FAK-PI3K signaling. Extracellular PKM2 activates integrin αvβ3-FAK-PI3K-NF- κ B survival signaling to promotes myofibroblast survival. Extracellular PKM2 activates integrin αvβ3-FAK-PI3K-PTEN signal to upregulate Arg-1 expression. Neutralization of extracellular PKM2 by an anti-PKM2 antibody attenuates lung fibrosis, providing a potential therapeutic strategy for lung fibrosis treatment.

2.3 Results

2.3.1 Extracellular PKM2 facilitates lung fibrosis progression

To investigate whether there is a correlation between extracellular PKM2 and lung fibrosis, we performed immune-histological analyses using tissue samples from human pulmonary fibrosis patients. Surprisingly, high levels of extracellular PKM2 were detected in patient lung tissues

whereas they were barely observed in the normal lung tissues (Fig. 2.1 A & B). Our results reveal a potential fibrosis-promoting function of extracellular PKM2 in lung fibrosis. To test the speculation, we used a well-established mouse model of lung fibrosis induced by bleomycin. Bacterially expressed PKM2 (rPKM2), PKM1 (rPKM1), or vehicle was added into the fibrosis induction 2.5 weeks after the first dose of bleomycin (Fig. 2.2 A). Gross examination of mouse indicated that the addition of rPKM2 led to more fibrosis features on the lung surface (Fig. 2.2 C), reduced body weight (Fig. 2.2 B) and increased lung weight (Fig. 2.2 D), compared to the rPKM1 treated group. The increase in lung weights implies enhanced collagen accumulation after rPKM2 addition. Sirius red staining of the lung sections and hydroxyproline assay demonstrated more and thicker collagen accumulation in the lungs of rPKM2-treated mice (Fig. 2.2 E, F & G). Additionally, IHC staining of α-SMA indicated that the addition of rPKM2 led to an increase in α-SMA positive myofibroblasts in fibrotic lungs (Fig. 2.2 F & H). These results suggest that the addition of rPKM2 into bleomycin exacerbates lung fibrosis progression. Then we asked whether administration of rPKM2 alone can induce lung fibrosis. To address this question, a group of mice was only treated by rPKM2 without bleomycin (Fig. 2.2 A). Clearly, administration of rPKM2 alone did not induce lung fibrosis (Fig. 2.2 B-H), suggesting that extracellular PKM2 could not initiate lung fibrosis.

2.3.2 Extracellular PKM2 protects myofibroblasts from apoptosis

How does extracellular PKM2 facilitate lung fibrosis progression? Fibroblasts are activated to myofibroblasts during fibrosis progression. Sustained activation and resistance to apoptosis of myofibroblasts lead to organ fibrosis progression (Bataller and Brenner, 2005; Yin et al., 2013). Since the extracellular PKM2 could not initiate lung fibrosis, we questioned whether extracellular PKM2 exerted its effects on myofibroblast turnover. To test this conjecture, we carried out

immunofluorescence (IF) staining using tissue sections from lungs of mice treated with bleomycin with or without addition of rPKM2. Evidently, with addition of rPKM2, significantly more lung myofibroblasts (α-SMA positive) were present (Fig. 2. 3 A & B). Co-staining with an apoptosis TUNEL kit indicated that addition of rPKM2 to the fibrosis induction resulted in less apoptosis of α-SMA positive myofibroblasts (Fig. 2.3 A & B). The results suggest that extracellular PKM2 may play a role in preventing myofibroblasts from apoptosis.

To verify the role of extracellular PKM2 in myofibroblast apoptosis protection, we employed normal human lung fibroblast (NHLF). To study the effects of extracellular PKM2 on myofibroblasts, we induced NHLFs to myofibroblasts by stimulating NHLFs with TGF-β. Hereafter, the NHLF-derived myofibroblasts refer to the NHLFs treated by TGF-β. Treatment of NHLF-derived myofibroblasts with Fas ligand and Cycloheximide (CHX) induced cell apoptosis. Addition of rPKM2 but not rPKM1 into culture medium protected NHLF-derived myofibroblasts from apoptosis induced by FasL + CHX, as evidenced by cell counting (Fig. 2.4 A & B) and Annexin V/PI FACS assays (Fig. 2.4 C & D). Furthermore, the addition of rPKM2 into culture medium resulted in a decrease in cleaved PARP and increases in BCL2 and cIAP1 in the cells (Fig. 2.4 E). Additionally, rPKM2 treatment restored the reduction of ATP level induced by Fas + CHX by more than 60% (Fig. 2.4 F), indicating that rPKM2 treatment reduced apoptotic rate in myofibroblasts.

2.3.3 Extracellular PKM2 upregulates Arginase-1 in myofibroblasts to promote proline synthesis

A hallmark of lung fibrosis is synthesis and secretion of excessive amounts of collagen by myofibroblasts. We asked whether extracellular PKM2 affected collagen synthesis and secretion in myofibroblasts. Thereby, we examined the collagen expression level in rPKM2-treated

myofibroblasts and found myofibroblasts expressed much higher levels of collagen after rPKM2 treatment compared with rPKM1 treatment (Fig. 2.5 A). Measurement of collagen in the culture medium showed that addition of rPKM2 into cell culture increased collagen secretion (Fig. 2.5 B & C). However, RT-qPCR analyses revealed that rPKM2 did not upregulate the collagen 1A mRNA in NHLF (Fig. 2.5 D), indicating that PKM2 did not regulate collagen expression at transcriptional level. Therefore, rPKM2 likely promoted collagen synthesis after mRNA synthesis in the cells. Due to unique amino acids composition, myofibroblasts must rapidly turn on glycine and proline production for rapid collagen synthesis. We measured the free amino acids in myofibroblasts treated by rPKM2 and observed a marked increase in proline level, accompanied by a dramatic reduction in arginine level (Fig. 2.5 E). Proline is mainly synthesized in cells by arginine – ornithine, catalyzing by arginase, and subsequent to proline or polyamine. We therefore quantified ornithine in NHLF-derived myofibroblasts upon rPKM2 treatment. Clearly, rPKM2 increased ornithine level (Fig 2.5. F). The decrease in arginine and increases in ornithine and proline suggest that rPKM2 might regulate the arginine metabolism enzyme, arginase. The myofibroblasts treated with rPKM2 displayed a higher level of arginase activity (Fig. 2.5 G). Furthermore, the uses of the arginase inhibitor (NOHA) and arginine-depleted medium abolished the collagen-promoting effects of PKM2 in myofibroblasts (Fig. 2.5 I & J), indicating PKM2 upregulated collagen producing by increasing arginase. There are two isoforms of arginase, Arginase-1 and Arginase-2. Arginase-1 is reported to be expressed and functionally important for collagen deposition in lung fibroblasts upon TGF-β induction (Kitowska, Zakrzewicz et al. 2008). Therefore, we analyzed the mRNA and protein levels of Arginase-1 after rPKM2 addition by RT-qPCR and immunoblots respectively. The results revealed that rPKM2 treatment increased Arginase-1 mRNA and protein levels in myofibroblasts (Fig. 2.5 A & H). Thus, our results suggest

that extracellular PKM2 facilitates collagen synthesis and secretion by upregulating Arginase-1 in myofibroblasts therefore increasing proline synthesis from arginine.

To verify that extracellular PKM2 upregulates Arginase-1 in myofibroblasts, we probed the expression of Arginase-1 in the lungs of mice that were treated with bleomycin with or without addition of rPKM2. Evidently, rPKM2 increased Arginase-1 and α-SMA co-staining in the fibrotic lungs (Fig 2.6. A & B). The proline level in lungs of rPKM2-treated mice was elevated and the arginine level was significantly diminished compared to rPKM1-treated mice (Fig 2.6. C). Therefore, our results show that extracellular PKM2 upregulates Arginase-1 in myofibroblasts during fibrosis progression to facilitate proline and subsequent collagen synthesis and secretion.

2.3.4 Extracellular PKM2 interacts with and activates integrin αvβ3

An open question was what would be the cell surface receptor(s) that mediated the effects of extracellular PKM2 on myofibroblasts. The αvβ3 integrin is reported to mediate the signaling from the extracellular matrix and ligands outside of cells (Fiore et al., 2018; Jun & Lau, 2018; Sarrazy et al., 2014). Immunoblot assay demonstrated NHLF-derived myofibroblasts expressed high levels of αv and β3 (Fig. 2.7 A). The rPKM2 and integrin αvβ3 interaction was further verified by cell attachment assay using culture plates coated with rPKM2. The NHLF-derived myofibroblasts which expressed high levels of αvβ3 attached strongly to the rPKM2 coated plates (Fig. 2.7 B & C). Furthermore, the attachment was completely blocked by LM609, an antibody that recognizes integrin αvβ3 and blocks integrin activation (Fig. 2.7 B & C). Additionally, the interaction of PKM2 with integrin αvβ3 was verified by co-immunoprecipitation of rPKM2 with β3 in cell extracts prepared from rPKM2-treated myofibroblasts (Fig. 2.7 D).

2.3.5 Extracellular PKM2 activates integrin αvβ3-FAK-PI3K signaling axis in myofibroblasts

Upon the binding of PKM2 to αvβ3, what are downstream signal transduction pathways? Since it is well established that activation of integrin signaling leads to activation of FAK and subsequent downstream PI3K (Wegener and Campbell, 2008), we reasoned whether the effects of extracellular PKM2 in myofibroblasts was mediated through activation of FAK and PI3K. We determined the activities of various signaling proteins including FAK and PI3K by examining their phosphorylation levels using immunoblots. The results revealed that the phosphorylation of FAK, PI3K and AKT (a downstream target of PI3K) were significantly enriched after rPKM2 addition, but not ERK (Fig. 2.8 A). Furthermore, PI3K activity assay demonstrated the PI3K activity was upregulated and activated in the NHLF-derived myofibroblasts upon rPKM2 treatments (Fig. 2.8 B). The activation of PI3K was abrogated by a FAK inhibitor, a PI3K inhibitor or an anti-αvβ3 antibody (Fig. 2.8 B). The above evidence indicates that extracellular PKM2 activates integrin αvβ3, FAK and PI3K. We then asked whether the activation of integrin αvβ3-FAK-PI3K mediated the apoptosis protection by extracellular PKM2. If so, the effects would be abolished by an anti-αvβ3 antibody or a FAK inhibitor or a PI3K inhibitor. As expected, the effects of rPKM2 on apoptosis protection of NHLF-derived myofibroblasts were inhibited by an anti-αvβ3 antibody or a FAK inhibitor or a PI3K inhibitor (Fig. 2.8 C). The blocking effect of the anti-αvβ3 antibody was further confirmed with the viable cell counting (Fig. 2.8 D & E). A well-known downstream target of activated PI3K is the activation of NF-κB survival signaling (Dan et al., 2008). Clearly, NF-κB was highly activated in NHLF-derived myofibroblasts in the presence of rPKM2, and activation of NF-κB was abolished in the presence of an anti-integrin αvβ3 antibody or a FAK inhibitor or a PI3K inhibitor (Fig. 2.8 F). The results indicate that the effects of extracellular PKM2

in protecting myofibroblasts from apoptosis are mediated via activation of NF-κB survival signaling.

Our next question is how extracellular PKM2 upregulates Arginase-1 in myofibroblasts. Is it also through activation of integrin αvβ3 and subsequent PI3K? If so, the upregulation of Arginase-1 by rPKM2 treatment would be abolished by integrin αvβ3 knockdown or an anti-αvβ3 antibody or a PI3K inhibitor. As expected, the PKM2-induced upregulation of Arginase-1 was inhibited by αvβ3 knockdown or the anti-αvβ3 antibody or the PI3K inhibitor (Fig. 2.8 G and H). Then we asked how PI3K signaling regulated Arginase-1 expression. It is well established that PI3K – PTEN pathway regulates Arginase-1 expression in macrophages (Sahin et al., 2014). Downregulation of PTEN in fibroblasts promotes myofibroblast differentiation and collagen synthesis (White et al., 2006). We reasoned whether extracellular PKM2 regulated Arginase-1 expression in myofibroblasts by the same pathway via PI3K-PTEN signaling axis. Thus, we probed the PTEN levels in the rPKM2 treated myofibroblasts. Addition of rPKM2 but not rPKM1 into culture medium strongly reduced PTEN in the cells (Fig 2.5. A). The results suggest that extracellular PKM2 may play a role in downregulation of PTEN during fibrosis progression, which subsequently control Arginase-1 expression. To test this conjecture, PTEN was exogenously expressed in NHLF-derived myofibroblasts that were subsequently treated by rPKM2. Immunoblot and RT-PCR analyses demonstrated that overexpression of PTEN reduced Arginase-1 protein and mRNA levels in the cells (Fig 2.8. I & J).

2.3.6 Neutralization of PKM2 attenuates lung fibrosis

If extracellular PKM2 facilitates lung fibrosis progression by protecting myofibroblasts from turnover and enhancing collagen production, it would be expected that an antibody against PKM2 would abolish its effects in promoting lung fibrosis. This would suggest a novel strategy

and target for lung fibrosis treatment. To confirm this speculation, we employed an in-house developed rabbit monoclonal antibody against PKM2, IgGPK (Zhang et al., 2016). Mice were induced to lung fibrosis by bleomycin, followed by treatments with vehicle, IgG control (IgGCon) or IgGPK (Fig. 2.9 A). At the end of the treatment, mice were sacrificed. Body weight, lung weight, and out-surface of lungs were examined. IgGPK treatment led to an increase in body weight and a decrease in lung weight compared to IgG treatment (Fig. 2.9 B & D). Lungs from IgGPK-treated mice showed less fibrotic-like, whitish patterns on their surfaces compared to those from IgG-treated mice (Fig. 2.9 C). Sirius red staining of lung tissue sections and hydroxyproline assay revealed a substantial decrease in collagen content and density, indicating less collagen accumulation in fibrotic lungs after the IgGPK treatment (Fig. 2.9 E, F & G). We also analyzed whether the IgGPK treatment indeed specifically led to relief of apoptosis protection of lung myofibroblasts, and thus led to apoptosis of lung myofibroblasts. Immunohistochemical analysis of α-SMA demonstrated IgGPK treatment resulted in a reduction in α-SMA positive myofibroblasts in fibrotic lungs (Fig. 2.9 F & H). IF staining of α-SMA also showed significantly less myofibroblasts (α-SMA positive) were present in fibrotic lungs from mice treated by IgGPK (Fig. 2.10 A & B). Co-staining α-SMA with an apoptosis TUNEL kit indicated that IgGPK treatment led to more apoptosis of α-SMA positive lung myofibroblasts (Fig. 2.10 A & B). Next we examined whether IgGPK treatment inhibited Arginase-1 expression in lung myofibroblasts. Co-staining α-SMA with Arginase-1 showed the treatment of IgGPK resulted in a notable decline in Arginase-1 expressing myofibroblasts (Fig. 2.10 C & D). Amino acid level measurement revealed IgGPK treatment led to a marked reduction in proline level, accompanied by an augment in arginine level (Fig. 2.10 E). We conclude that neutralization of PKM2 attenuates lung fibrosis by blocking myofibroblasts apoptotic resistance and Arginase-1 expression.

2.4 Discussion

The myofibroblasts are the key effector cells in fibrosis progression. One feature of myofibroblasts is that they are strongly resistant to turnover, which allows myofibroblasts to be continuously and actively present in fibrotic regions, eventually leading to the fibrosis. However, the mechanisms how myofibroblasts obtain potent resistance to turnover have not been well appreciated. Herein we report a novel mechanism that extracellular PKM2 protects myofibroblasts from apoptosis by activating integrin αvβ3-FAK-PI3K-NF-κB signal pathway.

Enhanced collagen synthesis is another determining feature of myofibroblasts, which process is controlled in various levels, including transcriptional and translational regulation (Ricard-Blum, Baffet, & Théret, 2018). The availability of amino acid constitutes of collagen evidently plays a role in controlling the collagen expression translationally. Proline is the second most abundant amino acid in collagen, accounting for approximately 23% of collagen (Gordon & Hahn, 2010), and the collagen metabolism is regulated by proline (Karna, Szoka, Huynh, & Palka, 2019). The proline can be converted from glutamine/glutamate or arginine. Supplementation of arginine promotes wound healing, whereas supplementation of glutamine/glutamate or proline in the diet achieves little or no effect (Albaugh et al., 2017), indicating the arginine-to-proline conversion is critical in regulation collagen production. Arginine-to-proline metabolism is highly controlled by the arginase, and the arginase activity is associated with collagen production (Kitowska, Zakrzewicz et al. 2008). However, what regulates arginase for facilitating collagen production is barely documented. Our study reports that extracellular PKM2 upregulates Arginase-1 and promotes proline and subsequent collagen production by integrin αvβ3-FAK-PI3K-PTEN signal pathway.

Overall, our investigations reveal that the extracellular PKM2 facilitates lung fibrosis by protecting myofibroblasts from apoptosis and promoting collagen synthesis in myofibroblasts. Our studies support the potential use of the anti-PKM2 antibody to attenuate lung fibrosis.

Whether the effects of extracellular PKM2 in lung fibrosis apply to fibrosis in other organs such as liver, kidney and heart is a question we are currently addressing. With preliminary data (unpublished), we observed the same effects of extracellular PKM2 in liver fibrosis, which made us speculate extracellular PKM2 could execute a universal role to promote apoptosis resistance and collagen synthesis in myofibroblasts in fibrosis of different organs. The ongoing projects would provide more clues.

As myofibroblasts also exist in the tumor stroma, the so-called cancer-associated fibroblasts, which is more and more recognized as essential players in tumor growth and metastasis. It is interesting to investigate whether the extracellular PKM2 also acts on these cancer-associated fibroblasts. High levels of circulated PKM2 has been reported in patients with various cancers, and it has been described that secreted PKM2 promotes tumor cell proliferation and migration (Yang, Li et al. 2015, Hsu, Hung et al. 2016, Kim, Kim et al. 2019). However, there is a lack of research studying the role of extracellular PKM2 on cancer-associated fibroblasts in cancer growth and metastasis. Basing on our observation in lung fibrosis, it is possible that extracellular PKM2 may prevent cancer-associated fibroblasts from apoptosis and promote their collagen production, which leads to cancer progression.

Proline can be converted from glutamine/glutamate and arginine. Glutamine/glutamate is believed to be an important source of proline (Barbul, 2008), given the fact that glutamine is the most abundant amino acid in the human body (~20% of circulating free amino acid and 60% of the free intracellular amino acids). Besides, myofibroblasts undergo metabolism reprogramming

and glutamine is reported critical for collagen synthesis in lung fibroblasts (Bernard et al., 2015; Hamanaka et al., 2019). However, we observed a marked increase in proline but did not observe a significant reduction in glutamine in NHLF-derived myofibroblasts after rPKM2 treatment. This phenomenon made us think why myofibroblasts do not turn to glutamine/glutamate metabolism for proline when the demand for collagen synthesis increases. A possible explanation would be that myofibroblasts require glutamine/glutamate for other purposes such as energy supply. Further works need to be done to test this hypothesis and uncover more details.

Figure 2.1. High levels of extracellular PKM2 are detected in lungs of patients with lung fibrosis (A) Representative images of immunohistochemistry analysis of PKM2 accumulation in normal human lung tissues and lung tissues from patients with pulmonary fibrosis. Red arrows indicate the areas with PKM2 extracellular accumulation patterns. (B) Quantification of PKM2 staining as in (A) by Frida software. The intensity of PKM2 is presented as the percentage of positive staining areas in the total area using four tissue cores of normal lung and six of fibrosis lung from the tissue array; five randomly selected view fields per core.

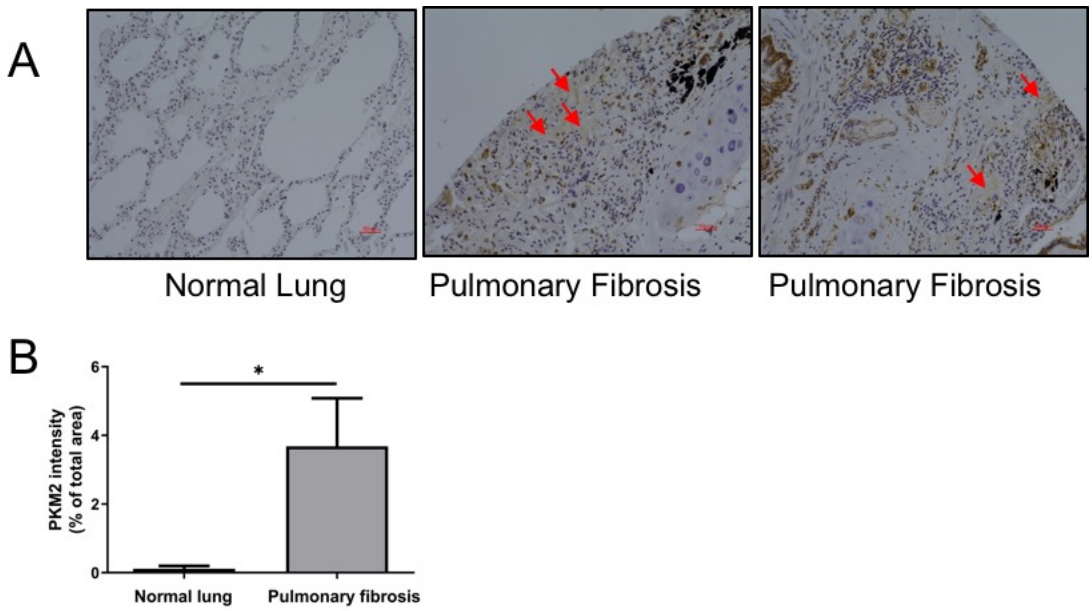

Figure 2.1 High levels of extracellular PKM2 are detected in lungs of patients with lung fibrosis

Figure 2.2. Treatment of rPKM2 promotes lung fibrosis development.

(A) Experimental scheme of bleomycin (BLM)-induced lung fibrosis model establishment and treatment with buffer/rPKM1/rPKM2. (B) The body weights were monitored. Black arrow indicates the time point when buffer/rPKM1/rPKM2 treatments start. (C) Representative photographs of lungs from mice treated with indicated agents 1-day post-fixation with 10% formalin. (D) Lung weights were measured at the endpoint. (E) Hydroxyproline level in lungs of mice with indicated treatments. (F) Representative images of Sirius Red staining (top panel) and α-SMA immunohistochemistry staining (bottom panel) in lung sections from the indicated groups of mice. (G and H) Quantification of Sirius Red stains (G) and α-SMA immunohistochemistry staining (H) of lung tissue sections from mice treated with indicated agents using Frida software. The positive staining areas were calculated as percentages of total area, using five randomly selected sections per mouse, a total of nine mice in each group. All columns and error bars represent means ± SD. * $p<0.05$, ** $p<0.01$, *** $p<0.001$.

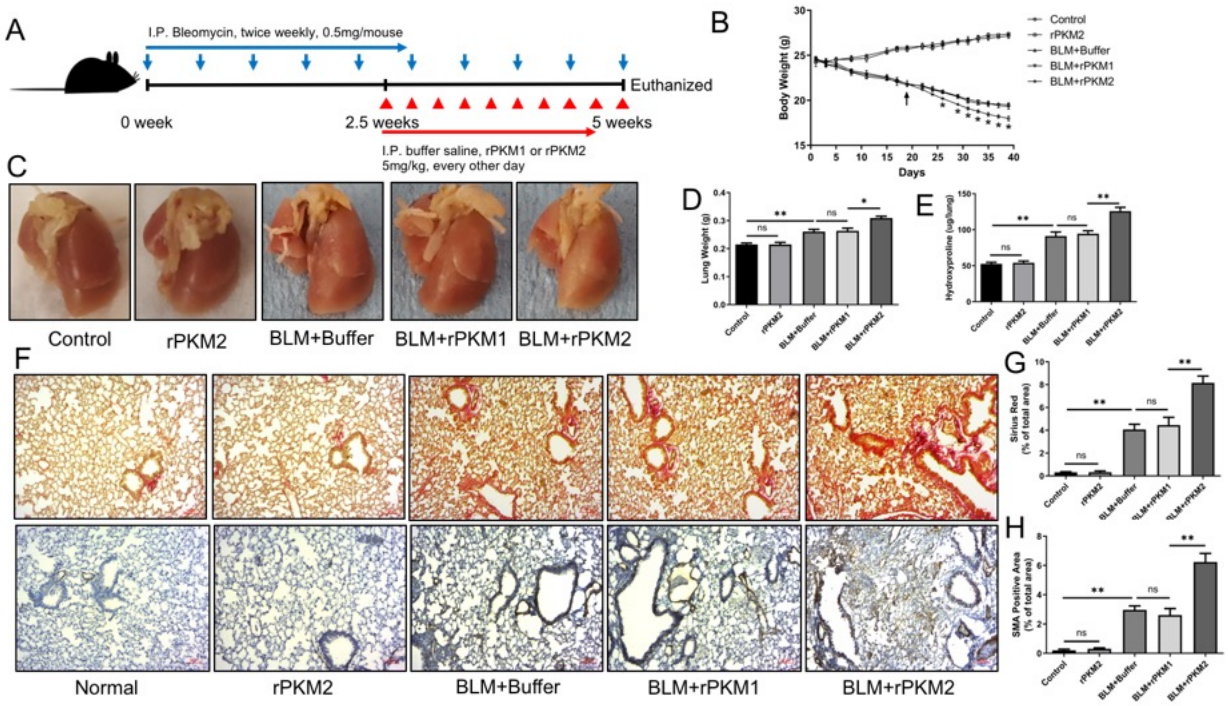

Figure 2.2 Treatment of rPKM2 promotes lung fibrosis development

Figure 2.3. Extracellular PKM2 decreases myofibroblast apoptosis in fibrotic lungs.

(A) Representative images of immunofluorescence staining of TUNEL (TdT-mediated dUTP nick end labeling, green) and αSMA (red) in lung frozen sections from mice treated by indicated agents. Nuclei are visualized by 4,6-diamidino-2-phenylindole (DAPI) staining (blue). White arrowheads indicate TUNEL and αSMA double-positive cells. (B) Quantification of αSMA and TUNEL staining using ImageJ. The TUNEL and αSMA double-positive cells were counted and presented as the double-positive cell number per view. All columns and error bars represent means ± SD. ** $p<0.01$, *** $p<0.001$.

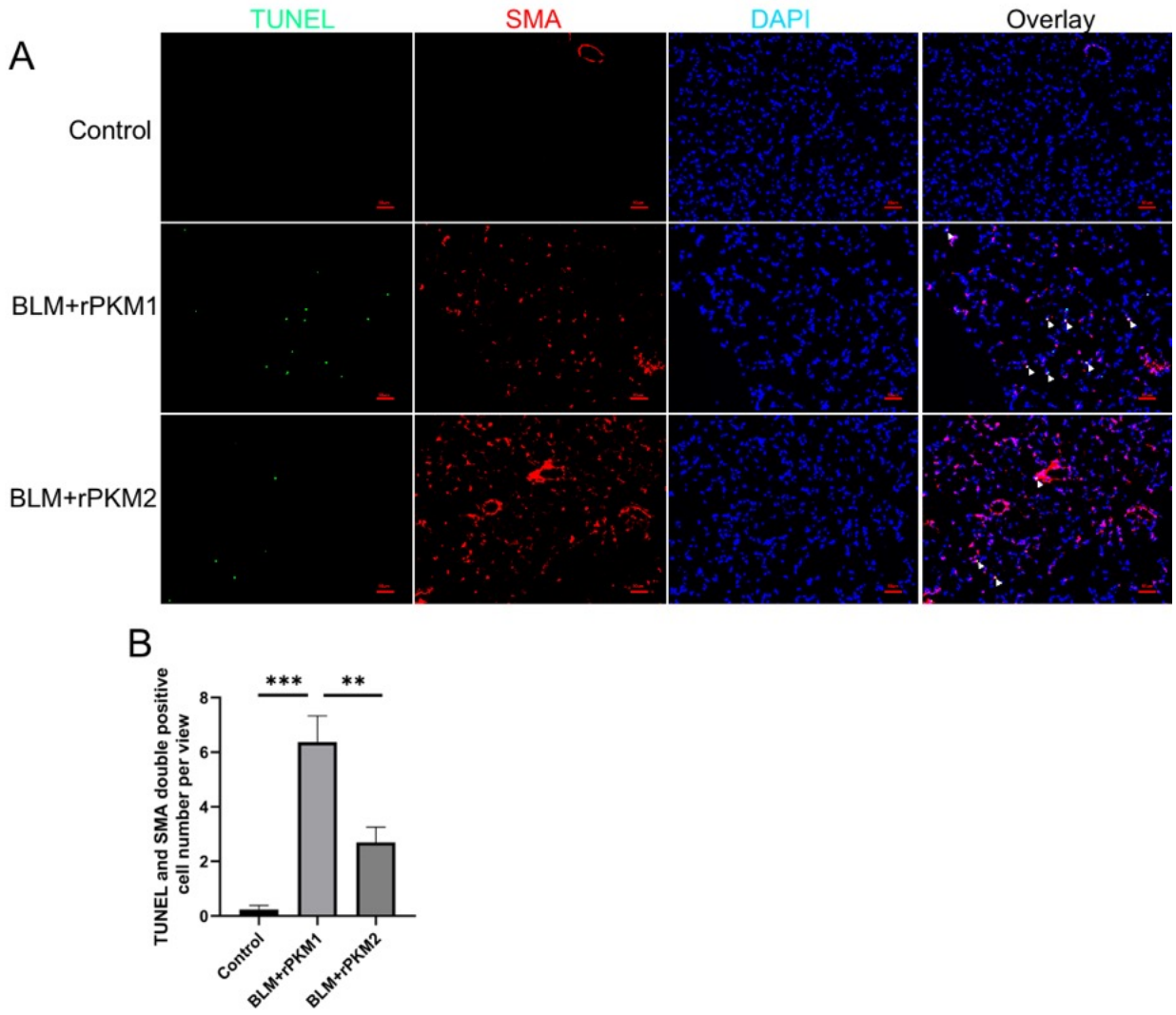

Figure 2.3 Extracellular PKM2 decreases myofibroblast apoptosis in fibrotic lungs.

Figure 2. 4. Extracellular PKM2 protects myofibroblasts against apoptosis.

The normal human lung fibroblasts (NHLFs) were induced to myofibroblasts by 1-day treatment of TGFβ1 (10 μg/ml), after serum-free starvation overnight. The NHLF-derived myofibroblasts were treated with rPKM2/rPKM1 (150 nM each) for 1 d, followed by apoptosis induction with Fas ligand (100ng/ml) and Cycloheximide (CHX, 100 μg/ml) for 10 h. After the treatment, cells were processed for microscopic photography (A), Annexin V/PI analysis (C), western blot analysis of apoptosis relevant proteins including PARP, BCL2 and cIAP (E) or ATP assay (F). (A) Representative microscope images of myofibroblasts after treatments of indicated agents. (B) Quantification of the viable cell number in (A). The viable cells were calculated as the attached cell number per view field using five randomly selected view fields each time for a total of three independent experiments. (C) Annexin V/PI analysis of NHLF-derived myofibroblasts treated with indicated agents by flow cytometry. (D) Quantification of apoptotic rate for Annexin V/PI assay. The apoptotic rates were qualified as the Annexin V positive cell percentages of total acquired cells. (E) Representative western blots showing PARP, BCL2 and cIAP1 and GAPDH in NHLF-derived myofibroblasts treated by indicated agents. (F) ATP level analysis of NHLF-derived myofibroblasts after indicated treatments. The ATP levels were presented as luminescence reading (RLU). All columns and error bars represent means $\pm$ SD, n $\geqslant$ 3. * $p<0.05$, *** $p<0.001$.

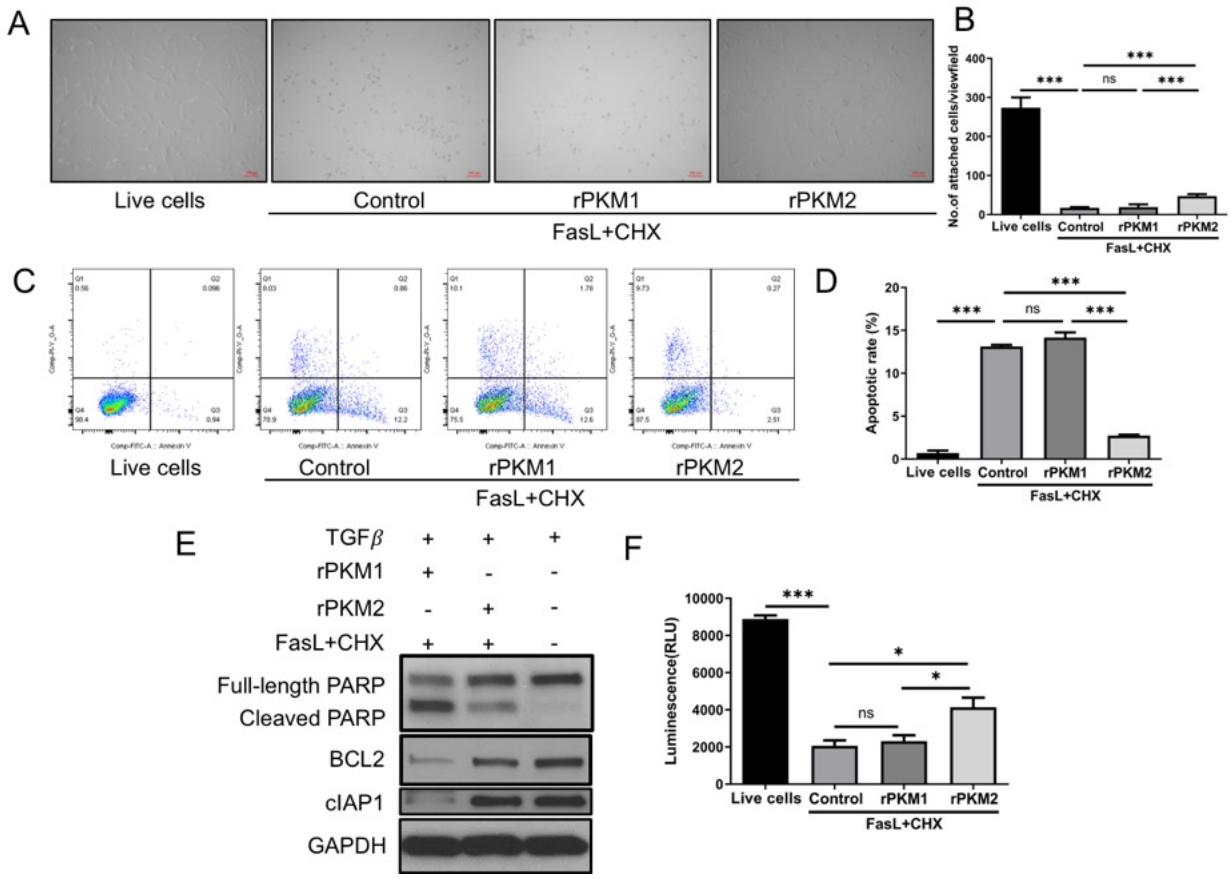

Figure 2.4 Extracellular PKM2 protects myofibroblasts against apoptosis.

Figure 2.5. Extracellular PKM2 upregulates Arg-1 in myofibroblasts, promoting proline synthesis for collagen production.

(A) Representative western blots showing expression of arginase 1 (Arg-1), collagen 1 (Col1a1) and PTEN. TGFβ1-induced myofibroblasts derived from NHLFs were treated with rPKM2 for 1 d (to examine Arg-1 and PTEN level) or 4 d (to examine collagen I level). rPKM1 serves as the isoform control for rPKM2. Actin serves as a loading control. (B) Representative images of tubes for collagen content measurements showing the collagen pellets. TGFβ1-induced myofibroblasts derived from NHLFs were treated with rPKM2 for 4 d and the culture media were collected for collagen content determination using Sirius Red. Arrows indicate the red collagen pellets, composed of the collagen-dye complex. (C) Quantification of collagen contents in (B). The collagen pellets were dissolved, and absorbance was measured. The quantification of collagen was expressed as relative fold changes of absorbance compared with the control group. Three independent repeats were performed, and data presented mean ± SD. (D and H) mRNA levels of *COL1A1* and *ARG1* were analyzed after rPKM2 treatment in TGFβ1-induced myofibroblasts derived from NHLFs by RT-qPCR. *ACTIN* serves as a reference gene. The mRNA levels were quantified using 2^-ΔΔCt and expressed as relative fold changes of mRNA level compared with the control group. Data are presented as mean ± SD (n=3). (E) Free amino acid levels were analyzed by LC-MS after rPKM2 treatment in lysates of TGFβ1-induced NHLF-derived lung myofibroblasts. The level of each amino acid was presented as relative abundance compared with rPKM1-treated control. (F) Measurement of ornithine level in NHLF-derived myofibroblasts after rPKM1 or rPKM2 treatment. (G) Arginase activity was measured after rPKM2 treatment in TGFβ1-induced NHLF-derived myofibroblasts. Arginase activities were qualified as relative fold changes compared with the control group. Data presented mean ± SD (n=3). (I and J) TGFβ1-

induced myofibroblasts derived from NHLFs were treated by rPKM2 for 4 days in the presence of NOHA (I) or specialized arginine-depleted medium (J) and subjected to expression analysis of collagen I (Col1a1) by western blots. The addition of arginase inhibitor (NOHA, 1 mM) or the medium replacement by specialized arginine-depleted medium occurs 30 min before rPKM2 treatment. All columns and error bars represent means $\pm$ SD, n $\geqslant$ 3. * $p<0.05$, ** $p<0.01$.

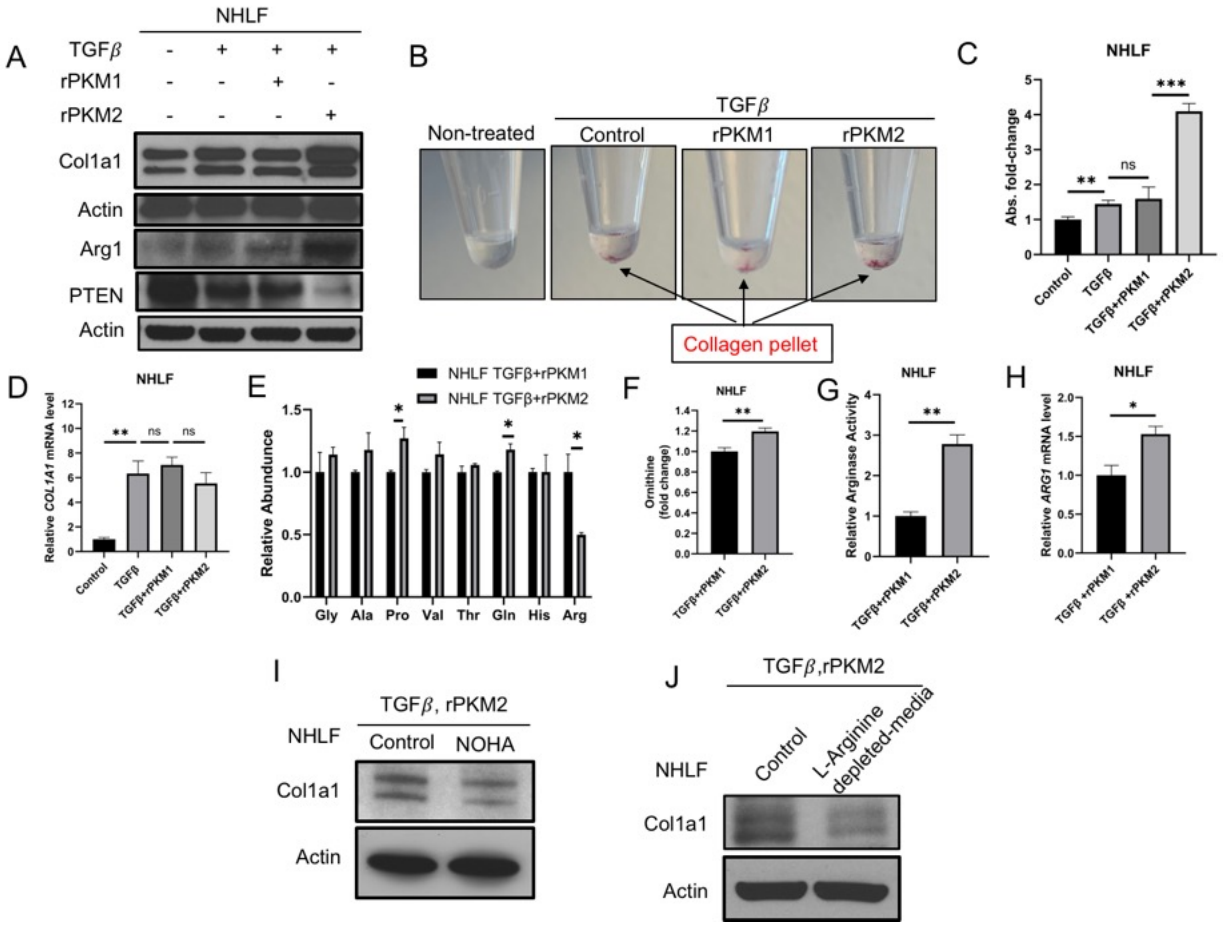

Figure 2.5 Extracellular PKM2 upregulates Arg-1 in myofibroblasts, promoting proline synthesis for collagen production.

Figure 2.6. Extracellular PKM2 enhances Arg-1 expression in myofibroblasts in fibrotic lungs. (A and B) Representative images of immunofluorescent co-staining of Arg-1 and αSMA in lung tissues from mice treated with indicated agents: Arg-1 (red). αSMA (red), nuclei (blue). Arrowheads indicate the Arginase-1 and αSMA double-positive cells, the Arginase-1-expressing myofibroblasts. (C) Free amino acid levels were analyzed in lung homogenates from mice treated with indicated agents. The levels of each amino acid were presented as relative abundance compared with the rPKM1-treated group. Data presented as means ± SE, n ⩾ 3. * $p<0.05$, ** $p<0.01$, *** $p<0.001$.

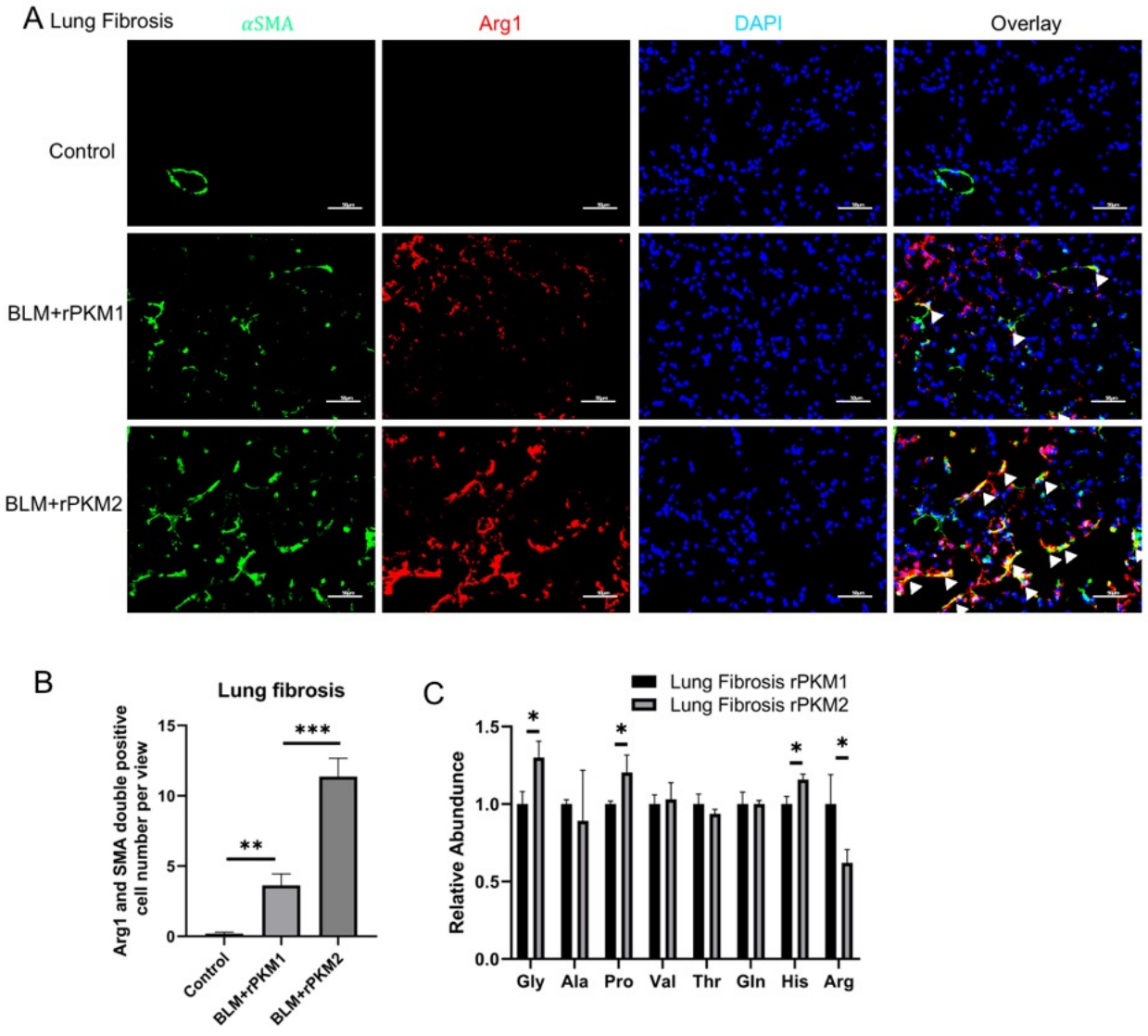

Figure 2.6 Extracellular PKM2 enhances Arg-1 expression in myofibroblasts in fibrotic lungs.

Figure 2.7. Extracellular PKM2 interacts with integrin αvβ3.

(A) Representative western blots showing expression levels of αv and β3 in NHLF-derived myofibroblasts by stimulation with TGFβ1 (10 μg/ml) for 1 day. GAPDH was used as a loading control. (B) Representative microscope images of cell attachment assay. NHLF-derived myofibroblasts by TGFβ1 induction were seeded on rPKM2-coated plates in the presence of the function-blocking antibody against αvβ3 (LM609, 10 μg/ml) or IgG control. After incubation, unattached cells were washed away, and the remaining cells were stained by crystal violet. rPKM1 serves as the isoform control for rPKM2. (C) Quantification of cell attachment assay. Attached cells were counted in five randomly selected view field per images. Experiments were done in triplicate and data presented as means ± SD. (D) Co-immunoprecipitation analysis of β3 and PKM2. TGFβ1-induced NHLF-derived myofibroblasts were treated with rPKM2 (150nM) for 1 h. Cell lysates were prepared and immunoprecipitated by the anti-His-tag antibody. rPKM2 is a His-tag protein. The Precipitated protein complex was analyzed by western blots for β3 and PKM2. The same amount of PKM2 input serves as a loading control. All columns and error bars represent means $\pm$ SD, n $\geqslant$ 3. *** $p<0.001$.

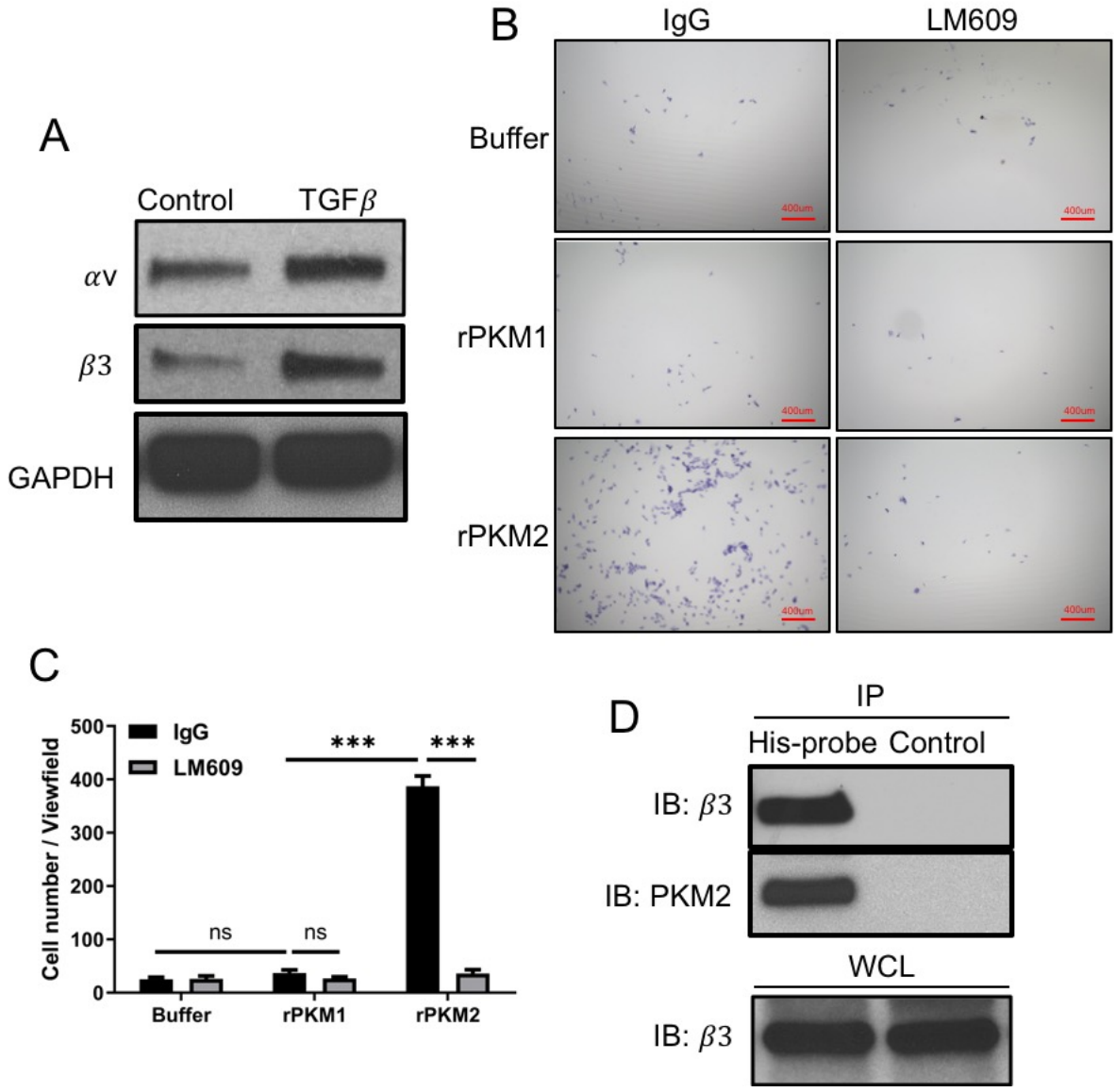

Figure 2.7 Extracellular PKM2 interacts with integrin αvβ3

Figure 2.8 Extracellular PKM2 activates integrin αvβ3-FAK-PI3K signaling axis in myofibroblasts

(A) The NHLFs were starved in serum-free medium overnight, followed by TGFβ1 (10 μg/ml) stimulation for 1 day then rPKM2 treatment (150nM) for an additional 30 min and assayed for activation of PI3K, AKT, FAK and ERK by detecting their phosphorylation with phospho-specific antibodies. Actin was used as a loading control. (B-F) NHLFs were induced to myofibroblasts by treatment of TGFβ1 (10 μg/ml) for a day, after serum-free starvation overnight. The myofibroblasts were treated with 150 nM rPKM2/rPKM1 for 1 d, in the presence of FI14 (FAK inhibitor), LY294002 (PI3K inhibitor) or LM609 (αvβ3 antibody) and assayed for PI3K (B) and NF-κB (F) activities. The inhibitors (20 μg/ml LY294002; 2.5 μM FI14) and LM609 (10 ng/ml) were added 30 min earlier than rPKM2 addition. Data were presented as fold changes compared with the control group. Cells treated as above were subjected to apoptosis induction by Fas ligand (100ng/ml) and CHX (100 μg/ml) for 10 h and examined for ATP assay (C) or microscopic photography (D). (C) ATP levels were measured in cells treated by indicated agents and the data were represented as luminescence readings in RLU. (D) Representative microscope images of cells in the presence of LM609 or IgG control. (E) Quantification of viable cell numbers. The quantification was performed by counting the attached cell number per view using five randomly selected view fields in each image. The experiment was repeated three times independently. (G) TGFβ1-induced myofibroblasts derived from NHLFs were treated with rPKM2 for 30 min (to examine p-PI3K level) or 1 d (to examine Arginase-1 level) in the presence of PI3K inhibitor (LY294002) or function-blocking anti-αvβ3 antibody (LM609) and analyzed for protein level of Arginase-1 or p-PI3K, respectively using western blots. The rPKM1 serves as isoform control for rPKM2. Actin serves as a loading control. (H) The β3 was knocked down with siRNA in TGFβ1-

induced lung myofibroblasts derived from NHLFs, followed by rPKM2 treatment for 30 min (to examine p-PI3K level) or 1 d (to examine Arginase-1). Actin serves as a loading control. Scrambled siRNA was used as a control for β3 siRNA. (I and J) PTEN was exogenously expressed using adenovirus ad-PTEN in NHLF-derived myofibroblasts. The cells were then treated by rPKM2 and subjected to the Immunoblot (I) and RT-qPCR (J) analyses of PTEN and Arg-1. All columns and error bars represent means ± SD, n ⩾ 3. * $p<0.05$, ** $p<0.01$, *** $p<0.001$.

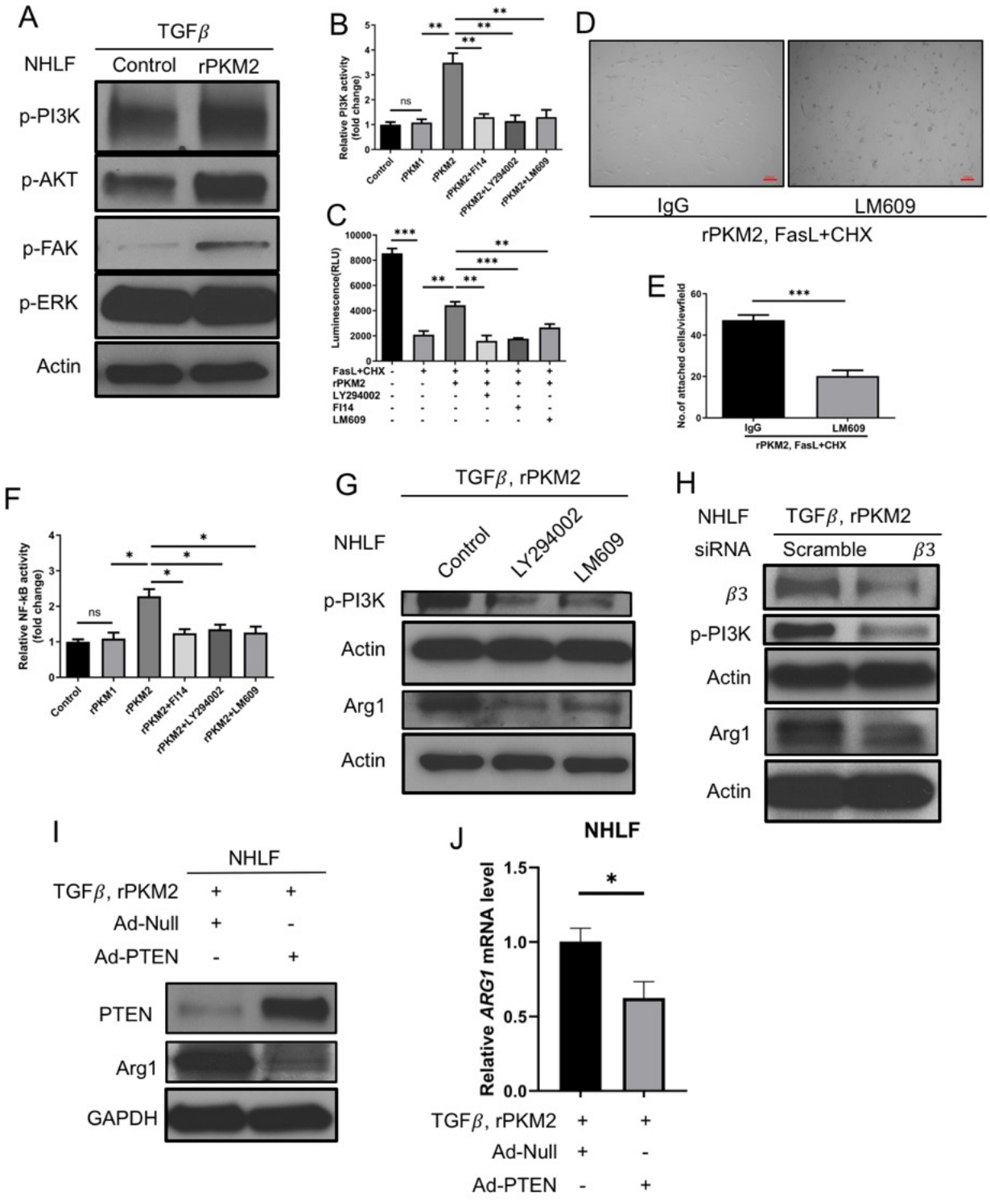

Figure 2.8 Extracellular PKM2 activates integrin αvβ3-FAK-PI3K signaling axis in myofibroblasts

Figure 2.9. Neutralization of rPKM2 attenuates lung fibrosis progression.

(A) Experimental scheme of BLM-induced lung fibrosis model establishment and treatment with IgGCon/IgGPK. (B) The body weights were monitored. Black arrow indicates the time point when IgGCon/IgGPK treatments start. (C) Representative photographs of lungs from mice treated with indicated agents 1-day post-fixation with 10% formalin. (D) Lung weights were measured at the endpoint. (E) Hydroxyproline level in lungs of mice after indicated treatments (F) Representative images of Sirius Red staining (top panel) and αSMA immunohistochemistry staining (bottom panel) of lung tissue treated with indicated agents. (G and H) Quantification of Sirius Red staining (G) and αSMA immunohistochemistry staining (H) of lung tissue sections from mice treated with indicated agents using Frida software. The positive staining areas were calculated as percentages of total area, using five randomly selected sections per mouse, a total of eight mice in each group. All columns and error bars represent means ± SD. * $p<0.05$, ** $p<0.01$, *** $p<0.001$.

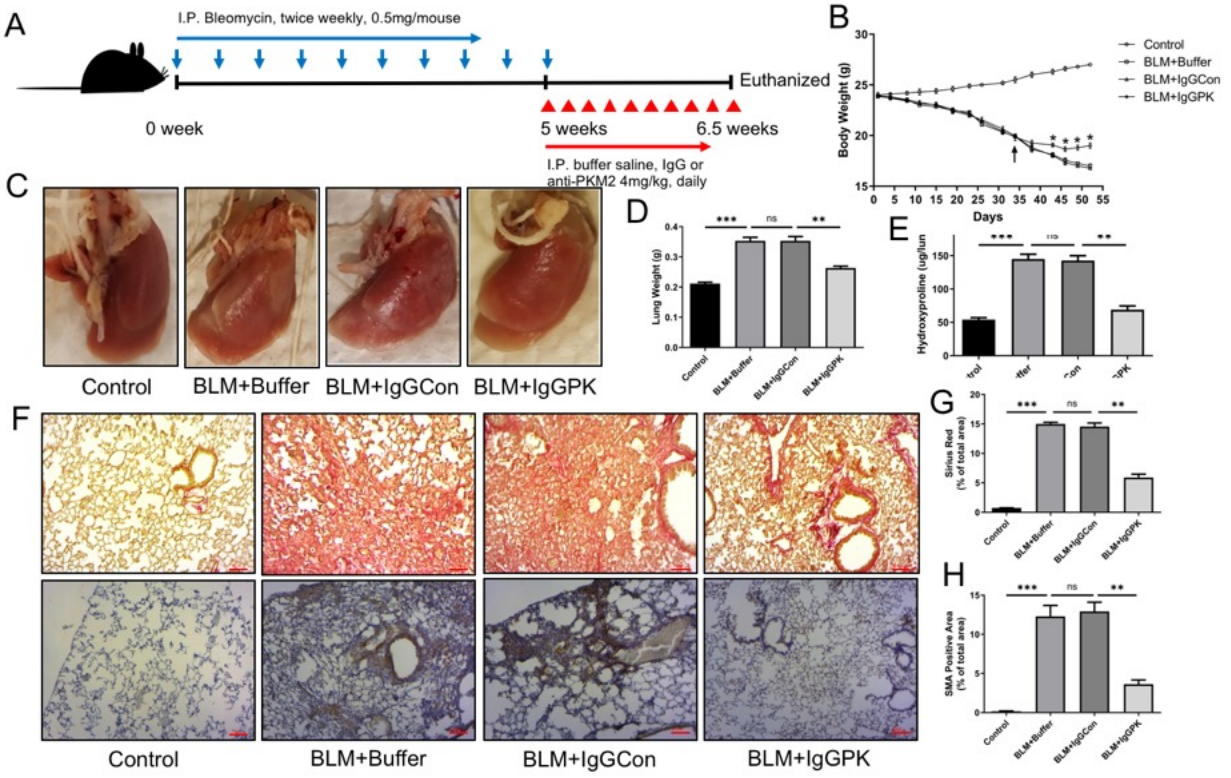

Figure 2.9 Neutralization of rPKM2 attenuates lung fibrosis progression.

Figure 2.10. Neutralization of PKM2 increases apoptosis and reduces Arg-1 expression in myofibroblasts in fibrotic lungs.

(A) Representative images of immunofluorescence staining of TUNEL (green) and αSMA (red) in lung frozen sections from mice treated by indicated agents. Nuclei are visualized by DAPI staining (blue). White arrowheads indicate TUNEL and αSMA double-positive cells. (B) Quantification of αSMA and TUNEL staining using ImageJ. The TUNEL and αSMA double-positive cells were counted and presented as the double-positive cell number per view. (C and D) Representative images of immunofluorescent co-staining of arginase 1 and αSMA in lung tissues from mice treated with indicated agents: arginase 1 (red). αSMA (red), nuclei (blue). Arrowheads indicate the Arginase-1 and αSMA double-positive cells, the Arginase-1-expressing myofibroblasts. (E) Free amino acid levels were analyzed in lung homogenates from mice treated with indicated agents. The levels of each amino acid were presented as relative abundance compared with the rPKM1-treated group. Data presented as means $\pm$ SE, n $\geqslant$ 3. * $p<0.05$, ** $p<0.01$, *** $p<0.001$.

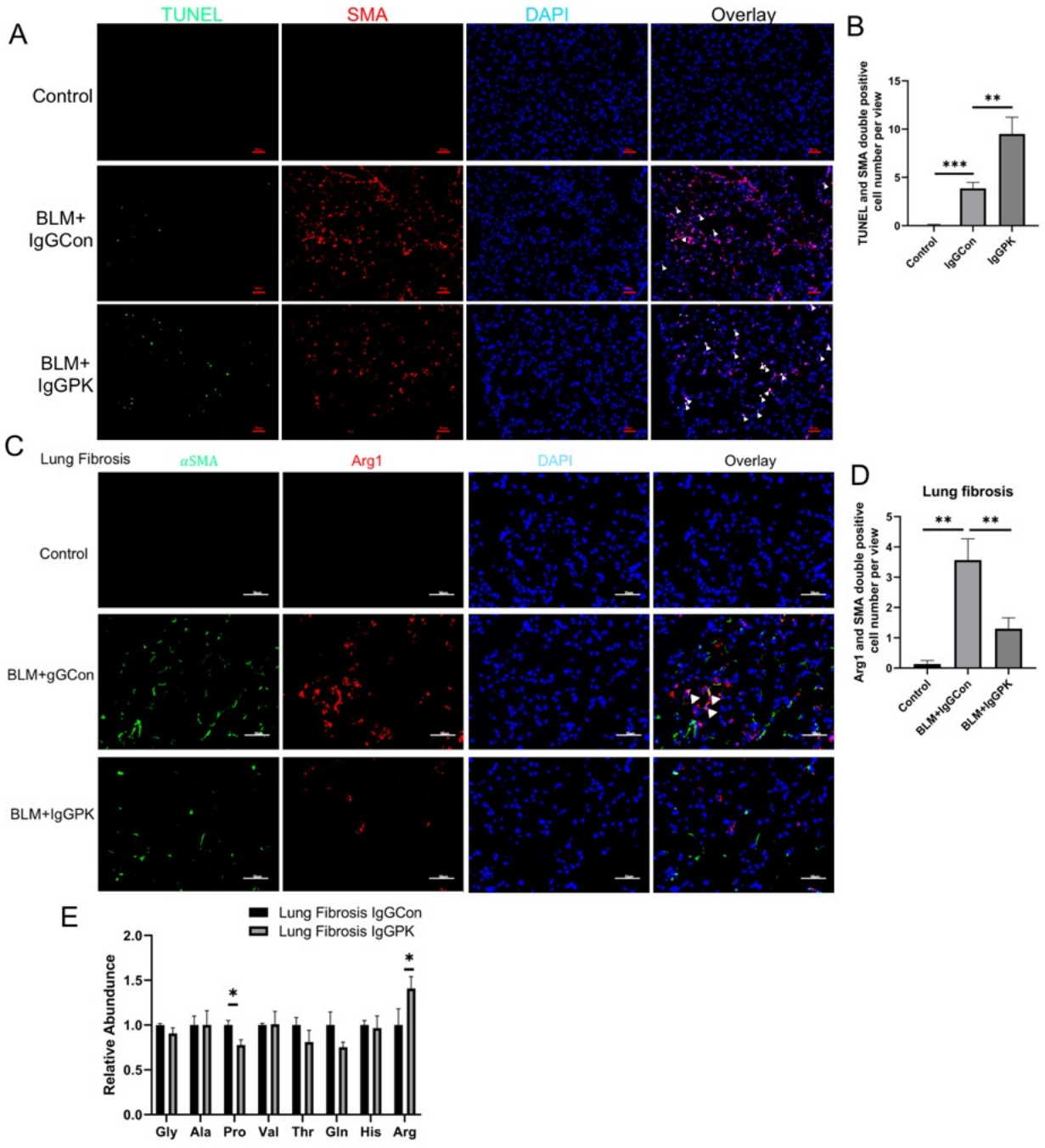

Figure 2.10 Neutralization of PKM2 increases apoptosis and reduces Arg-1 expression in myofibroblasts in fibrotic lungs.

Figure 2.11. Schematic diagram of the proposed mechanisms of extracellular PKM2 promoting lung fibrosis progression. On binding to αvβ3 integrin on the surface of myofibroblasts, PKM2 activates FAK and PI3K, triggering (1) enhanced apoptosis resistance of myofibroblasts via activation of NF-κB and (2) upregulation of Arginase-1, generating proline for collagen synthesis. Both roles of PKM2 result in myofibroblast persistence and further fibrosis progression.

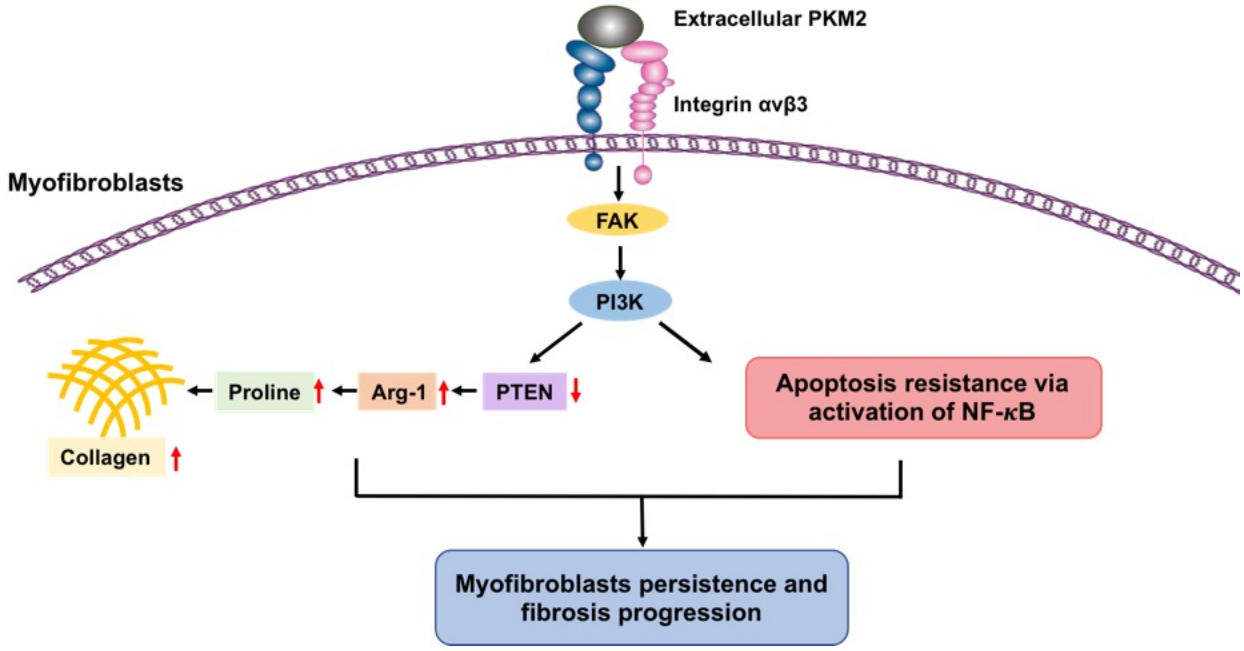

Figure 2.11 Schematic diagram of the proposed mechanisms of extracellular PKM2 promoting lung fibrosis progression.

3 Extracellular PKM2 promotes lung metastasis in 4T1 breast cancer

3.1 Abstract

Fibrosis is a hallmark of cancer. Fibrosis in cancer results from the increased deposition of a cross-linked collagen matrix by myofibroblasts. Fibrosis in cancer is a key driver for cancer growth and metastasis. High levels of PKM2 are identified in the blood circulation of cancer patients of many types. However, the effects of extracellular PKM2 on fibrosis in cancer has not been well studied. Here we show that the extracellular PKM2 enhances collagen accumulation in metastatic lungs and promotes lung metastasis in 4T1 breast cancer. Neutralization of PKM2 with antibody reduces collagen content and myofibroblast population at primary tumors, reduces tumor burden and provides survival benefit in 4T1 breast cancer. Additionally, neutralization of PKM2 with antibody leads to significant decreases in collagen deposition and myofibroblast population at metastatic lungs and reduces lung metastasis in 4T1 breast cancer. In summary, extracellular PKM2 increases fibrosis level in breast cancer which favors cancer growth and metastasis. Our study suggests a new therapeutic target for the treatment of breast cancer.

3.2 Introduction

Fibrosis in cancer, also called cancer-associated fibrosis, is an essential component of the cancer microenvironment which significantly impacts cancer growth and metastasis (Chandler, Liu, Buckanovich, & Coffman, 2019). Fibrosis in cancer results from the increased deposition of a cross-linked collagen matrix by myofibroblasts (Yamauchi, Barker, Gibbons, & Kurie, 2018). The myofibroblasts in cancer microenvironment is also known as cancer-associated fibroblasts (CAFs). Therefore, cancer-associated fibrosis is characterized by CAFs and CAF-secreted collagen. CAFs and CAF-secreted collagen in the tumor stroma not only promote tumor cell proliferation and growth at primary tumor sites by providing a tumor-promoting biochemical and

biomechanical context, they also enhance tumor metastasis through increasing primary tumor cell escape. Furthermore, the fibrosis at secondary metastatic sites prepare a permissive “soil” for metastasizing tumor cells to colonize (Cox & Erler, 2014). Additionally, when metastasizing tumor cells arrive to secondary metastatic sites, they trigger more myofibroblast activation locally through a paracrine mechanism, which further leads to enhanced colonization of the organ (Cox & Erler, 2014). Overall, CAFs and CAF-mediated collagen remodeling are responsible for driving cancer-associated fibrosis and creating fibrotic milieus at both primary tumor and secondary metastatic sites that enhance tumor progression and metastasis.

Pyruvate kinase M2 is long known as a metabolic enzyme in glycolysis. Whereas, after its non-canonical role being discovered as a critical player in converting metabolism to anabolism (so-called “Warburg effect”) in tumor cells, this multi-functional protein has attracted research enthusiasms of cancer biologists. Considerable advances in recent decades extended our knowledge of its multidimensional non-glycolytic roles as a protein kinase and a transcriptional co-activator. Thanks to recent discoveries of PKM2's extracellular localization, people realize the importance of extracellular PKM2 as a signal protein. A remarkable high level of PKM2 is found in circulation of patients of various cancer types. Extracellular PKM2 promotes angiogenesis for tumor growth and facilitates wound healing process (Li, Zhang, Qiao, Yang, & Liu, 2014; Zhang, Li, Liu, & Liu, 2016). But the importance of extracellular PKM2 has not been elucidated thoughtfully. Here we report extracellular PKM2 has an impact on fibrosis in breast cancer. The extracellular PKM2 increases fibrosis level in breast cancer which favors cancer growth and metastasis. Our study suggests a new therapeutic target for the treating cancer.

3.3 Results

3.3.1 The application of rPKM2 promotes 4T1 tumor metastasis to lungs.

Fibrosis in cancer is recognized as a key feature of cancer, which facilitates cancer growth and metastasis. Our previous finding demonstrates that the extracellular PKM2 promotes fibrosis in the lung. Therefore, we hypothesized that extracellular PKM2 could have an impact on fibrosis in cancer, ultimately affecting the local tumor development and malignant metastasis. To test this hypothesis, we established the 4T1 breast cancer model and treated the mice with rPKM1 or rPKM2 (Fig. 3.1 A). At the end of the treatment, mice were sacrificed, and organs were harvested for further analysis. The rPKM2 treatment did not make any difference on tumor volume (data not shown). A possible explanation is that the concentration of extracellular PKM2 at primary tumors is already saturated since cancer cells are known to secret very high levels of PKM2. The examination of lung metastasis demonstrated that the rPKM2 addition increased the lung metastatic nodules compared to rPKM1 addition (Fig.3.1 B). To determine the role of extracellular PKM2 in cancer-associated fibrosis, we assessed collagen content using Sirius Red staining. The results showed the rPKM2 treatment enhanced collagen deposition in the lungs compared to rPKM1 treatment (Fig.3.1 C & D). This evidence suggested rPKM2 addition increased fibrosis level in metastatic sites, which could be the reason that lung metastasis was enhanced after rPKM2 treatment. However, the rPKM2 treatment did not change collagen level in primary tumor sites (Fig.3.1 E & F), which is actually consistent with our observation that rPKM2 addition did not affect primary tumor volume.

3.3.2 Anti-PKM2 antibody treatment slows primary tumor growth in 4T1 mice.

To examine the effects of neutralization of extracellular PKM2 in cancer, we treated 4T1 breast cancer mice with an in-house developed anti-PKM2 antibody or IgG control (Fig. 3.2 A).

The monitoring of mice survival showed that the anti-PKM2 treatment displayed a survival benefit for 4T1 mice (Fig. 3.2 B). The measurement of tumor volume indicated that the anti-PKM2 antibody treatment reduced the mice tumor burden compared to IgG treatment (Fig.3.2 C), indicating anti-PKM2 antibody slowed tumor growth. We then examined the fibrosis level at primary tumors. The Sirius Red staining demonstrated less collagen accumulation in 4T1 mice treated with anti-PKM2 antibody (Fig.3.2 D & E). IHC staining of α-SMA indicated that anti-PKM2 antibody treatment led to a reduction in α-SMA positive myofibroblasts in primary tumors (Fig.3.2 F & G). Together, our results demonstrate the anti-PKM2 antibody treatment decreases fibrosis level at primary tumor sites, slows tumor growth and provides survival benefit in 4T1 breast cancer model.

3.3.3 Anti-PKM2 antibody treatment reduces lung metastasis in 4T1 mice.

As we have observed changes at primary tumor after the anti-PKM2 antibody treatment, we then went on to analyze the lung metastasis. The careful examination of metastasis on the lung surface after dissection demonstrated that the lung metastatic nodules were less in anti-PKM2 antibody treated mice compared to IgG treated mice (Fig. 3.3 A & B). Analysis of H&E staining indicated that lung metastasis area was also reduced after the treatment of anti-PKM2 antibody (Fig.3.3 C & D). We then assessed the fibrosis level in metastatic lungs. The Sirius Red staining showed that the addition of the anti-PKM2 antibody resulted in curtailed collagen deposition (Fig. 3.4 A&B). The IHC staining of αSMA demonstrated a significant decline in αSMA positive myofibroblasts after anti-PKM2 antibody treatment (Fig. 3.4 C & D). The above evidence suggests that neutralization of PKM2 with anti-PKM2 antibody decreases fibrosis level in metastatic lungs and diminishes the lung metastasis in 4T1 breast cancer model.

3.4 Discussion

PKM2, despite its canonical role in glycolysis, exhibits plasticity as a multi-functional protein associated with its diversity of locations (Amin, Yang, & Li, 2019). Its enrichment in cancer patient blood circulation fuels considerable research enthusiasms, and extracellular PKM2 is discovered to promote proliferation and migration of different cancer cell types (Hsu et al., 2016; Kim et al., 2019; Yang et al., 2015), enhance angiogenesis and metastasis during cancer progression (Li et al., 2014; Wang et al., 2020). There is a lack of study on the interaction between extracellular PKM2 and cancer-associated fibrosis. We here report extracellular PKM2 enhances cancer-associated fibrosis and promotes tumor growth and metastasis. Our study provides a potential therapeutic target for the treatment of cancer that could be translated to clinical practice.

We observed that rPKM2 treatment decreased lung metastasis in 4T1 cancer model but did not have an inhibitory effect on primary tumor. This could be because that the concentration in tumor stroma is much higher than that in local lung tissue. It is known that cancer cells actively secret high levels of PKM2. So, it is possible that the PKM2 level around tumor area is already high enough, so the additional supply of rPKM2 would not have much more effects on primary tumors. While the local concentration of PKM2 in lung area is relatively lower and the addition of rPKM2 displayed more significant effects on lung sites. This explanation is supported by our observation in the anti-PKM2 treatment that better effect were achieved in lung sites than in the primary tumors.

Though we found the anti-PKM2 antibody was effective on inhibiting tumor growth and lung metastasis in 4T1 mice, the effects are relatively moderate. A reason could be the affinity of the antibody clone 16-2 we used. When we were developing the anti-PKM2 antibody, we created antibodies against PKM2 protein from human source, to make it easy for clinical application in

the future. But when we performed *in vivo* experiments, we applied the antibody in mice. It happens that an antibody clone with high affinity to human protein has low affinity to mouse homolog. So, the antibody clone 16-2 has high affinity to human PKM2, but its affinity to mouse PKM2 could be low. This is the question which we are trying to address currently.

Moreover, we are excited to investigate the mechanism how extracellular PKM2 acts on cancer-associated fibrosis. Basing on our previous finding in lung fibrosis, we propose that extracellular PKM2 promotes cancer-associated fibrosis by preventing myofibroblasts from apoptosis and enhancing collagen production in myofibroblasts. Further works need to be done to test this hypothesis, including *in vitro* experiments such as treating myofibroblasts isolated from tumor stroma with rPKM2 and *in vivo* experiments such as staining the tissues from treated mice with TUNEL and αSMA.

Another question that needs to be addressed is how extracellular PKM2 enhances metastasis. Is it through increasing chances of tumor cell migration by acting on myofibroblasts in primary sites or through promoting metastatic niche developments by acting on myofibroblasts in the metastatic site or both? The extracellular PKM2 definitely has effects on the primary tumor site, as judged by the decreased tumor volume after anti-PKM2 antibody treatment. The survival benefits of the anti-PKM2 antibody are ascribed not only to the decreased primary tumor volume but also to the diminished the metastatic nodule number and size, indicating extracellular PKM2 acts on myofibroblasts on both primary and the metastatic sites.

Furthermore, if we focus on the metastatic sites, whether extracellular PKM2 promotes the enlargement of metastatic niche or it increases the seeding of metastatic niches is another interesting question to answer. Basing on our hypothesized apoptosis inhibitory role of PKM2, it seems that PKM2 promoting the expansion of pre-established nodules is more easily understood.

However, the mature myofibroblasts could educate precursor cells and transform them into myofibroblasts by secreting a large number of mediators. If the extracellular PKM2 secreted by myofibroblasts is one of such mediators, it would help myofibroblasts turn more cells into their allies and promotes metastatic niche origination. Further efforts need to be made to clarify this question. Overall, our studies suggest that extracellular PKM2 could be a therapeutic option to target fibrosis in cancer.

Figure 3.1. The application of rPKM2 promotes 4T1 tumor metastasis to lungs.

(A) Experimental scheme of 4T1 breast cancer model establishment and treatment with rPKM1/rPKM2. (B) Quantification of metastatic nodules in lungs from rPKM1 and rPKM2-treated groups. (C and E) Histologic analysis of collagen level by Sirius Red staining in lung sections (C) and primary tumor sites (E). Red represents collagen fiber presence. Brown represents the cytoplasm of cells. (D and F) Quantification of Sirius Red staining in lung sections (C) and primary tumor sites (E). The positive staining areas were calculated as percentages of total area, using five randomly selected sections per mouse, a total of ten mice in each group. All columns and error bars represent means ± SD. * $p<0.05$.

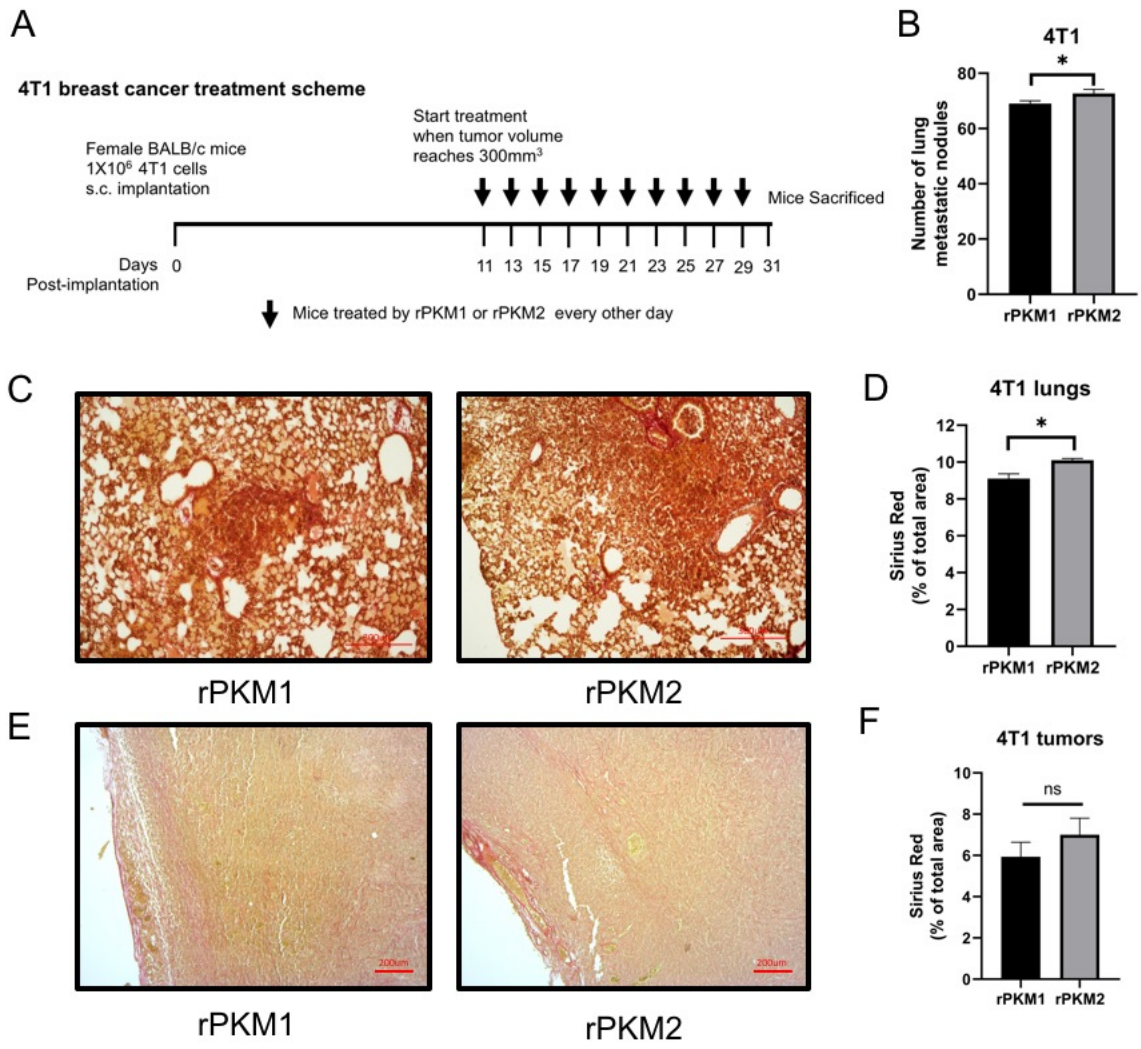

Figure 3.1 The application of rPKM2 promotes 4T1 tumor metastasis to lungs.

Figure 3.2. Neutralization of PKM2 slows 4T1 breast cancer growth.

(A) Experimental scheme of 4T1 breast cancer model establishment and treatment with Buffer/IgGPK. (B) The survival rate was monitored after tumor cell implantation (day 0). (C) The primary tumor volume was measured by using calipers and calculated with the formula: 1/2 × long diameter × short diameter^2. Representative images of Sirius Red staining (D) and immunohistochemistry staining of αSMA (F) tumor tissue sections from the indicated groups of mice. (F) Brown: targeted protein marker as indicated. Blue: nuclei counterstained by hematoxylin. (E and G) Quantification of Sirius Red staining (E) and the immunohistochemistry staining of αSMA (G) in lung tissue sections from mice treated with indicated agents using Frida software. The positive staining areas were calculated as percentages of total area, using five randomly selected sections per mouse, a total of ten mice in each group. All columns and error bars represent means ± SD. * $p<0.05$.

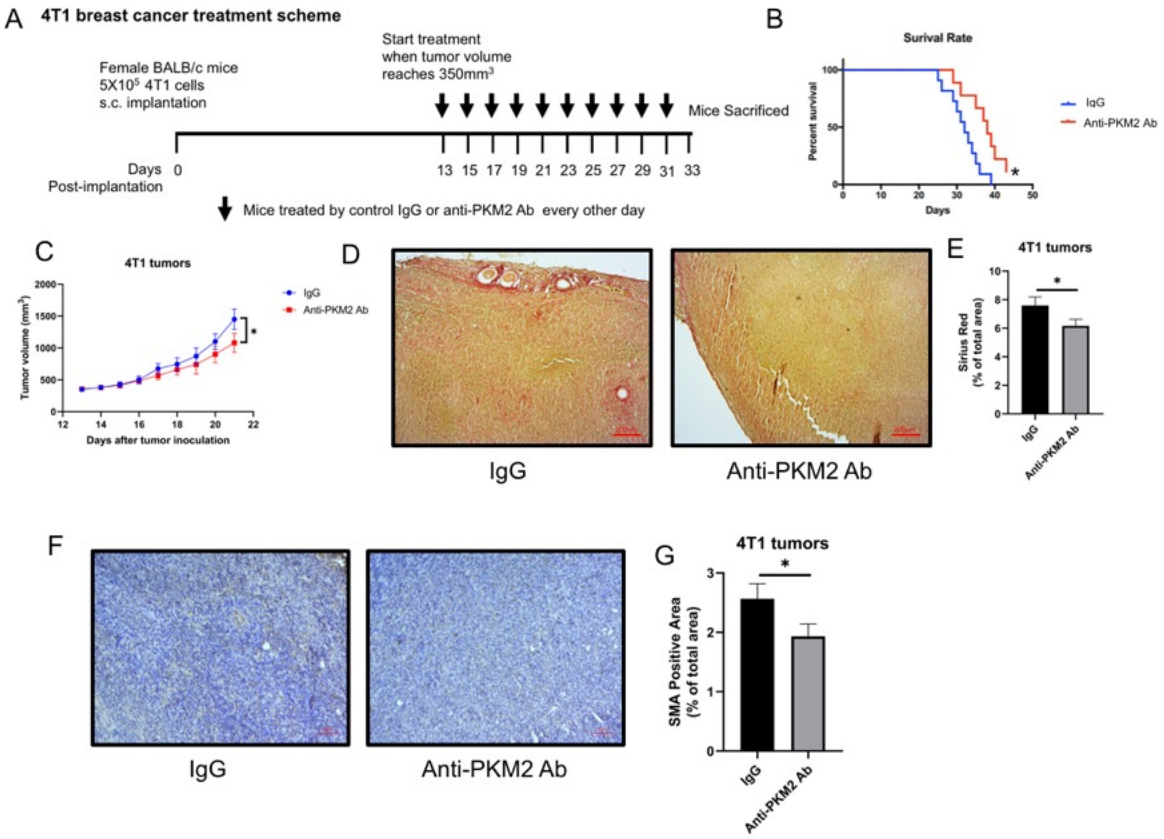

Figure 3.2 Neutralization of PKM2 slows 4T1 breast cancer growth.

Figure 3.3. Neutralization of PKM2 decreases lung metastatic nodules in 4T1 breast cancer.

(A) Representative photographs of lungs harvested at the endpoint. (B) Quantification of metastatic nodules in lungs from anti-PKM2 and buffer treated groups. (C) The representative images of hematoxylin and eosin (H&E) staining of lungs showing the metastatic nodules. (D) Quantification of total lung metastatic nodule area in the lung sections stained with H&E. The metastatic nodule areas were calculated as percentages of total area, using five randomly selected sections per mouse, a total of ten mice in each group. All columns and error bars represent means ± SD. ** $p<0.01$.

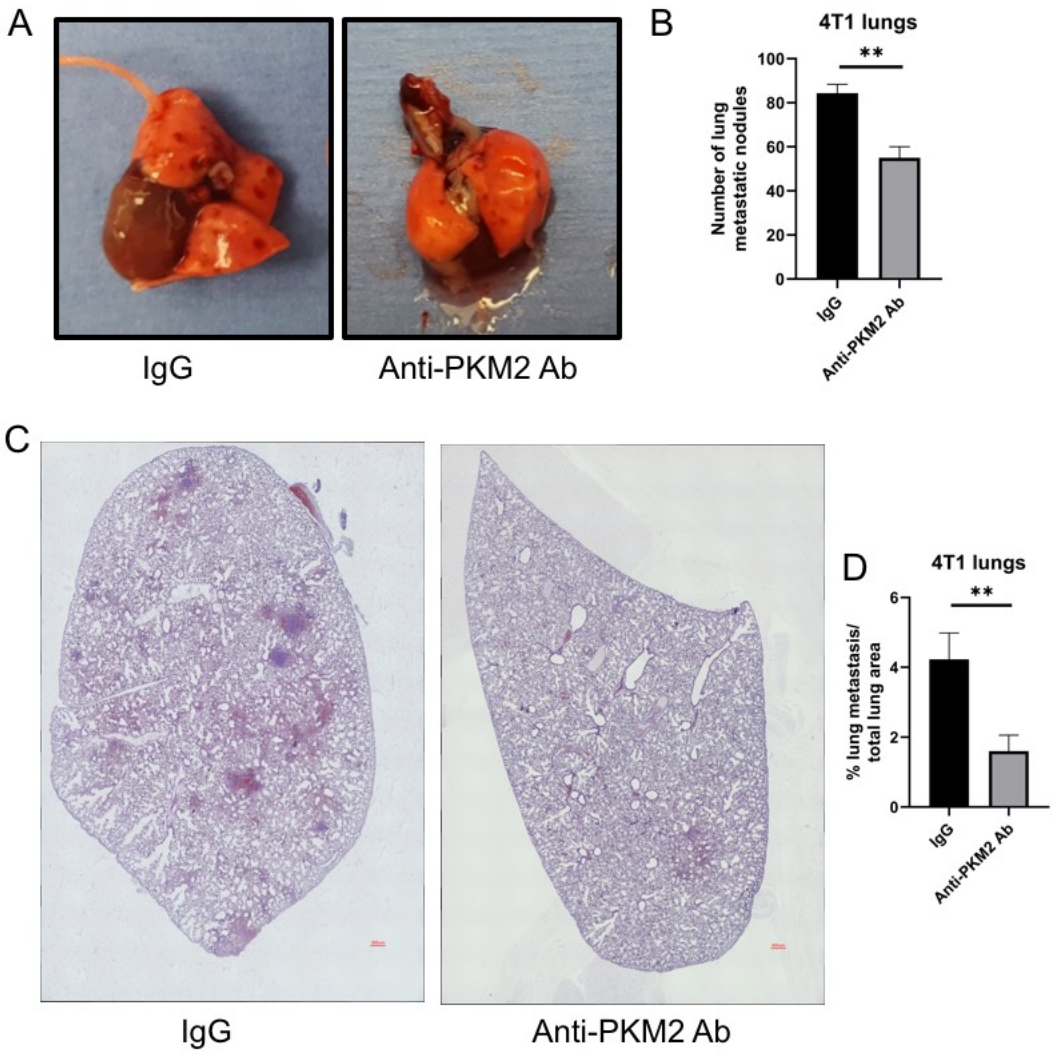

Figure 3.3 Neutralization of PKM2 decreases lung metastatic nodules in 4T1 breast cancer.

Figure 3.4. Neutralization of PKM2 reduces fibrosis level in lungs from 4T1 breast cancer mice. Representative images of Sirius Red staining (A) and immunohistochemistry staining of αSMA (C) in lung sections from the indicated groups of mice. (A) Red represents collagen fiber presence. Brown represents the cytoplasm of cells. (C) Brown: targeted protein marker as indicated. Blue: nuclei counterstained by hematoxylin. Quantification of Sirius Red staining (B) and immunohistochemistry staining of αSMA (D) of lung tissue sections from mice treated with indicated agents using Frida software. The positive staining areas were calculated as percentages of total area, using five randomly selected sections per mouse, a total of ten mice in each group. All columns and error bars represent means ± SD. ** $p<0.01$.

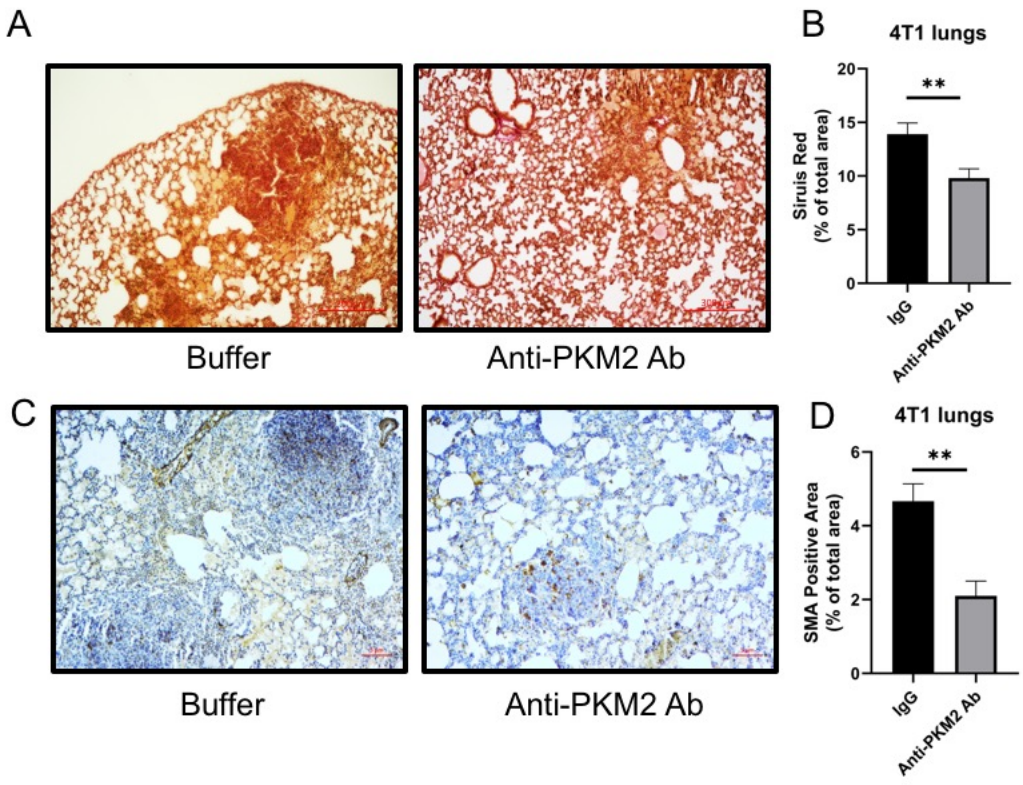

Figure 3.4 Neutralization of rPKM2 reduces fibrosis level in lungs from 4T1 breast cancer mice.

4 Conclusions and Discussions

4.1 Extracellular PKM2 facilitates lung fibrosis progression.

Our lab has a long history studying extracellular PKM2's roles in physiologic and pathologic conditions. The fundamental works in our lab have revealed that extracellular PKM2 is a multi-function player in various conditions. The high level of PKM2 in the blood circulation of cancer patients has been shown to promote tumor cell growth and angiogenesis (Li, Zhang, Qiao, Yang, & Liu, 2014). The extracellular PKM2 found in wound sites facilitates the wound healing process via angiogenesis, and neutrophils are the main source of secreted PKM2 at the early wound healing phase (Zhang, Li, Liu, & Liu, 2016). Our further investigations have disclosed that secreted PKM2 is involved in tissue repair and regeneration in liver (unpublished data). In my part of work, the effect of extracellular PKM2 in lung fibrosis progression has been examined.

We observed an increased extracellular PKM2 level in patient tissues who were diagnosed with chronic inflammation associated with lung fibrosis. The phenomenon brought up a question why the extracellular PKM2 level is increased in the fibrotic lungs. Thus, we took a deep inspection at the role of extracellular PKM2 in lung fibrosis.

The lung fibrosis animal model induced by bleomycin was used for our purpose of research. We found the addition of rPKM2 to the mice promoted lung fibrosis progression. We observed that the body weights of rPKM2-treated mice dropped dramatically due to the worsen health condition after treatments. Also, the average lung weights of the rPKM2-treated mice were greater than those of rPKM1-treated mice probably because the accumulated collagen deposition after rPKM2 treatment contributed to the increased weight of lungs. After organ dissection, the lungs from the rPKM2-treated group showed more whitish, fibrotic-like patterns on the surface, indicating the more collagen deposition after rPKM2 treatment. Further specific collagen staining

with Sirius red staining confirmed that the collagen level was increased in rPKM2-treated mouse tissues.

Myofibroblasts are the primary source of collagen production, thus play an essential role in fibrosis progression. Since we found that extracellular PKM2 enhanced collagen deposition during lung fibrosis progression, we then asked whether extracellular PKM2 had a correlation with collagen-producing myofibroblasts? Myofibroblasts are characterized by stress fiber and the expression of αSMA. We used the immunohistochemistry staining method to determine the expression of αSMA in mice tissues. The results demonstrated that the expression of αSMA was increased after rPKM2 treatment, suggesting the number of myofibroblasts in rPKM2-treated mice was greater. One of the most important reasons why the myofibroblasts are deleterious is that they acquire strong resistance to apoptosis. Therefore, we asked a further question, whether the increase in the myofibroblast number after rPKM2 addition was caused by the decrease in myofibroblast apoptosis? We moved forward to test our hypothesis. Apoptosis level was assessed by a widely used TUNEL assay, co-stained with αSMA marker, to specifically detect the apoptosis in myofibroblasts. The immunofluorescent staining results demonstrated that the number of apoptotic myofibroblasts was lower in rPKM2-treated mice.

To confirm the apoptosis protective effects of the extracellular PKM2, we utilized a PKM2 neutralization antibody in bleomycin-induced lung fibrosis model. We carried out the same sets of experiments to check PKM2 neutralization effects. The results unveiled that, consistent with what we observed previously, neutralization of PKM2 diminished lung fibrosis development, supported by the evidence that the average body weights were increased in the anti-PKM2 antibody treated group, while the average lung weights were decreased, along with less whitish, fibrotic-like patterns on the surface of lungs. Further histology analysis verified that collagen deposition and

αSMA positive myofibroblast number were both reduced after anti-PKM2 antibody treatment. Moreover, the apoptotic rate of myofibroblasts was ameliorated.

4.2 Extracellular PKM2 protects myofibroblasts against apoptosis.

The *in vivo* study of PKM2 on lung fibrosis pointed out that extracellular PKM2 manipulated the apoptosis of myofibroblast, driving us to investigate the underlying mechanisms. In the first place, we carried out *in vitro* experiments to inspect the apoptosis protection role of rPKM2 on myofibroblasts. The NHLFs were activated to myofibroblasts by TGFβ1 and then induced to apoptosis by Fas Ligand and CHX. We observed that a greater number of cells were alive in the rPKM2-treated group compared with the rPKM1-treated group. We then used the Annexin V/PI staining to detect apoptosis rate, and the apoptosis rate was lower in rPKM2-treated group. Moreover, apoptosis-related proteins are examined by western blot, and the results showed that the protein level of cleaved-PARP (cleaved by caspases in apoptosis) was lower while the anti-apoptotic proteins BCL2 and cIAP1 were higher in rPKM2-treated group. In addition, the ATP level was used as an indicator of cell growth, and the ATP level was higher after rPKM2 treatment.

Together, the extracellular PKM2 exhibits apoptosis protection effects on NHLF-derived myofibroblasts. The next key question was how extracellular PKM2 protected myofibroblasts from apoptosis. The integrin αvβ3 is noted to be highly expressed in pathologic conditions such as cancer. We detected the expression of αv and β3 with western blot and found that the expressions of both subunits were intensively increased in myofibroblasts after TGF β1 stimulation. Therefore, we hypothesized that αvβ3 was a potential binding partner of PKM2. The co-IP result showed that β3 was pulled down together with PKM2, and the cell attachment assay supported that the αvβ3 antibody, LM609, abolished the attachment of myofibroblasts to rPKM2-coated plates. Also, the

LM609 abolished the anti-apoptotic effect of rPKM2 on myofibroblasts, indicated by viable cell numbers and the ATP levels. We continued to inspect the downstream pathway after PKM2 binding to αvβ3. We screened several essential players associated with survival pathways and found the p-FAK, p-PI3K and p-AKT protein levels were increased after rPKM2 treatment while p-ERK protein level was not significantly increased. Furthermore, the PI3K activity was enhanced after rPKM2 treatment. The inhibition of FAK and PI3K by specific inhibitors FI14 and LY294002, respectively, abolished the anti-apoptotic effects of rPKM2 on myofibroblast, shown by ATP level examination. Such evidence indicated that FAK, PI3K and AKT were involved in the downstream of the apoptosis protective role of extracellular PKM2. As NF-κB is the common transcription factor downstream of PI3K signaling, we then measured the NF-κB activity and found that PKM2 increased NF-κB activity in myofibroblasts. In addition, the inhibition of FAK, PI3K or αvβ3 by FI14, LY294002 or LM609 respectively abolished the increase of PI3K activity by PKM2; the same thing happened with NF-κB activity.

Overall, we addressed that the apoptosis protective role of extracellular PKM2 is through αvβ3-FAK-PI3K-NF-κB pathway.

4.3 Extracellular PKM2 enhances collagen synthesis in myofibroblasts by upregulating Arginase-1.

Besides apoptosis resistance, another vital reason that myofibroblasts are detrimental is that they have potent collagen production capacity. So, we tried to evaluate whether PKM2 promoted collagen production. We found that rPKM2 treatment increased collagen type I expression in myofibroblasts using western blot, and the secreted collagen 1 level in the culture medium was also increased. However, the mRNA level of collagen 1 was not changed significantly, verified by RT-qPCR. These results pointed out that PKM2 did not upregulate

collagen 1 transcriptionally. Therefore, we thought the change of collagen 1 could come from translational modulation. Proline, the principle amino acid constituent of collagen 1 which makes up ~23% of collagen, caught our attention. A growing body of evidence reported that proline biosynthesis is enhanced in disease conditions, converted from arginine by arginase through the urea cycle. Therefore we measured the proline level. The MS analysis of various amino acids indicated that the proline level was significantly enhanced in myofibroblasts after rPKM2 treatment, along with a notable reduction in arginine level. The arginase activity was increased in rPKM2-treated myofibroblasts. The protein and mRNA levels of Argninase-1 were enhanced as well. To further confirm the connection between proline and collagen, we used the arginine-depleted medium to culture myofibroblast and found that the increase in collagen production by rPKM2 treatment was abolished. In addition, the arginase inhibitor, NOHA, also diminished the promotion on collagen synthesis by rPKM2. We further tested our hypothesis *in vivo* and performed amino acid analysis on tissue samples using LC-MS. We observed an increase in proline and a reduction in arginine in rPKM2-treatment mice, and the opposite effects in anti-PKM2 antibody-treated mice. The Arginase-1 and αSMA co-staining results suggested that the percentage of Arginase-1-expressing myofibroblasts was augmented in rPKM2-treated group while the percentage was decreased in anti-PKM2 antibody-treated group.

Furthermore, we desired to understand whether the upregulation of Arginase-1 by PKM2 was also mediated by integrin αvβ3. β3 knockdown blocked the effect of rPKM2 on increasing the expression of Arginase-1 and p-PI3K in myofibroblasts. Additionally, the inhibition of PI3K or αvβ3 by inhibitor LY294002 and LM609, respectively, abolished the increase in Arginase-1 and p-PI3K protein levels upregulated by rPKM2 addition. Therefore, the upregulation of Arginase-1 by PKM2 is mediated by integrin αvβ3-PI3K signaling.

4.4 Extracellular PKM2 promotes lung metastasis of breast cancer.

Cancer-associated fibroblasts attract tremendous research enthusiasm due to their detrimental and diverse roles in manifesting cancer microenvironment, arising as the most notable therapeutic target in cancer research. As cancer-associated fibroblasts are the myofibroblasts in the cancer microenvironment, we extended our research field to cancer and sought to understand the extracellular PKM2's effects on cancer-associated fibroblasts. Mounting evidence implicates that cancer-associated fibroblasts are responsible for cancer metastatic niche initiation as cancer-associated fibroblasts secret considerable and divergent cytokines, chemokines and growth factors and synthesize ECM to establish a local environment favoring cancer growth. To do so, the cancer-associated fibroblasts not only promote the growth and migration of cancer cells but also transforms normal cells in metastatic sites into cancer-supporting phenotypes. The ECM produced by cancer-associated fibroblasts serves as a platform for cancer migration and colonization. The lung is the most frequent metastatic location, and the metastasis in the lung is most lethal due to that the lung is the respiratory organ in the body. So, we induced the 4T1 cancer model in which frequent metastasis to lung organ was observed, then treated the 4T1 mice with rPKM2 or anti-PKM2 antibody.

In the 4T1 cancer model, we observed that anti-PKM2 antibody-treated mice has a higher survival rate, along with reduced primary tumor size. After dissection, we found the metastatic nodule number was less in anti-PKM2 antibody-treated group by counting the nodule numbers on the surface of the lung tissues. The histology studies revealed that collagen deposition was diminished after anti-PKM2 antibody treatment, and αSMA positive cancer-associated fibroblast cell number was less in metastatic lung tissues. Consistent with our observations in lung tissues, we found the collagen production and cancer-associated fibroblast number were both less in

primary tumor sites after anti-PKM2 antibody treatment. In addition to anti-PKM2 antibody treatment, we also carried out experiments testing the effects of adding rPKM2. The results demonstrated that rPKM2 addition enhanced collagen production in metastatic lung sites and increased lung metastasis.

In summary, the extracellular PKM2 enhances metastasis to lungs in breast cancer.

4.5 Conclusions and Future Perspectives

Our investigation uncloses that the extracellular PKM2, which is increased during fibrosis pathogenesis, contributes to the persistent activity of pro-fibrotic myofibroblasts by protecting these cells against apoptosis and augmenting their collagen synthesis translationally through upregulating the Arginase-1.

The extracellular PKM2 binds to integrin αvβ3 on the cell surface of myofibroblasts and triggers the FAK/PI3K signaling axis. Our discovery not only provides a new perspective for understanding the fibrosis development mechanism but also implies a potential target for the clinical practice in fibrosis disease treatments.

Lung fibrosis is a detrimental disease condition independently or associated with divergent diseases as a secondary effect. Lung fibrosis causes organ failure and the final mortality. Fibrosis could happen to any organ when stimulated with continuous injury. Fibroses in all organs are likely to share common pathogenesis, at least partially. The effects of extracellular PKM2 in lung fibrosis development could be a universal phenomenon in various organ fibrosis. Understanding the role of extracellular PKM2 in a bigger picture could provide new insights into the way we view the organ fibrosis of different types. In fact, we already have evidence to show that extracellular PKM2 also plays a critical role in liver fibrosis/cirrhosis. In future works, we are interested in extending our knowledge of the extracellular PKM2 to other fibrotic diseases. Cardiac fibrosis is a

devastating health issue worldwide associated with almost all forms of heart disease, in which cardiac fibroblasts-derived myofibroblasts are ascribed to disease development (Travers Joshua, Kamal Fadia, Robbins, Yutzey Katherine, & Blaxall Burns, 2016). We plan to examine the effects of extracellular PKM2 in cardiac fibrosis progress. Kidney in another major organ of the human body. Kidney fibrosis is also a significant problem that affects 50% seniors over 70 and approximately 10% of the global population (Humphreys, 2018; Liu, 2006) and the myofibroblasts are stated as a contributor to its aggressiveness. We are also interested in looking at the association between extracellular PKM2 and renal fibrosis.

Another main conclusion interpreted from our results is that extracellular PKM2 promotes lung metastasis. Further work need be done to explore the mechanisms. Basing on our theory in lung fibrosis, it is likely that extracellular PKM2 in cancer may protect cancer-associated fibroblasts against apoptosis and enhance their collagen synthesis feature. To verify *in vitro*, the apoptosis rate of rPKM2 treated cancer-associated fibroblasts can be exanimated and compared with that of the rPKM1-treated group using various approaches. To confirm *in vivo*, the TUNEL assay can be performed to check the apoptosis rate. However, due to a lack of a universal marker for heterogeneous cancer-associated fibroblasts, it is tricky to track the presence of those cells in tissues.

It is exciting to know that the extracellular PKM2 changes the number of cancer-associated fibroblasts. It is of great importance to test our theory in other cancer models, especially those types rich in cancer-associated fibroblasts, such as pancreatic cancers. Pancreatic cancer is the first leading cause of death worldwide and is characterized by excessive ECM and pancreatic stellate cell-derived myofibroblasts (Ohlund et al., 2017). It is interesting to explore how the extracellular PKM2 affects pancreatic cancer.

Besides the myofibroblast apoptosis protective role of PKM2, we report for the first time that extracellular PKM2 enhances the collagen synthesis in myofibroblasts by upregulating Arginase-1. Although arginase has caught increasing attention as a critical player in inflammatory and lung fibrosis, the current studies mostly have focused on the arginase in macrophages. Arginase competes with NO synthase for a common substrate, arginine. NO, the destructive product of NO synthase, mediates the cytotoxic response of macrophages. The fundamental theory about arginase in pulmonary fibrosis is that arginase activity limits the utilization of arginine by NO synthase, thus suppresses the cytotoxic effects of macrophages (Maarsingh, Pera, & Meurs, 2008). Our discovery emphasizes the role of arginase as an enzyme to produce proline as building materials for collagen, which, though less known of, could be of great importance during fibrosis development. Evidence implies that, compared to proline itself, or its common substrates, glutamine and glutamates, the arginine is more favored under wound healing (Barbul, 2008). The possible reason would be that myofibroblasts, just like the cancer cells, undergo glutamine starvation as their energy substantially comes from glutamine; thus, they prefer using arginine to produced proline as the substrates for collagen synthesis. It is very interesting to test this hypothesis and understand more about organ fibrosis. It is interesting to test this hypothesis and understand more about arginase regulation in fibrosis progression.

One important finding of this research work is that extracellular PKM2 causes an increase in Arginase-1 in myofibroblasts. Arginase-1 is well studied in macrophages. It is a crucial effector and a phenotype marker for macrophages. The increase of Arginase-1 expression is recognized as an indicator of macrophage polarization to M2 macrophages. M2 macrophages are a subtype of the macrophage which plays an essential role for constructive immunity during the progression of various diseases including fibrosis and cancer. The integrin αvβ3 is reported to be heavily

expressed on the surface of macrophages (Antonov et al., 2011). Therefore, it is possible that the extracellular PKM2 could bind with integrin αvβ3 on the surface of macrophages and induce the upregulation of Arginase-1 in macrophages, leading to a macrophage phenotype switch to M2 type. Proline produced by the arginase pathway in M2 macrophages is well described as an essential substrate for collagen synthesis during pathological vascular remodeling, fibrosis, and stiffness (Hannemann et al., 2019). Moreover, M2 macrophages are documented to be a master mediator during fibrosis (Hannemann et al., 2019). Especially, they are the dominant source of TGFβ which enhances pro-fibrotic signaling and induces myofibroblast activation. Besides our observation that the extracellular PKM2 increases Arginase-1 in myofibroblasts to promote proline and subsequent collagen production, we speculate that the extracellular PKM2 would drive an increase in Arginase-1 expression in macrophages and lead to macrophage phenotype switch to M2, which could enhance proline supply to myofibroblasts for collagen synthesis and increase TGFβ secretion to promote pro-fibrotic signaling. Therefore, the potential role of the extracellular PKM2 on macrophages would provide additional significance of extracellular PKM2 in fibrosis progression. This direction is also our ongoing project and one of our future perspectives. We are also interested to investigate if the myofibroblasts and macrophages share the similar integrin αvβ3-FAK-PI3K signaling pathway for Arginase-1 upregulation upon the activation of the extracellular PKM2. This would also be exciting since it may provide strong evidence for the potent role of the extracellular PKM2 as a master regulator in tissue repair and regeneration from a big picture perspective.

5 Materials and Methods

5.1 Materials

5.1.1 Chemicals, Reagents and Solution

Table 5.1 1 Chemicals, Reagents and Solutions

Acetic Acid	VWR international
40% Acrylamide/Bis Solution	Bio-Rad
Agar	Sigma Aldrich
Ampicillin	Sigma Aldrich
Bovine Serum Albumin	Sigma Aldrich
Bromophenol Blue	EMD
Calcium Chloride	Sigma Aldrich
Cell Culture Grade Water	Corning
Coomassie blue	Sigma Aldrich
Crystal Violet	Sigma Aldrich
Dithiothreitol	Sigma Aldrich
Dimethyl Sulfoxide	Sigma Aldrich
Dulbecco's Modified Eagle Medium	Cellgro
ECL Western Blot substrate	Thermo Scientific
Eagle's minimal essential medium	Cellgro
Ethanol	VWR International
Ethylenediaminetetraacetic Acid	Sigma Aldrich
Fetal Bovine Serum	Corning
FAK inhibitor 14	Millipore
FBM™ Basal Medium	Lonza
FGM™-2 Single Quots™ supplements	Lonza
Flow Cytometry Staining Buffer	Thermo Fisher
10% Formalin	Thermo Fisher
Glycerol	VWR International
Glutamine solution (100×)	ThermoFisher
Hank's Balanced Salt Solution	Corning
Hydrogen Peroxide (30%)	Thermo Fisher
4-(2-hydroxyethyl)-1-piperazineethanesulfonic acid	Sigma Aldrich
Hydrochloric acid	VWR International

Imidazole	Sigma Aldrich
Isopropanol	VWR International
Isopropyl ß-D-1-thiogalactopyranoside	Sigma Aldrich
Kanamycin	Sigma Aldrich
LY294002	Sigma Aldrich
Magnesium Chloride	Sigma Aldrich
Methanol	VWR International
Minimal Essential Medium	Cellgro
Mounting Medium	Electron Microscopy Sciences
4% Paraformaldehyde solution in PBS	Thermo Fisher
Penicillin-Streptomycin solution	Cellgro
Phenylmethylsulfonyl Fluoride	Sigma Aldrich
Phosphate-buffered Saline	Cellgro
Ponceau solution	Sigma Aldrich
Potassium Chloride	Sigma Aldrich
Prolong gold anti-fade reagent with DAPI	Life Technologies
Protein A agarose	Thermo Scientific
Protein inhibitor cocktail (100×)	Thermo Scientific
Phosphatase inhibitor cocktail I (100×)	Thermo Scientific
RIPA buffer (100×)	Millipore
Sodium Chloride	VWR International
Sodium Citrate	Sigma Aldrich
Sodium Dodecyl Sulfate	Sigma Aldrich
Sodium Hydroxide	Sigma Aldrich
Sodium Pyruvate solution	Cellgro
Tris base	VWR International
Triton X-100	Sigma Aldrich
0.25% Trypsin-EDTA	Cellgro
Tween-20	Sigma Aldrich
Western Blot Stripping Buffer	Thermo Scientific
Xylene	VWR International

5.1.2 Antibodies

Table 5.1 2 Antibodies

Alexa Fluor 488(Goat Anti-Mouse IgG H&L)	Thermo Fisher
Alexa Fluor 488(Goat Anti-Rabbit IgG H&L)	Thermo Fisher
Alexa Fluor 555(Goat Anti-Mouse IgG H&L)	Thermo Fisher
Alexa Fluor 555(Goat Anti-Rabbit IgG H&L)	Thermo Fisher

α-Smooth Muscle Actin Antibody	Abcam
α-Smooth Muscle Actin Antibody	Sigma Aldrich
αv antibody	Santa Cruz Biotechnology
αvβ3 antibody (Clone LM609)	Millipore
Arginase 1 antibody	Santa Cruz Biotechnology
β3 antibody	Santa Cruz Biotechnology
β-Actin antibody	Santa Cruz Biotechnology
BCL2 antibody	Thermo Fisher
cIAP1 antibody	Thermo Fisher
Col1a1 antibody	Santa Cruz Biotechnology
GAPDH antibody	Santa Cruz Biotechnology
Goat anti-Rabbit Secondary Antibody, HRP	Thermo Fisher
Goat anti-Mouse Secondary Antibody, HRP	Thermo Fisher
p-AKT antibody	Santa Cruz Biotechnology
p-ERKantibody	Santa Cruz Biotechnology
PKM2 antibody	Cell Signaling Technology
p-PI3K antibody	Thermo Fisher

5.1.3 Primer sequences

Table 5.1 3 List of primer sequences used in qPCR

gene	Primer sequences
ARG1	Forward: 5'-ACTTAAAGAACAAGAGTGTGATGTG-3'
	Reverse: 5'-ATTGCCAAACTGTGGTCTCC-3'
COL1A1	Forward: 5'-GGTCAGATGGGCCCCCG-3'
	Reverse: 5'-GCACCATCATTTCCACGAGC-3'
ACTB	Forward: 5'-AGCACTGTGTTGGCGTACAG-3'
	Reverse: 5'-AGAGCTACGAGCTGCCTGAC-3'

5.1.4 Kits

Table 5.1 4 Kits

EnerCount Cell Growth Assay Kit	Codex Biosolutions
FITC Annexin V/Dead Cell Apoptosis Kit	Thermo Fisher

Lipofectamine 3000 Transfection Reagent	Thermo Fisher
NFkB p65 Transcription Factor Assay Kit	Abcam
NovaUltra H&E Stain Kit	IHC World
NovaUltra Sirius Red Stain Kit	IHC World
PI3K-Glo™ Class I Profiling Kit	Promega
Lipid Kinase Assays: PI3K-Glo™ Class I Profiling Kit	Promega
TdT In Situ Apoptosis Detection Kit-Fluorescein	R&D

5.1.5 Cell Lines

Table 5.1 5 Cell Lines

Normal Human Lung Fibroblast (NHLF)	Lonza
HEK-293	ATCC
4T1	ATCC
B16-F10	ATCC

5.1.6 Instruments

Table 5.1 6 Instruments

ÄKTA™ Pure Chromatography Systems	GE Healthcare
API 3200 LC/MS/MS System	AB Sciex
BD LSRFortessa™ cell analyzer	BD Biosciences
Biophotometer	Eppendorf
Class II Biosafety Cabinet	Labconco
CO_2 Incubator	Thermo Fisher
7500 Fast Real-Time PCR System	Life Technologies
Histocenter 3	Shandon
Keyence Fluorescent Microscope	Keyence
Kodak X-OMAT 2000A	Kodak
Leica CM3050 Research Cryostat	Leica
MD Plate Reader UV/Vis	Molecular Dynamics
Microtome	Leica
Nanodrop	Thermo Fisher
STP-120 Spin Processor	Fisher
Vacufuge Concentrator	Eppendorf
ZEISS Microscope	Zeiss

5.2 Methods

5.2.1 Recombinant protein expression

The rPKM2-expressing plasmids were transformed into competent BL21(DE3) E. coli cells.

Firstly, a 100 μl aliquot of the competent BL21(DE3) E. coli cell stock was taken out from -80ºC freezer. The competent cell stock was placed on ice to thaw. Then, the plasmid DNA was added into the thawed competent cells and mixed gently by pipetting up and down. The mixture was incubated on ice for 5 mins, followed by heat shock at 42ºC for 1 min, and then kept on ice for another 5 mins. The cells were then transferred into 1ml of LB broth and shaked at 37ºC for 1 hour. The cell culture was plated onto LB agar plates with kanamycin. The plates were incubated at 37ºC overnight.

The next step was to make a starter culture of 250 ml for protein expression. One colony was picked from the plates with a sterile inoculation loop and added into the LB broth with kanamycin (100 mg/ml) in a flask. The flask was put into a shaker, 200 rpm at 37ºC until the absorbance at 600 nm was between 0.5 to 1.5. The starter cell culture can be used for expansion. The remaining culture can be stored at 4ºC. 100 ml of starter culture was transferred into 1 L of LB broth with kanamycin in a flask. The flask was incubated in a shaker, 200 rpm at 37ºC until the absorbance at 600nm was between 0.8 and 1. Then 0.3mM IPTG was added into the flask to induce the protein expression. The flask was incubated in the shaker, 180 rpm at 16ºC overnight. After incubation, the culture was centrifuged at 4 ºC, 5000 rpm. The supernatants were discarded, and the pellets were stored at -80 ºC freezer.

5.2.2 Recombinant protein isolation purification

The first step is lysis and sonication of the bacteria. The bacteria pellets were resuspended with Buffer A (50 mM Tris, 50 mM NaCl, 20mM imidazole, pH 7.4) with 0.5mM PMSF with a 10 ml pipet. The suspension was taken to sonication for 15 min, followed by centrifugation at 14,000 rpm for 15 min at 4°C. The supernatant was transferred to a new tube and filtered with a 0.45μm filter. The filtrate was loaded to the FPLC system of ÄKTA purifier under a preset protocol. The protein was eluted by gradually increasing the concentration of imidazole using Buffer B (50 mM Tris, 50 mM NaCl, 500mM imidazole, 10% glycerol, pH 7.4). Those eluted fractions which covered the majority of the protein peak were collected and combined together. The mixed eluted sample was transferred to a dialysis bag containing dialysis buffer (50 mM Tris, 50 mM NaCl, 10% glycerol, pH 7.4) and dialyzed with vortex at 4 °C overnight. After that, 10 μl of the dialyzed sample was taken out for confirmation of PKM2 protein with SDS-PAGE, followed by coomassie blue staining or Western blot with PKM2 antibody. The purified recombinant PKM2 proteins were sterilized by filtering with 0.22 μm filter and then aliquoted and kept at -80 °C for longtime storage.

5.2.3 Cell culture

The NHLF primary cells were purchased from Lonza and maintained in specialized fibroblast growth medium 2 containing 2% FBS and insulin, hFGF-B and GA-1000 as supplements. The arginine deficient DEME for SILAC (Thermo Fisher) replaced regular fibroblast medium as the culture medium for NHLF, depending on the purpose of certain experiments as indicated. The HEK-293 cells were maintained in MEM medium with 10% FBS, while the 4T1 cell in RPMI-1640 medium with 10% FBS and B16 cells in DMEM medium with 10% FBS. All the cells were kept in a cell culture incubator at 37 °C/ 5% CO_2. For experiments described herein,

NHLFs were plated at 30,000 cells/well in six-well plates or 180,000 cells in 100 mm dishes, depending on specific experiment requirements. NHLFs were starved in fibroblast basal medium without supplements overnight and activated with TGF-β1 (10 ng/ml) for 1 d to induce myofibroblast differentiation. Then depending on different settings of experiments, different treatments were carried out. For PI3K and NF-κB activity determination, cells were treated with 150 nM rPKM2 for 1 d. For apoptosis-related detection, the cells were pre-treated with 150 nM rPKM2 for 30 min, followed by 100 ng/ml Fas Ligand and 100 μg/ml CHX with rPKM2 presenting continuously for 10 h. The inhibitors (20 μg/ml LY294002; 2.5 μM FI14; 1 mM NOHA) and antibody (10 ng/ml LM609) were added 30 min earlier than rPKM2 addition. After treatment, cells were harvested at the indicated time points for the measurement of mRNA, protein levels, or apoptosis assay.

Murine TNBC 4T1 cell line and melanoma cell line B16-F10 cells were obtained from the American Type Culture Collection (ATCC). The 4T1 cells were cultured in RPMI-1640 medium containing 10% fetal bovine serum (FBS), 1% penicillin and 1% streptomycin and B16 cells in Dulbecco's modified Eagle's minimal essential medium (DMEM) supplemented with 10% FBS, 1% penicillin and 1% streptomycin. Cell lines were maintained in a 5% CO2 atmosphere at 37 °C.

5.2.4 RNA isolation and RT-qPCR analysis.

The total RNA of cells was isolated using the RNeasy Plus mini kit (Qiagen) according to the manufacturer's instructions. For RT-qPCR, 0.5 μg of total RNA was reverse-transcribed to cDNA using Maxima First Strand cDNA Synthesis Kit (Thermo Fisher K1641). Real-time qPCR was then performed using 2 μl of cDNA using Luna Universal qPCR Master Mix (NEB M3003) with SYBR® Green as the fluorescent dye and the 7500 Fast Real-Time PCR System (Life Technologies). The primer pairs are listed in Table 2, used at a final concentration of 250 nM.

ACTIN was used as the reference gene. The relative transcript abundance of target genes compared with the reference gene was expressed in the cycle threshold (ΔCt) as ΔCt = Ct(target) – Ct(reference). The relative difference in transcript levels of the treated group compared with the control group was expressed as ΔΔCt = ΔCt(treated) – ΔCt(control). The relative fold changes in the transcript level were represented as $2^{\wedge-\Delta\Delta Ct}$.

5.2.5 SDS-PAGE and Western Blot

After the treatment, the culture medium was removed from the plates or dishes and cells were washed three times with ice-cold PBS buffer. Then the cells were scraped off with a rubber scraper and centrifuged at 1000 rpm, 4 ℃ for 10 min. The superannuants were discarded, and the cell pellets were resuspended with RIPA buffer premixed with protease inhibitors cocktail and phosphatase inhibitors. The mixtures were placed on a rotator and incubated at 4 ℃ for 30 min, after which, the lysates were centrifuged at 14000 rpm, 4 ℃ for 10 min. The supernatants were transferred to new tubes and stored at -20 /-80℃ freezer. The protein concentrations were determined using the Quick Start Bradford 1×Dye Reagent (Bio-Rad, Cat. # 5000205) and a Biophotometer. For western blot analysis, an equal amount of protein sample was taken out and mixed with 5× loading buffer (175 mM Tris-HCl pH 7.0, 5 mM EDTA, 10% SDS, 20% sucrose, 0.01% bromophenol blue, and 28.8 mM β-mercaptoethanol) and heated at 95℃ for 10 min. The samples and protein ladder were loaded in SDS-PAGE gel and ran at constant voltage 80 V first at the stacking stage, and then at 80 V at the separating stage.

After the SDS-PAGE, the proteins were transferred to a nitrocellulose membrane at a constant current of 250 mA for 2 h at 4℃. The membrane was blocked in the blocking solution, 5% BSA prepared in TBST (20mM Tris-HCl pH 7.5, 150 mM NaCl, 0.1% Tween-20) at room temperature for 1 h. After blocking, the membrane was incubated with the primary antibody

diluted in the blocking solution on a flat shaker at 4 ℃ overnight, followed by three times washing with TBST buffer, 10 min each time. Then the membrane was incubated with respective secondary antibody diluted in blocking solution on a flat shaker at 4 ℃ overnight, followed by three times washing with TBST buffer, 10 min each time. The specific bands were detected by autoradiography using chemiluminescence reagents.

5.2.6 Immunoprecipitation

Cell lysates were centrifuged at 14,000 rpm, 4 °C for 10 min and the supernatant collected. The supernatants were pre-cleared by incubating with 1μg normal rabbit IgG and 20 μl protein A/G beads (Santa Cruz) for 60 min at 4 °C. Following centrifugation, 2 μg anti-His-tag antibody (Sc-8036; Clone H-3; Santa Cruz Biotechnology) and 20 μl protein A/G beads were added to the supernatant, and this was rotated at 4 °C for 4 h. Following centrifugation, the beads were washed twice with IP lysis buffer. Then the samples were mixed with sample buffer and boiled for 10 min at 95°C followed by SDS-PAGE and western blotting using the following antibodies: β3 integrin 1:1000 (ab119992; Abcam); PKM2 1:1000 (4053s; Cell signaling technology).

5.2.7 Amino acids isolation and Mass spectrometry analysis

1×10^6 Cells or 100 mg tissues were used for amino acid analysis with LC-MS. Cells were washed with 0.9% NaCl, scraped off and centrifuged at 1000 rpm, 4 ℃ for 10 min, after which the pellets were saved for the next step. 100 mg of tissues were weighed and homogenized in liquid nitrogen. The tissue dry powder was collected for the next step. 50% pre-cold Methanol was added for fixation. Then chloroform was added to lyse the cells at 4℃ for 30 min on the rotator. The lysates were centrifuged at 14000 rpm, 4℃ for 10 min and the top aqueous layer was used as samples for LC-MS analysis with a Sciex API3200 esi-triple quadrupole mass spectrometer coupled with an Agilent 1200 HPLC. 10 μl of each standard and sample was injected into the

system. Amino Acid Standard H (Thermo Fisher Cat. # 20088) was used as standard. The MS parameters used are as follows: Ion source (IS) voltage, 5400 v, ion source temperature 450C, collision energy 5v. Analyst 1.5.1 was used for data analysis.

5.2.8 Immunohistochemistry staining.

Tissues were fixed in 10% formalin and embedded in paraffin blocks then cut into 6 μm sections.

The tissue sections were baked at 60 ℃ for 2 hours and then dewaxed and rehydrated by immersion in the following solutions in order (three times xylene, twice 100% ethanol, 90% ethanol, 70% ethanol, 50% ethanol, 30% ethanol, and distilled water). Antigen retrieval was performed by incubating tissue sections in 10 mM Sodium Citrate buffer, pH 6.0 in a pressure cooker for 10 min. After the sections were cooled down at the room temperature, they were washed in PBS for 5 min. The endogenous peroxidase activity was blocked with 3% H_2O_2 for 10 min, followed by washing with PBS for 5 min. The sections were then blocked with the blocking buffer, 5% BSA in PBST (0.1% Tween-20 in PBS) and then incubated with the primary antibody diluted in the blocking buffer at 4 ℃ overnight. The sections were washed with PBST three times, 5 min each time. The sections were then incubated with respective HRP polymer at room temperature for 30 min, followed by the same washing step as above. The DAB substrate chromogen solution was prepared freshly by mixing 1 ml of DAB diluent with 1 drop of DAB concentrate using ImmPACT DAB Peroxidase (HRP) Substrate (Vector Laboratories, Cat. # SK 4150). DAB substrate was added onto the slides and the color development was monitored carefully under a microscope. Hematoxylin was used for counterstain. The sections were dehydrated by immersion in the same set of solutions in reverse order and then mounted with mounting medium.

IHC staining results were quantified using FRIDA (FRamework for Image Dataset Analysis) software. All images for analysis were saved in the same folder and a mask was selected by picking positive staining regions in different images. Once the mask was defined, the software calculates the positive area for all images.

5.2.9 Immunofluorescent staining.

The frozen sections were warmed up at room temperature and fixed with ice-cold methanol for 10min, followed by washing with PBS for 5 min. Then the tissue was circled with a PAP pen, and blocked with blocking buffer, 5% BSA diluted in PBST (0.1% Tween-20 in PBS buffer) for 30 min. The sections were incubated with the primary antibody diluted in the blocking buffer at 4 ℃ overnight. The sections were washed with PBST three times, 5 min each time. After washing, the sections were incubated with respective fluorescent secondary antibody diluted in the blocking buffer at room temperature for 1 h, followed by the same washing procedure. If double staining was required, the sections were blocked with the blocking buffer again and incubated with the second primary antibody for 2h at room temperature. After washing, the sections were incubated with another fluorescent secondary antibody for 1 h. The same washing procedure was performed, after which the sections were mounted with Prolong Gold Antifade Mountant with DAPI. The staining was analyzed with a Keyence fluorescent microscope.

IF staining results were quantified with ImageJ software. The total positive staining area was measured.

5.2.10 Collagen assay.

The collagen contents in the culture medium were determined with Sirius Red (IHC world), followed the procedure previously described (Chen et al., 2013; Kliment, Englert, Crum, & Oury, 2011). Equal volumes of culture medium were added to 1 ml of Sirius Red dye, followed by 1 h

incubation in a shaker. After centrifugation at 12,000 rpm for 10 min, the pellets of collagen-dye complex were washed with acidified water (5% acetic acid) twice. Then 250 μl 0.1 M NaOH was added and incubated for 5 min. The contents of tubes were transferred to a 96-well plate and read at 540 nm on an MD plate reader (Molecular Dynamics). Collagen contents were calculated using a standard curve with type 1 collagen (Sigma).

5.2.11 Cell growth assay

The cell growth was examined by measuring ATP changes in cells using Codex EnerCount™ Cell Growth Assay Kit (Codex Biosolutions), following the manufacturer's instructions. Cells were grown on a 96 well plate. After the treatments, the freshly made working reagent was added to the culture media. The plate was incubated at room temperature for 1 h, after which the luminescence was read on a plate reader Victor UV/Vis/Fluorescent Plate Reader (PerkinElmer).

5.2.12 Annexin V/PI apoptosis detection with flow cytometry

The cells were detached with accutase solution (BD Biosciences) and stained with Dead Cell Apoptosis Kit with Annexin V FITC and PI (Thermo Fisher, Cat. # V13242). Briefly, the cells were washed twice in PBS and once in Binding Buffer and resuspended in Binding Buffer at 10^6 cells/ml. 5 µl of FITC-conjugated Annexin V was added to the cell suspension and incubated 15 min RT at dark, followed by one wash and resuspension in Binding Buffer. 5 µl of Propidium Iodide was added in and incubated for 5 min. The samples were analyzed by LSRFortessa™ cell analyzer (BD Biosciences), and the data were analyzed by FlowJo software (FlowJo).

5.2.13 Animal model and treatment.

All animal experiments were performed according to the guidelines of Georgia State University and were approved by IACUC. 6-week old male C57BL/6J mice were administrated

25mg/kg bleomycin twice a week for 5 weeks and treated with appropriate agents for the indicated time period. rPKM1 and rPKM2 are recombinant proteins expressed in bacteria. IgGCon is normal rabbit IgG used as control. IgGPK are in-house developed rabbit antibody against human PKM2, clone 16-2. At the end of the treatments, animals were sacrificed, and organs were harvested and processed for embedding and sectioning or immediately snap-frozen in liquid nitrogen for subsequent analyses. Statistical analyses were done in comparison to the control group.

4T1 cells ($0.5\text{-}1\times 10^6$) or B16-F10 (0.2×10^6) were suspended in PBS and implanted in 100µl volume of 1:1 mixture of cell suspension and growth factor-reduced Matrigel (BD Biosciences) into the mammary glands of BALB/c female mice or C57BL/6J mice (aged 6-10 weeks) dorsal site subcutaneously, respectively. The tumor volumes were monitored by measuring two principal perpendicular diameters of the tumor with calipers and calculating the tumor volume using the formula: $V = 0.5\times W^2\times L$. W=width (mm), L=length (mm). When the tumor reached indicated volume, the mice were treated with appropriate agents for the indicated time period. rPKM1 and rPKM2 are recombinant proteins expressed in bacteria. IgG is normal rabbit IgG used as control. IgGPK is in-house developed rabbit antibody against human PKM2, clone 16-2. At the end of the treatments, animals were sacrificed, and organs were harvested and processed for embedding and sectioning or immediately snap-frozen in liquid nitrogen for subsequent analyses. Statistical analyses were done in comparison to the control group. To determine the effects of application of different agents on lung metastatic tumor frequency in vivo, the visible tumor number was counted immediately after lungs were harvested. Lung tissue blocks were sectioned into 6-µm sections and stained by H&E. The number of metastases was scored using 5 sections per mouse.

5.2.14 Sirius red

Sirius Red staining was carried out using NovaUltra Sirius Red Stain Kit from IHC WORLD following the instruction of the manufacturer.

5.2.15 Hematoxylin and eosin (H&E) staining

The paraffin slides were baked at 60 ℃ for 2 hours, and rehydrated by immersing into the following solution in order (xylene, 100% ethanol, 90% ethanol, 70% ethanol, 50% ethanol, 30% ethanol). Next, the slides were incubated with Mayer's Hematoxylin for 10 min and washed under tap water for 10 min. The slides were immersed in Eosin for 30 sec and washed under tap water. The slides were immersed into the previous solutions in reverse order for dehydration, after which the slides were mounted with mounting medium and covered by coverslips.

5.2.16 Statistical analysis.

Statistical analyses were carried out using the GraphPad Prism software. Data were statistically analyzed by comparing two appropriate groups. The p values were calculated using the unpaired two-tailed Student t-test. In all figures and tables, ns means $p > 0.05$, * means $p < 0.05$, ** means $P < 0.01$, and *** means $P < 0.001$.

REFERENCES

Barbul, A. (2008). Proline precursors to sustain Mammalian collagen synthesis. J Nutr, 138(10), 2021s-2024s. doi:10.1093/jn/138.10.2021S

Humphreys, B. D. (2018). Mechanisms of Renal Fibrosis. Annual Review of Physiology, 80(1), 309-326. doi:10.1146/annurev-physiol-022516-034227

Li, L., Zhang, Y., Qiao, J., Yang, J. J., & Liu, Z. R. (2014). Pyruvate kinase M2 in blood circulation facilitates tumor growth by promoting angiogenesis. J Biol Chem, 289(37), 25812-25821. doi:10.1074/jbc.M114.576934

Liu, Y. (2006). Renal fibrosis: new insights into the pathogenesis and therapeutics. Kidney Int, 69(2), 213-217. doi:10.1038/sj.ki.5000054

Maarsingh, H., Pera, T., & Meurs, H. (2008). Arginase and pulmonary diseases. Naunyn-Schmiedeberg's archives of pharmacology, 378(2), 171-184. doi:10.1007/s00210-008-0286-7

Ohlund, D., Handly-Santana, A., Biffi, G., Elyada, E., Almeida, A. S., Ponz-Sarvise, M., . . . Tuveson, D. A. (2017). Distinct populations of inflammatory fibroblasts and myofibroblasts in pancreatic cancer. J Exp Med, 214(3), 579-596. doi:10.1084/jem.20162024

Travers Joshua, G., Kamal Fadia, A., Robbins, J., Yutzey Katherine, E., & Blaxall Burns, C. (2016). Cardiac Fibrosis. Circulation Research, 118(6), 1021-1040. doi:10.1161/CIRCRESAHA.115.306565

Zhang, Y., Li, L., Liu, Y., & Liu, Z. R. (2016). PKM2 released by neutrophils at wound site facilitates early wound healing by promoting angiogenesis. Wound Repair Regen, 24(2), 328-336. doi:10.1111/wrr.12411

Albaugh, V. L., Mukherjee, K., & Barbul, A. (2017). Proline Precursors and Collagen Synthesis: Biochemical Challenges of Nutrient Supplementation and Wound Healing. The Journal of nutrition, 147(11), 2011-2017. doi:10.3945/jn.117.256404

Balkwill, F. R., Capasso, M., & Hagemann, T. (2012). The tumor microenvironment at a glance. Journal of Cell Science, 125(23), 5591. doi:10.1242/jcs.116392

Barratt, S. L., Creamer, A., Hayton, C., & Chaudhuri, N. (2018). Idiopathic Pulmonary Fibrosis (IPF): An Overview. Journal of clinical medicine, 7(8), 201. doi:10.3390/jcm7080201

Bochaton-Piallat, M.-L., Gabbiani, G., & Hinz, B. (2016). The myofibroblast in wound healing and fibrosis: answered and unanswered questions. F1000Research, 5, F1000 Faculty Rev-1752. doi:10.12688/f1000research.8190.1

Buschow, S. I., van Balkom, B. W., Aalberts, M., Heck, A. J., Wauben, M., & Stoorvogel, W. (2010). MHC class II-associated proteins in B-cell exosomes and potential functional implications for exosome biogenesis. Immunol Cell Biol, 88(8), 851-856. doi:10.1038/icb.2010.64

Caldwell, R. W., Rodriguez, P. C., Toque, H. A., Narayanan, S. P., & Caldwell, R. B. (2018). Arginase: A Multifaceted Enzyme Important in Health and Disease. Physiological Reviews, 98(2), 641-665. doi:10.1152/physrev.00037.2016

Gelse, K., Pöschl, E., & Aigner, T. (2003). Collagens—structure, function, and biosynthesis. Advanced Drug Delivery Reviews, 55(12), 1531-1546. doi:https://doi.org/10.1016/j.addr.2003.08.002

Gonzalez, A. C. d. O., Costa, T. F., Andrade, Z. d. A., & Medrado, A. R. A. P. (2016). Wound healing - A literature review. Anais brasileiros de dermatologia, 91(5), 614-620. doi:10.1590/abd1806-4841.20164741

Gordon, M. K., & Hahn, R. A. (2010). Collagens. Cell and tissue research, 339(1), 247-257. doi:10.1007/s00441-009-0844-4

Guo, S., & Dipietro, L. A. (2010). Factors affecting wound healing. Journal of dental research, 89(3), 219-229. doi:10.1177/0022034509359125

Harvey, L. D., & Chan, S. Y. (2018). YAPping About Glutaminolysis in Hepatic Fibrosis. Gastroenterology, 154(5), 1231-1233. doi:10.1053/j.gastro.2018.03.007

Hinz, B. (2016). Myofibroblasts. Experimental Eye Research, 142, 56-70. doi:https://doi.org/10.1016/j.exer.2015.07.009

Hinz, B., Phan, S. H., Thannickal, V. J., Galli, A., Bochaton-Piallat, M.-L., & Gabbiani, G. (2007). The myofibroblast: one function, multiple origins. The American journal of pathology, 170(6), 1807-1816. doi:10.2353/ajpath.2007.070112

Hirata, E., & Sahai, E. (2017). Tumor Microenvironment and Differential Responses to Therapy. Cold Spring Harbor perspectives in medicine, 7(7), a026781. doi:10.1101/cshperspect.a026781

Hosios, A. M., Fiske, B. P., Gui, D. Y., & Vander Heiden, M. G. (2015). Lack of Evidence for PKM2 Protein Kinase Activity. Molecular cell, 59(5), 850-857. doi:10.1016/j.molcel.2015.07.013

Hsu, M. C., Hung, W. C., Yamaguchi, H., Lim, S. O., Liao, H. W., Tsai, C. H., & Hung, M. C. (2016). Extracellular PKM2 induces cancer proliferation by activating the EGFR signaling pathway. Am J Cancer Res, 6(3), 628-638.

Israelsen, W. J., Dayton, T. L., Davidson, S. M., Fiske, B. P., Hosios, A. M., Bellinger, G., . . . Vander Heiden, M. G. (2013). PKM2 isoform-specific deletion reveals a differential requirement for pyruvate kinase in tumor cells. Cell, 155(2), 397-409. doi:10.1016/j.cell.2013.09.025

Jun, J.-I., & Lau, L. F. (2018). Resolution of organ fibrosis. The Journal of clinical investigation, 128(1), 97-107. doi:10.1172/JCI93563

Jun, J. I., & Lau, L. F. (2010). The matricellular protein CCN1 induces fibroblast senescence and restricts fibrosis in cutaneous wound healing. Nat Cell Biol, 12(7), 676-685. doi:10.1038/ncb2070

Karna, E., Szoka, L., Huynh, T. Y. L., & Palka, J. A. (2019). Proline-dependent regulation of collagen metabolism. Cell Mol Life Sci. doi:10.1007/s00018-019-03363-3

Kim, H., Kim, S. H., Hwang, D., An, J., Chung, H. S., Yang, E. G., & Kim, S. Y. (2019). Extracellular pyruvate kinase M2 facilitates cell migration by upregulating claudin-1 expression in colon cancer cells. Biochem Cell Biol, 1-8. doi:10.1139/bcb-2019-0139

King, T. E., Pardo, A., & Selman, M. (2011). Idiopathic pulmonary fibrosis. The Lancet, 378(9807), 1949-1961. doi:https://doi.org/10.1016/S0140-6736(11)60052-4

Kitowska, K., Zakrzewicz, D., Königshoff, M., Chrobak, I., Grimminger, F., Seeger, W., . . . Eickelberg, O. (2008). Functional role and species-specific contribution of arginases in pulmonary fibrosis. American Journal of Physiology-Lung Cellular and Molecular Physiology
, 294(1), L34-L45. doi:10.1152/ajplung.00007.2007

Meyer, K. C. (2017). Pulmonary fibrosis, part I: epidemiology, pathogenesis, and diagnosis. Expert Rev Respir Med, 11(5), 343-359. doi:10.1080/17476348.2017.1312346

Ricard-Blum, S., Baffet, G., & Théret, N. (2018). Molecular and tissue alterations of collagens in fibrosis. Matrix Biology, 68-69, 122-149. doi:https://doi.org/10.1016/j.matbio.2018.02.004

Richeldi, L., Collard, H. R., & Jones, M. G. (2017). Idiopathic pulmonary fibrosis. Lancet, 389(10082), 1941-1952. doi:10.1016/s0140-6736(17)30866-8

Rockey, D. C., Bell, P. D., & Hill, J. A. (2015). Fibrosis--a common pathway to organ injury and failure. N Engl J Med, 372(12), 1138-1149. doi:10.1056/NEJMra1300575

Stempien-Otero, A., Kim, D.-H., & Davis, J. (2016). Molecular networks underlying myofibroblast fate and fibrosis. Journal of molecular and cellular cardiology, 97, 153-161. doi:10.1016/j.yjmcc.2016.05.002

Tao, L., Huang, G., Song, H., Chen, Y., & Chen, L. (2017). Cancer associated fibroblasts: An essential role in the tumor microenvironment. Oncology letters, 14(3), 2611-2620. doi:10.3892/ol.2017.6497

Wang, C., Zhang, S., Liu, J., Tian, Y., Ma, B., Xu, S., . . . Luo, Y. (2020). Secreted Pyruvate Kinase M2 Promotes Lung Cancer Metastasis through Activating the Integrin Beta1/FAK Signaling Pathway. Cell Rep, 30(6), 1780-1797.e1786. doi:10.1016/j.celrep.2020.01.037

Wu, T., & Dai, Y. (2017). Tumor microenvironment and therapeutic response. Cancer Letters, 387, 61-68. doi:https://doi.org/10.1016/j.canlet.2016.01.043

Wynn, T. A. (2008). Cellular and molecular mechanisms of fibrosis. The Journal of pathology, 214(2), 199-210. doi:10.1002/path.2277

Yang, P., Li, Z., Wang, Y., Zhang, L., Wu, H., & Li, Z. (2015). Secreted pyruvate kinase M2 facilitates cell migration via PI3K/Akt and Wnt/beta-catenin pathway in colon cancer cells. Biochem Biophys Res Commun, 459(2), 327-332. doi:10.1016/j.bbrc.2015.02.112

Amin, S., Yang, P., & Li, Z. (2019). Pyruvate kinase M2: A multifarious enzyme in non-canonical localization to promote cancer progression. Biochim Biophys Acta Rev Cancer, 1871(2), 331-341. doi:10.1016/j.bbcan.2019.02.003

Bernard, K., Logsdon, N. J., Benavides, G. A., Sanders, Y., Zhang, J., Darley-Usmar, V. M., & Thannickal, V. J. (2018). Glutaminolysis is required for transforming growth factor-beta1-induced myofibroblast differentiation and activation. J Biol Chem, 293(4), 1218-1228. doi:10.1074/jbc.RA117.000444

Bernard, K., Logsdon, N. J., Ravi, S., Xie, N., Persons, B. P., Rangarajan, S., . . . Thannickal, V. J. (2015). Metabolic Reprogramming Is Required for Myofibroblast Contractility and Differentiation. J Biol Chem, 290(42), 25427-25438. doi:10.1074/jbc.M115.646984

Du, K., Chitneni, S. K., Suzuki, A., Wang, Y., Henao, R., Hyun, J., . . . Diehl, A. M. (2019). Increased Glutaminolysis Marks Active Scarring in Nonalcoholic Steatohepatitis Progression. Cellular and Molecular Gastroenterology and Hepatology. doi:https://doi.org/10.1016/j.jcmgh.2019.12.006

Fiore, V. F., Wong, S. S., Tran, C., Tan, C., Xu, W., Sulchek, T., . . . Barker, T. H. (2018). αvβ3 Integrin drives fibroblast contraction and strain stiffening of soft provisional matrix during progressive fibrosis. JCI insight, 3(20), e97597. doi:10.1172/jci.insight.97597

Ge, J., Cui, H., Xie, N., Banerjee, S., Guo, S., Dubey, S., . . . Liu, G. (2018). Glutaminolysis Promotes Collagen Translation and Stability via α-Ketoglutarate-mediated mTOR Activation and Proline Hydroxylation. American journal of respiratory cell and molecular biology, 58(3), 378-390. doi:10.1165/rcmb.2017-0238OC

Hamanaka, R. B., O'Leary, E. M., Witt, L. J., Tian, Y., Gokalp, G. A., Meliton, A. Y., . . . Mutlu, G. M. (2019). Glutamine Metabolism Is Required for Collagen Protein Synthesis in Lung Fibroblasts. Am J Respir Cell Mol Biol, 61(5), 597-606. doi:10.1165/rcmb.2019-0008OC

Hsu, M. C., & Hung, W. C. (2018). Pyruvate kinase M2 fuels multiple aspects of cancer cells: from cellular metabolism, transcriptional regulation to extracellular signaling. Mol Cancer, 17(1), 35. doi:10.1186/s12943-018-0791-3

Konigshoff, M., Kramer, M., Balsara, N., Wilhelm, J., Amarie, O. V., Jahn, A., . . . Eickelberg, O. (2009). WNT1-inducible signaling protein-1 mediates pulmonary fibrosis in mice and is

upregulated in humans with idiopathic pulmonary fibrosis. The Journal of clinical investigation, 119(4), 772-787. doi:10.1172/jci33950

Nieweld, C., & Summer, R. (2019). Activated Fibroblasts: Gluttonous for Glutamine. Am J Respir Cell Mol Biol, 61(5), 554-555. doi:10.1165/rcmb.2019-0155ED

Rangarajan, S., Bone, N. B., Zmijewska, A. A., Jiang, S., Park, D. W., Bernard, K., . . . Zmijewski, J. W. (2018). Metformin reverses established lung fibrosis in a bleomycin model. Nat Med, 24(8), 1121-1127. doi:10.1038/s41591-018-0087-6

Sarrazy, V., Koehler, A., Chow, M. L., Zimina, E., Li, C. X., Kato, H., . . . Hinz, B. (2014). Integrins alphavbeta5 and alphavbeta3 promote latent TGF-beta1 activation by human cardiac fibroblast contraction. Cardiovasc Res, 102(3), 407-417. doi:10.1093/cvr/cvu053

Chen, C., Yang, S., Zhang, M., Zhang, Z., Zhang, B., Han, D., . . . Zhang, L. (2013). In vitro Sirius Red collagen assay measures the pattern shift from soluble to deposited collagen. Adv Exp Med Biol, 765, 47-53. doi:10.1007/978-1-4614-4989-8_7

Friman, T., Gustafsson, R., Stuhr, L. B., Chidiac, J., Heldin, N.-E., Reed, R. K., . . . Rubin, K. (2012). Increased fibrosis and interstitial fluid pressure in two different types of syngeneic murine carcinoma grown in integrin β3-subunit deficient mice. PLoS One, 7(3), e34082.

Horton, M. A. (1997). The αvβ3 integrin “vitronectin receptor”. The International Journal of Biochemistry & Cell Biology, 29(5), 721-725.

Kendall, R. T., & Feghali-Bostwick, C. A. (2014). Fibroblasts in fibrosis: novel roles and mediators. Frontiers in Pharmacology, 5(123). doi:10.3389/fphar.2014.00123

Kliment, C. R., Englert, J. M., Crum, L. P., & Oury, T. D. (2011). A novel method for accurate collagen and biochemical assessment of pulmonary tissue utilizing one animal. Int J Clin Exp Pathol, 4(4), 349-355.

Kumar, C. C. (1998). Signaling by integrin receptors. Oncogene, 17(11), 1365-1373.

Patsenker, E., Popov, Y., Stickel, F., Schneider, V., Ledermann, M., Sägesser, H., . . . Schuppan, D. (2009). Pharmacological inhibition of integrin alphavbeta3 aggravates experimental liver fibrosis and suppresses hepatic angiogenesis. Hepatology (Baltimore, Md.), 50(5), 1501-1511. doi:10.1002/hep.23144

Reynolds, L. E., Wyder, L., Lively, J. C., Taverna, D., Robinson, S. D., Huang, X., . . . Hodivala-Dilke, K. M. (2002). Enhanced pathological angiogenesis in mice lacking beta3 integrin or beta3 and beta5 integrins. Nat Med, 8(1), 27-34. doi:10.1038/nm0102-27

Robinson, S. D., Reynolds, L. E., Wyder, L., Hicklin, D. J., & Hodivala-Dilke, K. M. (2004). Beta3-integrin regulates vascular endothelial growth factor-A-dependent permeability. Arterioscler Thromb Vasc Biol, 24(11), 2108-2114. doi:10.1161/01.ATV.0000143857.27408.de

Sahin, E., Haubenwallner, S., Kuttke, M., Kollmann, I., Halfmann, A., Dohnal, A. M., . . . Schabbauer, G. (2014). Macrophage PTEN regulates expression and secretion of arginase I modulating innate and adaptive immune responses. J Immunol, 193(4), 1717-1727. doi:10.4049/jimmunol.1302167

Takada, Y., Ye, X., & Simon, S. (2007). The integrins. Genome Biology, 8(5), 215. doi:10.1186/gb-2007-8-5-215

Weis, S. M., & Cheresh, D. A. (2011). αV integrins in angiogenesis and cancer. Cold Spring Harbor perspectives in medicine, 1(1), a006478-a006478. doi:10.1101/cshperspect.a006478

Weng, S., Zemany, L., Standley, K. N., Novack, D. V., La Regina, M., Bernal-Mizrachi, C., . . . Semenkovich, C. F. (2003). Beta3 integrin deficiency promotes atherosclerosis and pulmonary inflammation in high-fat-fed, hyperlipidemic mice. Proc Natl Acad Sci U S A, 100(11), 6730-6735. doi:10.1073/pnas.1137612100

White, E. S., Atrasz, R. G., Hu, B., Phan, S. H., Stambolic, V., Mak, T. W., . . . Toews, G. B. (2006). Negative regulation of myofibroblast differentiation by PTEN (Phosphatase and Tensin Homolog Deleted on chromosome 10). American journal of respiratory and critical care medicine, 173(1), 112-121. doi:10.1164/rccm.200507-1058OC

Chandler, C., Liu, T., Buckanovich, R., & Coffman, L. G. (2019). The double edge sword of fibrosis in cancer. Translational Research, 209, 55-67. doi:https://doi.org/10.1016/j.trsl.2019.02.006

Cox, T. R., & Erler, J. T. (2014). Molecular Pathways: Connecting Fibrosis and Solid Tumor Metastasis. Clinical Cancer Research, 20(14), 3637. doi:10.1158/1078-0432.CCR-13-1059

Yamauchi, M., Barker, T. H., Gibbons, D. L., & Kurie, J. M. (2018). The fibrotic tumor stroma. The Journal of clinical investigation, 128(1), 16-25. doi:10.1172/JCI93554

Chandler, C., Liu, T., Buckanovich, R., & Coffman, L. G. (2019). The double edge sword of fibrosis in cancer. Translational Research, 209, 55-67. doi:https://doi.org/10.1016/j.trsl.2019.02.006

Chen, C., Yang, S., Zhang, M., Zhang, Z., Zhang, B., Han, D., . . . Zhang, L. (2013). In vitro Sirius Red collagen assay measures the pattern shift from soluble to deposited collagen. Adv Exp Med Biol, 765, 47-53. doi:10.1007/978-1-4614-4989-8_7

Cox, T. R., & Erler, J. T. (2014). Molecular Pathways: Connecting Fibrosis and Solid Tumor Metastasis. Clinical Cancer Research, 20(14), 3637. doi:10.1158/1078-0432.CCR-13-1059

Friman, T., Gustafsson, R., Stuhr, L. B., Chidiac, J., Heldin, N.-E., Reed, R. K., . . . Rubin, K. (2012). Increased fibrosis and interstitial fluid pressure in two different types of syngeneic murine carcinoma grown in integrin β3-subunit deficient mice. PLoS One, 7(3), e34082.

Horton, M. A. (1997). The αvβ3 integrin “vitronectin receptor”. The International Journal of Biochemistry & Cell Biology, 29(5), 721-725.

Karna, E., Szoka, L., Huynh, T. Y. L., & Palka, J. A. (2019). Proline-dependent regulation of collagen metabolism. Cell Mol Life Sci. doi:10.1007/s00018-019-03363-3

Kendall, R. T., & Feghali-Bostwick, C. A. (2014). Fibroblasts in fibrosis: novel roles and mediators. Frontiers in Pharmacology, 5(123). doi:10.3389/fphar.2014.00123

Kliment, C. R., Englert, J. M., Crum, L. P., & Oury, T. D. (2011). A novel method for accurate collagen and biochemical assessment of pulmonary tissue utilizing one animal. Int J Clin Exp Pathol, 4(4), 349-355.

Kumar, C. C. (1998). Signaling by integrin receptors. Oncogene, 17(11), 1365-1373.

Patsenker, E., Popov, Y., Stickel, F., Schneider, V., Ledermann, M., Sägesser, H., . . . Schuppan, D. (2009). Pharmacological inhibition of integrin alphavbeta3 aggravates experimental liver fibrosis and suppresses hepatic angiogenesis. Hepatology (Baltimore, Md.), 50(5), 1501-1511. doi:10.1002/hep.23144

Reynolds, L. E., Wyder, L., Lively, J. C., Taverna, D., Robinson, S. D., Huang, X., . . . Hodivala-Dilke, K. M. (2002). Enhanced pathological angiogenesis in mice lacking beta3 integrin or beta3 and beta5 integrins. Nat Med, 8(1), 27-34. doi:10.1038/nm0102-27

Robinson, S. D., Reynolds, L. E., Wyder, L., Hicklin, D. J., & Hodivala-Dilke, K. M. (2004). Beta3-integrin regulates vascular endothelial growth factor-A-dependent permeability. Arterioscler Thromb Vasc Biol, 24(11), 2108-2114. doi:10.1161/01.ATV.0000143857.27408.de

Sahin, E., Haubenwallner, S., Kuttke, M., Kollmann, I., Halfmann, A., Dohnal, A. M., . . . Schabbauer, G. (2014). Macrophage PTEN regulates expression and secretion of arginase I

modulating innate and adaptive immune responses. J Immunol, 193(4), 1717-1727. doi:10.4049/jimmunol.1302167

Takada, Y., Ye, X., & Simon, S. (2007). The integrins. Genome Biology, 8(5), 215. doi:10.1186/gb-2007-8-5-215

Weis, S. M., & Cheresh, D. A. (2011). αV integrins in angiogenesis and cancer. Cold Spring Harbor perspectives in medicine, 1(1), a006478-a006478. doi:10.1101/cshperspect.a006478

Weng, S., Zemany, L., Standley, K. N., Novack, D. V., La Regina, M., Bernal-Mizrachi, C., . . . Semenkovich, C. F. (2003). Beta3 integrin deficiency promotes atherosclerosis and pulmonary inflammation in high-fat-fed, hyperlipidemic mice. Proc Natl Acad Sci U S A, 100(11), 6730-6735. doi:10.1073/pnas.1137612100

White, E. S., Atrasz, R. G., Hu, B., Phan, S. H., Stambolic, V., Mak, T. W., . . . Toews, G. B. (2006). Negative regulation of myofibroblast differentiation by PTEN (Phosphatase and Tensin Homolog Deleted on chromosome 10). American journal of respiratory and critical care medicine, 173(1), 112-121. doi:10.1164/rccm.200507-1058OC

Yamauchi, M., Barker, T. H., Gibbons, D. L., & Kurie, J. M. (2018). The fibrotic tumor stroma. The Journal of clinical investigation, 128(1), 16-25. doi:10.1172/JCI93554